arXiv:1008.3349v1 [math.GT] 19 Aug 2010

KNOT DOUBLING OPERATORS AND BORDERED HEEGAARD FLOER HOMOLOGY

ADAM SIMON LEVINE

Abstract. We use bordered Heegaard Floer homology to compute the τ invariant of a family of satellite knots obtained via twisted infection along two components of the Borromean rings, a generalization of Whitehead doubling. We show that τ of the resulting knot depends only on the two twisting parameters and the values of τ for the two companion knots. We also include some notes on bordered Heegaard Floer homology that may serve as a useful introduction to the subject.

1. Introduction

A knot in the 3-sphere is called *topologically slice* if it bounds a locally flatly embedded disk in the 4-ball, and *smoothly slice* if the disk can be taken to be smoothly embedded. Two knots are called (topologically or smoothly) *concordant* if they are the ends of an embedded annulus in $S^3 \times I$; thus, a knot is slice if and only if it is concordant to the unknot. More generally, a link is (topologically or smoothly) *slice* if it bounds a disjoint union of appropriately embedded disks. The study of concordance — especially the relationship between the notions of topological and smooth sliceness — is one of the major areas of active research in knot theory, and it is closely tied to the perplexing differences between topological and smooth 4-manifold theory.

While all known explicit constructions of slice disks use smooth techniques, the early obstructions to sliceness — including the Alexander polynomial, the signature, J. Levine's algebraic concordance group, and Casson–Gordon invariants — arise from the algebraic topology of the complement of a slice disk, so they only obstruct a knot from being topologically slice. However, in the 1980s, Freedman [3] showed that any knot whose Alexander polynomial is 1 is topologically slice, even though it is difficult to describe the slice disks explicitly. In particular, the *untwisted positive and negative Whitehead doubles* of any knot K, denoted $Wh_\pm(K)$ (Figure 1), are topologically slice. Around the same time, the advent of Donaldson's gauge theory made it possible to show that some of these examples are not smoothly slice. Akbulut [unpublished] first proved in 1983 that the positive, untwisted Whitehead double of the right-handed trefoil is not smoothly slice. Later, using results of Kronheimer and Mrowka on Seiberg–Witten theory, Rudolph [21] showed that any nontrivial knot that is *strongly quasipositive* cannot be smoothly slice. In particular, the positive, untwisted Whitehead double of a strongly quasipositive knot is strongly quasipositive; thus, by induction, any iterated positive Whitehead double of a strongly quasipositive

---

The author was supported by NSF grants DMS-0739392 and DMS-1004622.

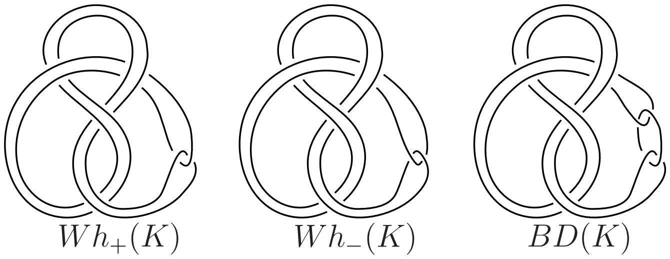

FIGURE 1. The positive and negative Whitehead doubles and the Bing double of the figure-eight knot.

knot is topologically but not smoothly slice. Bižaca [1] used this result to give explicit constructions of exotic smooth structures on $\mathbb{R}^4$.

Using Heegaard Floer homology, Ozsváth and Szabó [14] defined an additive, integer-valued knot invariant $\tau(K)$, defined as the minimum Alexander grading of an element of $\widehat{\mathrm{HFK}}(S^3, K)$ that survives to the E^∞ page of the spectral sequence from $\widehat{\mathrm{HFK}}(S^3, K)$ to $\widehat{\mathrm{HF}}(S^3)$. The τ invariant provides a lower bound on the genus of smooth surfaces in the four-ball bounded by K: $|\tau(K)| \le g_4(K)$. In particular, if K is smoothly slice, then $\tau(K) = 0$. This fact can be used to generalize many of the previously known results about knots that are topologically but not smoothly slice. For example, Hedden [4] computed the value of τ for all *twisted Whitehead doubles* in terms of τ of the original knot:

$$\tau(Wh_+(K,t)) = \begin{cases} 1 & t < 2\tau(K) \\ 0 & t \ge 2\tau(K). \end{cases} \tag{1}$$

(An analogous formula for negative Whitehead doubles follows from the fact that $\tau(\bar{K}) = -\tau(K)$.) In particular, if $\tau(K) > 0$, then $\tau(Wh_+(K,0)) = 1$, so $Wh_+(K,0)$ (the untwisted Whitehead double of K) is not smoothly slice. Since τ of a strongly quasipositive knot is equal to its genus [12], Rudolph's result follows from Hedden's. There is a famous conjecture (Problem 1.38 on Kirby's problem list [8]) that the untwisted Whitehead double of K is smoothly slice if and only if K is smoothly slice. However, it is not yet known whether, for instance, the positive Whitehead double of the left-handed trefoil is smoothly slice. Indeed, it seems that gauge theory invariants have a fundamental asymmetry that makes them unable to detect such examples, which likely places the "only if" direction of this conjecture beyond the scope of currently existing techniques.

We consider the following generalization of Whitehead doubling. For knots J, K and integers s, t, let $D_{J,s}(K,t)$ denote the knot shown in Figure 2(a); the box marked K, t (resp. J, s) indicates that the strands are tied along t-framed (resp. s-framed) parallel copies of the tangle $K \smallsetminus \{\mathrm{pt}\}$ (resp. $J \smallsetminus \{\mathrm{pt}\}$). (We give a more formal definition below.) If J is the unknot and $s = \pm 1$, then $D_{J,s}(K,t)$ is the t-twisted $\mp$ Whitehead double of K.

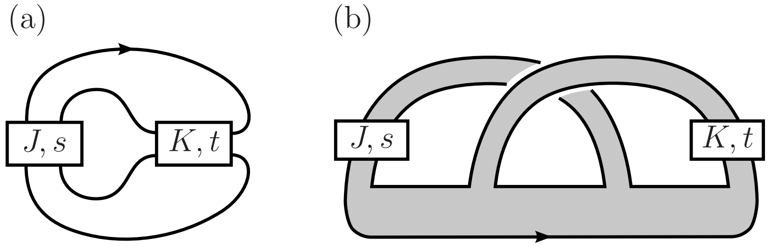

FIGURE 2. (a) The knot $D_{J,s}(K,t)$. (b) A genus-1 Seifert surface for $D_{J,s}(K,t)$.

A genus-1 Seifert surface for $D_{J,s}(K,t)$ is shown in Figure 2(b). From the Seifert form of this surface, we can compute that the Alexander polynomial of $D_{J,s}(K,t)$ is

$$\Delta_{D_{J,s}(K,t)}(T) = stT + (1 - 2st) + stT^{-1}.$$

In particular, this equals 1 whenever $s = 0$ or $t = 0$. By Freedman's theorem, $D_{J,s}(K,0)$ is therefore topologically slice. Moreover, if K is smoothly slice, then $D_{J,s}(K,0)$ is smoothly slice for any (J,s). To see this, perform a ribbon move to eliminate the band that is tied into J; the resulting two-component link, consisting of two parallel copies of K with linking number 0, is then the boundary of two parallel copies of a slice disk for K. The conjecture about untwisted Whitehead doubles described above has many potential generalizations in terms of $D_{J,s}(K,0)$ satellites, all equally difficult.

As a partial result in this direction, we prove the following theorem, which generalizes Hedden's result:

Theorem 1.1. *Let J and K be knots, and let $s,t \in \mathbb{Z}$. Then*

$$\tau(D_{J,s}(K,t)) = \begin{cases} 1 & s < 2\tau(J) \text{ and } t < 2\tau(K) \\ -1 & s > 2\tau(J) \text{ and } t > 2\tau(K) \\ 0 & \text{otherwise.} \end{cases}$$

In particular, if $\tau(K) > 0$ and $s < 2\tau(J)$, or if $\tau(K) < 0$ and $s > 2\tau(J)$, then $D_{J,s}(K,0)$ is topologically but not smoothly slice.

We now provide a more rigorous description of $D_{J,s}(K,t)$. Suppose L is a link in S^3, and γ is an oriented curve in $S^3 \smallsetminus L$ that is unknotted in S^3. For any knot $K \subset S^3$ and $t \in \mathbb{Z}$, we may form a new link $I_{\gamma,K,t}(L)$, the *t-twisted infection of L by K along γ*, by deleting a neighborhood of γ and gluing in a copy of the exterior of K by a map that takes a Seifert-framed longitude of K to a meridian of γ and a meridian of K to a t-framed longitude of γ. Since $S^3 \smallsetminus \gamma = S^1 \times D^2$, the resulting 3-manifold is simply ∞ surgery on K, i.e. S^3; the new link $I_{\gamma,K,t}(L)$ is defined as the image of L. Infecting along the boundary of a disk perpendicular to a group of strands formalizes the notion of "tying the strands into a knot." Moreover, given an unlink $\gamma_1, \dots, \gamma_n$ disjoint from L, we may infect simultaneously along all the γ_i; the result may be denoted $I_{\gamma_1,K_1,t_1;\cdots;\gamma_n,K_n,t_n}(L)$, and the order of the tuples (γ_i, K_i, t_i) does not matter.

Let $B = B_1 \cup B_2 \cup B_3$ denote the Borromean rings, oriented as shown in Figure 3. Then $D_{J,s}(K,t)$ is the knot obtained from B_3 by s-twisted infection by J along B_1

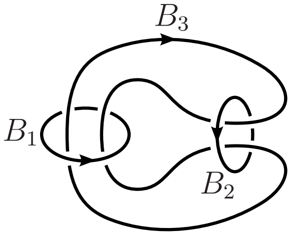

Figure 3. The Borromean rings.

and t-twisted infection by K along B_2:

$$D_{J,s}(K,t) = I_{B_1,J,s;\,B_2,K,t}(B_3).$$

The theory of *bordered Heegaard Floer homology*, developed recently by Lipshitz, Ozsváth, and Thurston [11, 10], is well-suited to the problem of computing Heegaard Floer invariants of knots obtained via infection. Briefly, it associates to a 3-manifold with boundary a module over an algebra associated to the boundary, so that if a 3-manifold Y is decomposed as $Y = Y_1 \cup_\phi Y_2$, where $\phi : \partial Y_1 \xrightarrow{\cong} \partial Y_2$, the chain complex $\widehat{\mathrm{CF}}(Y)$ may be computed as the derived tensor product of the invariants associated to Y_1 and Y_2. If a knot K is contained (nulhomologously) in, say, Y_1, then we may obtain the filtration on $\widehat{\mathrm{CF}}(Y)$ corresponding to K via a filtration on the algebraic invariant of Y_1. The theory also includes bimodules associated to manifolds with two boundary components.

In our setting, let Y denote the exterior of $B_1 \cup B_2$, and let X_J and X_K denote the exteriors of J and K, respectively. For suitable gluing maps $\phi_1 : \partial X_J \to \partial_1 Y$ and $\phi_2 : \partial X_K \to \partial_2 Y$ (where $\partial Y = \partial_1 Y \amalg \partial_2 Y$), the glued-up manifold $(Y \cup_{\phi_1} X_J) \cup_{\phi_2} X_K$ is S^3, and the image of $B_3 \subset Y$ is $D_{J,s}(K,t)$. We shall define suitable *bordered structures* $\mathcal{Y}$, $\mathcal{X}_J^s$, and $\mathcal{X}_K^t$ on Y, X_J, and X_K, respectively, so as to induce these gluing maps. By the *gluing theorem* of Lipshitz, Ozsváth, and Thurston, the filtered chain complex for $(S^3, D_{J,s}(K,t))$ can then computed as a special tensor product of the modules associated to $\mathcal{Y}$, $\mathcal{X}_J^s$, and $\mathcal{X}_K^t$:

$$\widehat{\mathrm{CF}}(S^3, D_{J,s}(K,t)) \simeq (\widehat{\mathrm{CFAA}}(\mathcal{Y}, B_3, 0) \boxtimes \widehat{\mathrm{CFD}}(\mathcal{X}_J^s)) \boxtimes \widehat{\mathrm{CFD}}(\mathcal{X}_K^t).$$

All of this terminology will be explained in Section 2. Using the formula for $\widehat{\mathrm{CFD}}(\mathcal{X}_J^s)$ and $\widehat{\mathrm{CFD}}(\mathcal{X}_K^t)$ proven by Lipshitz, Ozsváth, and Thurston [11] and a direct computation of $\widehat{\mathrm{CFAA}}(\mathcal{Y}, B_3, 0)$ using holomorphic disks (given in Section 3), we shall explicitly evaluate this double tensor product and compute its homology in Section 4, leading to the proof of Theorem 1.1. While the proof is fairly technical, it illustrates the power of the new bordered techniques: using a single computation involving holomorphic disks (which can in principle be performed entirely combinatorially) and some lengthy but straightforward algebra, we are able to obtain a statement about the Floer homology an infinite family of knots.

In Section 5, we present a few more results concerning knots of the form $D_{J,s}(K,t)$. Following the approach of Livingston and Naik [13], we show that if ν is any concordance invariant that shares certain formal properties with τ — e.g., Rasmussen's s invariant coming from Khovanov homology — then $\nu(D_{J,s}(K,t)) = \tau(D_{J,s}(K,t))$ when $|s|$ and $|t|$ are sufficiently large. We also provide a family of examples of knots of the form $D_{J,s}(K,t)$ that are smoothly slice, generalizing a result of Casson about Whitehead doubles.

Finally, Theorem 1.1 has a useful application to the study of Whitehead doubles of links, which was the author's original motivation for considering it. Specifically, we consider the Whitehead doubles of links obtained by *iterated Bing doubling*. Given a knot K, the *(untwisted) Bing double* of K is the satellite link $BD(K) = I_{B_1,K,0}(B_2 \cup B_3)$, as shown in Figure 1. More generally, given a link L, we may replace a component by its Bing double (contained in a tubular neighborhood of that component), and iterate this procedure. Bing doubling one component of the Hopf link yields the Borromean rings; accordingly, we define the family of *generalized Borromean links* as the set of all links obtained as iterated Bing doubles of the Hopf link. Using Theorem 1.1, the author proves in [9]:

Corollary 1.2. *Let L be any link obtained by iterated Bing doubling from either:*

1. *Any knot K with $\tau(K) > 0$, or*
2. *The Hopf link.*

Then the all-positive Whitehead double of L, $Wh_+(L)$, is not smoothly slice.

The links in (1) are boundary links, so their Whitehead doubles are all topologically slice by a result of Freedman [2]. On the other hand, it is not yet known whether the Whitehead doubles of iterated Bing doubles of the Hopf link are topologically slice; indeed, this question is one of the major unsolved problems in four-dimensional topological surgery theory. Once again, we see a strong dependence on chirality; our proof breaks down when claps of both signs are used. For further details, see [9].

Acknowledgements. This paper made up a large portion of the author's thesis at Columbia University. The author is grateful to his advisor, Peter Ozsváth, and the other members of his defense committee, Robert Lipshitz, Dylan Thurston, Paul Melvin, and Denis Auroux, for their suggestions, and to Rumen Zarev, Ina Petkova, Jen Hom, and Matthew Hedden for many helpful conversations about bordered Heegaard Floer homology. Additionally, he thanks the Mathematical Sciences Research Institute for hosting him in Spring 2010, when much of this research was conducted.

2. Background on bordered Heegaard Floer homology

In this section, we give a brief description of the bordered Heegaard Floer invariants, with the aim of defining the terms used later in the paper and illustrating the procedures for computation. We discuss only bordered manifolds with toroidal boundary components, which has the advantage of greatly simplifying some of the definitions. All of this material can be found in the two *magna opera* of Lipshitz, Ozsváth, and Thurston [11, 10].

2.1. **Algebraic objects.** We first recall the main algebraic constructions used in [11, 10], with the aim of describing how to work with them computationally. Let $(\mathcal{A}, d)$ be a unital differential algebra over $\mathbb{F} = \mathbb{F}_2$. (All of the definitions that follow can be stated in terms of differential graded algebras, but we suppress all grading information for brevity.) Let $\mathcal{I} \subset \mathcal{A}$ denote the subring of idempotents in $\mathcal{A}$, and assume that $\{\iota_i\}$ is an orthogonal basis for $\mathcal{I}$ over $\mathbb{F}$ with the property that $\sum_i \iota_i = \mathbf{1}$, the identity element of $\mathcal{A}$.

- A *(right)* $\mathcal{A}_\infty$ *algebra* or *type A structure* over $\mathcal{A}$ is an $\mathbb{F}$-vector space M, equipped with a right action of $\mathcal{I}$ such that $M = \bigoplus_i M\iota_i$ as a vector space, and multiplication maps

  $$m_{k+1} \colon M \underset{\mathcal{I}}{\otimes} \underbrace{\mathcal{A} \underset{\mathcal{I}}{\otimes} \dots \underset{\mathcal{I}}{\otimes} \mathcal{A}}_{k \text{ times}} \to M$$

  satisfying the $\mathcal{A}_\infty$ relations: for any $x \in M$ and $a_1, \dots, a_n \in \mathcal{A}$,

  $$\begin{aligned} 0 = &\sum_{i=0}^{n} m_{n-i+1}(m_{i+1}(x, a_1, \dots, a_i), a_{i+1}, \dots, a_n) \\ &+ \sum_{i=1}^{n} m_{n+1}(x, a_1, \dots, a_{i-1}, d(a_i), a_{i+1}, \dots, a_n) \\ &+ \sum_{i=1}^{n-1} m_n(x, a_1, \dots, a_{i-1}, a_i a_{i+1}, a_{i+2}, \dots, a_n). \end{aligned} \tag{2}$$

  We also require that $m_2(x, \mathbf{1}) = x$ and $m_k(x, \dots, \mathbf{1}, \dots) = 0$ for $k > 2$.

  The module M is called *bounded* if $m_k = 0$ for all k sufficiently large. If M is a bounded type A structure with basis $\{x_1, \dots, x_n\}$, we encode the multiplications using a matrix whose entries are formal sums of finite sequences of elements of $\mathcal{A}$, where having an $(a_1, \dots, a_k)$ term in the i, j^{th} entry means that the coefficient of x_j in $m_{k+1}(x_i, a_1, \dots, a_k)$ is nonzero. We write 1 rather than an empty sequence to signify the m_1 multiplication. For brevity, we frequently write $a_1 \cdots a_k$ rather than $(a_1, \dots, a_k)$; in this context, concatenation is *not* interpreted as multiplication in the algebra $\mathcal{A}$.
- A *(left) type D structure* over $\mathcal{A}$ is an $\mathbb{F}$-vector space N, equipped with a left action of $\mathcal{I}$ such that $N = \bigoplus_i \iota_i N$, and a map

  $$\delta_1 \colon N \to A \underset{\mathcal{I}}{\otimes} N$$

  satisfying the relation

  $$(\mu \otimes \mathrm{id}_N) \circ (\mathrm{id}_{\mathcal{A}} \otimes \delta_1) \circ \delta_1 + (d \otimes \mathrm{id}_N) \circ \delta_1 = 0, \tag{3}$$

  where $\mu \colon \mathcal{A} \otimes \mathcal{A} \to \mathcal{A}$ denotes the multiplication on $\mathcal{A}$.

  If N is a type D structure, the tensor product $\mathcal{A} \underset{\mathcal{I}}{\otimes} N$ is naturally a left differential module over $\mathcal{A}$, with module structure given by $a \cdot (b \otimes x) = ab \otimes x$, and differential $\partial(a \otimes x) = a \cdot \delta_1(x) + d(a) \otimes x$. Condition (3) translates to $\partial^2 = 0$.

Given a type-D module N, define maps

$$\delta_k\colon N \to \underbrace{\mathcal{A} \underset{\mathcal{I}}{\otimes} \dots \underset{\mathcal{I}}{\otimes} \mathcal{A}}_{k \text{ times}} \underset{\mathcal{I}}{\otimes} N$$

by $\delta_0 = \mathrm{id}_N$ and $\delta_k = (\mathrm{id}_{\mathcal{A}^{\otimes k-1}} \otimes \delta_1) \circ \delta_{k-1}$. We say N is *bounded* if $\delta_k = 0$ for all k sufficiently large.

Given a basis $\{y_1, \dots, y_n\}$ for N, we may encode δ_1 as an $n \times n$ matrix (b_{ij}) with entries in $\mathcal{A}$, such that $\delta_1 x_i = \sum_{j=1}^n b_{ij} \otimes x_j$. To encode δ_k in matrix form, we take the k^{th} power of the matrix for δ_1, except that instead of evaluating multiplication in $\mathcal{A}$, we simply concatenate tensor products of elements.

If $d = 0$, (3) is equivalent to the statement that the square of the matrix for δ_1 (where now we do evaluate multiplication in $\mathcal{A}$) is zero.

- If M is a right type A structure, N is a left type D structure, and at least one of them is bounded, we may form the *box tensor product* $M \boxtimes N$. As a vector space, this is $M \underset{\mathcal{I}}{\otimes} N$, with differential

$$\partial^{\boxtimes}(x \otimes y) = \sum_{k=0}^{\infty} (m_{k+1} \otimes \mathrm{id}_N)(x \otimes \delta_k(y)).$$

Given matrix representations of the multiplications on M and the δ_k maps on N, it is easy to write down the differential on $M \boxtimes N$ in terms of the basis $\{x_i \otimes y_j\}$.

- Now let $(\mathcal{A}, d_{\mathcal{A}})$ and $(\mathcal{B}, d_{\mathcal{B}})$ be differential algebras. Lipshitz, Ozsváth, and Thurston [10] define various types of $(\mathcal{A}, \mathcal{B})$-bimodules. We do not define these in full detail, but we mention some of the basic notions.

A *type DD structure* is simply a type D structure over the ring $\mathcal{A} \underset{\mathbb{F}}{\otimes} \mathcal{B}$. That is, the map δ_1 outputs terms of the form $a \otimes b \otimes x$, where $a \in \mathcal{A}$ and $b \in \mathcal{B}$.

A *type AA structure* consists of a vector space M with multiplications

$$m_{1,i,j}\colon M \otimes \mathcal{A}^{\otimes i} \otimes \mathcal{B}^{\otimes j} \to M,$$

satisfying a version of the $\mathcal{A}_\infty$ relation (2). As above, all tensor products are taken over the rings of idempotents, $\mathcal{I}_\rho \subset \mathcal{A}$ and $\mathcal{I}_\sigma \subset \mathcal{B}$. Our notation differs a bit from that of [10] in that we think of both algebras as acting on the right.

A *type DA structure* is a vector space N with maps

$$\delta_1^{1+j}\colon N \otimes \mathcal{B}^{\otimes j} \to \mathcal{A} \otimes N$$

satisfying an appropriate relation that combines (2) and (3). A *type AD structure* is defined similarly, except that the roles of $\mathcal{A}$ and $\mathcal{B}$ are interchanged.

The box tensor product of two bimodules, or of a module and a bimodule, can be defined assuming at least one of the factors is bounded (in an appropriate sense). See [10, Subsection 2.3.2] for details.

- A filtration on a type A structure M is a filtration $\dots \subseteq \mathcal{F}_p \subseteq \mathcal{F}_{p+1} \subseteq \dots$ of M as a vector space, such that $m_{k+1}(\mathcal{F}_p \otimes \mathcal{A}^{\otimes k}) \subseteq \mathcal{F}_p$ for any $a_1, \dots, a_k$. Similarly, a filtration on a type D structure N is a filtration of N such that $\delta_1(\mathcal{F}_p) \subseteq \mathcal{A} \otimes \mathcal{F}_p$. It is easy to extend these definitions to the various types of bimodules. A filtration on M or N naturally induces a filtration on $M \boxtimes N$.

2.2. **The torus algebra.** The *pointed matched circle for the torus*, $\mathcal{Z}$, consists of an oriented circle Z, equipped with a basepoint $z \in Z$, a tuple $\mathbf{a} = (a_1, a_2, a_3, a_4)$ of points in $Z \smallsetminus \{z\}$ (ordered according to the orientation on $Z \smallsetminus \{z\}$), and the equivalence relation $a_1 \sim a_3$, $a_2 \sim a_4$. The genus-1, one-boundary-component surface $F^\circ(\mathcal{Z})$ is obtained by identifying Z with the boundary of a disk D and attaching 1-handles h_1 and h_2 that connect a_1 to a_3 and a_2 to a_4, respectively. By attaching a 2-handle along $\partial F^\circ(\mathcal{Z})$, we obtain the closed surface $F(\mathcal{Z})$. There is an orientation-reversing involution $r\colon Z \to Z$ that fixes z, interchanges a_1 and a_4, and interchanges a_2 and a_3, which extends to a diffeomorphism $r\colon F(\mathcal{Z}) \to -F(\mathcal{Z})$ that interchanges h_1 and h_2.

The algebra $\mathcal{A} = \mathcal{A}(\mathcal{Z}, 0)$ is generated as a vector space over $\mathbb{F}$ by two *idempotents* ι_0, ι_1 and six *Reeb elements* $\rho_1, \rho_2, \rho_3, \rho_{12}, \rho_{23}, \rho_{123}$. For each sequence of consecutive integers $I = (i_1, \dots, i_k) \subset \{1, 2, 3\}$, we have $\iota_{[i_1-1]}\rho_I = \rho_I \iota_{[i_k]} = \rho_I$, where $[j]$ denotes the residue of j modulo 2. The nonzero multiplications among the Reeb elements are: $\rho_1\rho_2 = \rho_{12}$, $\rho_2\rho_3 = \rho_{23}$, $\rho_1\rho_{23} = \rho_{12}\rho_3 = \rho_{123}$. All other products are zero, as is the differential. Let $\mathcal{I}$ denote the subring of idempotents of $\mathcal{A}$; it is generated as a vector space by ι_0 and ι_1. The identity element is $\mathbf{1} = \iota_0 + \iota_1$.

By abuse of notation, we identify ρ_1 with the oriented arc of Z from a_1 to a_2, ρ_2 with the arc from a_2 to a_3, ρ_3 with the arc from a_3 to a_4, and ρ_{12}, ρ_{23}, and ρ_{123} with the appropriate concatenations.

2.3. **Bordered 3-manifolds and their invariants.** A *bordered* 3*-manifold with boundary* $F(\mathcal{Z})$ consists of the data $\mathcal{Y} = (Y, \Delta, z', \phi)$, where Y is an oriented 3-manifold with a single boundary component, Δ is a disk in ∂Y, $z' \in \partial\Delta$, and $\phi : F(\mathcal{Z}) \to \partial(Y)$ is a diffeomorphism taking D to Δ and z to z'. The map ϕ is specified (up to isotopy fixing Δ pointwise) by the images of the core arcs of the two one-handles in $F^\circ(\mathcal{Z})$. We may analogously define a *bordered* 3*-manifold with boundary* $-F(\mathcal{Z})$. The diffeomorphism $r\colon F(\mathcal{Z}) \to -F(\mathcal{Z})$ provides a one-to-one correspondence between these two types of bordered manifolds.

A bordered 3-manifold $\mathcal{Y}$ may be presented by a bordered Heegaard diagram

$$\mathcal{H} = (\Sigma, \{\alpha_1^c, \dots, \alpha_{g-1}^c, \alpha_1^a, \alpha_2^a\}, \{\beta_1, \dots, \beta_g\}, z),$$

where Σ is a surface of genus g with one boundary components, $\{\alpha_1^c, \dots, \alpha_{g-1}^c\}$ and $\{\beta_1, \dots, \beta_g\}$ are tuples of homologically linearly independent, disjoint circles in Σ, and α_1^a and α_2^a are properly embedded arcs that are disjoint from the α circles and linearly independent from them in $H_1(\Sigma, \partial\Sigma)$. If we identify $(\partial\Sigma, z, \partial\Sigma \cap (\alpha_1^a \cup \alpha_2^a))$ with $\mathcal{Z}$ — where $\partial\Sigma$ is given the boundary orientation — we obtain a bordered 3-manifold with boundary parametrized by $F(\mathcal{Z})$ by attaching handles along the α and

β circles. If instead we identify $\partial\Sigma$ with $-\mathcal{Z}$, we obtain a bordered 3-manifold with boundary parametrized by $-F(\mathcal{Z})$.

Let $\mathfrak{S}(\mathcal{H})$ denote the set of unordered g-tuples of points $\mathbf{x} = \{x_1, \dots, x_g\}$ such that each α circle and each β circle contains exactly one point of $\mathbf{x}$ and each α arc contains at most one point of $\mathbf{x}$. Let $X(\mathcal{H})$ denote the $\mathbb{F}_2$-vector space spanned by $\mathfrak{S}(H)$.

For generators $\mathbf{x}, \mathbf{y} \in \mathfrak{S}(\mathcal{H})$, let $\pi_2(\mathbf{x}, \mathbf{y})$ denote the set of homology classes of maps $u\colon S \to \Sigma \times [0,1] \times [-2,2]$, where S is a surface with boundary, taking ∂S to

$$\begin{aligned}((\boldsymbol{\alpha} \times \{1\} \cup \boldsymbol{\beta} \times \{2\} \cup (\partial\Sigma \smallsetminus z) \times [0,1]) \times [-2,2]) \cup \\ (\mathbf{x} \times [0,1] \times \{-2\}) \cup (\mathbf{y} \times [0,1] \times \{2\})\end{aligned}$$

and mapping to the relative fundamental homology class of $(\mathbf{x} \times [0,1] \times \{-2\}) \cup (\mathbf{y} \times [0,1] \times \{2\})$. Each element $B \in \pi_2(\mathbf{x}, \mathbf{y})$ is determined by its *domain*, the projection of B to $H_2(\Sigma, \boldsymbol{\alpha} \cup \boldsymbol{\beta} \cup \partial\Sigma; \mathbb{Z})$. The group $H_2(\Sigma, \boldsymbol{\alpha} \cup \boldsymbol{\beta} \cup \partial\Sigma; \mathbb{Z})$ is freely generated by the closures of the components of $\Sigma \smallsetminus (\boldsymbol{\alpha} \cup \boldsymbol{\beta})$, which we call *regions.* The domain of any $B \in \pi_2(\mathbf{x}, \mathbf{y})$ satisfies the following conditions:

- The multiplicity of the region containing the basepoint z is 0.[1]
- For each point $p \in \boldsymbol{\alpha} \cap \boldsymbol{\beta}$, if we identify an oriented neighborhood of p with $\mathbb{R}^2$, taking p to the origin and the α and β segments containing p to the x- and y-axes, respectively, and let $n_1(p)$, $n_2(p)$, $n_3(p)$, and $n_4(p)$ denote the multiplicities in D of the regions in the four quadrants, then

$$n_1(p) - n_2(p) + n_3(p) - n_4(p) = \begin{cases} 1 & p \in \mathbf{x} \smallsetminus \mathbf{y} \\ -1 & p \in \mathbf{y} \smallsetminus \mathbf{x} \\ 0 & \text{otherwise.} \end{cases} \tag{4}$$

Thus, finding the elements of $\pi_2(\mathbf{x}, \mathbf{y})$ is a simple matter of linear algebra. A homology class $B \in \pi_2(\mathbf{x}, \mathbf{y})$ is called *positive* if the regions in its domain all have non-negative multiplicity; only positive classes can support holomorphic representatives.

We shall describe only the invariant $\widehat{\mathrm{CFD}}$ here, since we do not compute $\widehat{\mathrm{CFA}}$ explicitly from a Heegaard diagram in this paper.

We identify the boundary of Σ with $-\mathcal{Z}$. Assume that the α arcs are labeled so that $\alpha_1^a \cap \partial\Sigma = \{a_1, a_3\}$ and $\alpha_2^a \cap \partial\Sigma = \{a_2, a_4\}$.

Define a function $I_D\colon \mathfrak{S}(\mathcal{H}) \to \{\iota_0, \iota_1\}$ by

$$I_D(\mathbf{x}) = \begin{cases} \iota_0 & \mathbf{x} \cap \alpha_2^a \neq \varnothing \\ \iota_1 & \mathbf{x} \cap \alpha_1^a \neq \varnothing. \end{cases} \tag{5}$$

Define a left action of $\mathcal{I}$ on $X(\mathcal{H})$ by $\iota_i \cdot \mathbf{x} = \delta(\iota_i, I_D(\mathbf{x}))\mathbf{x}$, where δ is the Kronecker delta.

For each of the oriented arcs $\rho_I \subset \mathcal{Z}$, let $-\rho_I$ denote ρ_I with its opposite orientation. (That is, $-\rho_1$ goes from a_2 to a_1, etc.) Given $\mathbf{x} \in \mathfrak{S}(\mathcal{H})$ and a sequence

---

[1] In classical Heegaard Floer homology, the definition of $\pi_2(\mathbf{x}, \mathbf{y})$ does not include this requirement.

$\vec{\rho} = (-\rho_{I_1}, \dots, -\rho_{I_k})$, the pair $(\mathbf{x}, \vec{\rho})$ is called *strongly boundary monotonic* if the initial point of $-\rho_{I_1}$ is on the same α circle as $\mathbf{x}$, and for each $i > 1$, the initial point of $-\rho_{I_i}$ and the final point of $-\rho_{I_{i-1}}$ are paired in $\mathbb{Z}$.

If $B \in \pi_2(\mathbf{x}, \mathbf{y})$ is a positive class, then $\partial^\partial B$ (the intersection of the domain of B with the boundary of Σ) may be expressed (non-uniquely) as a sum of arcs $-\rho_{I_i}$. Specifically, we say that the pair $(B, \vec{\rho})$ is *compatible* if $(\mathbf{x}, \vec{\rho})$ is strongly boundary monotonic and $\partial^\partial B = \sum_{i=1}^k (-\rho_{I_i})$. If $(B, \vec{\rho})$ is compatible, the *index* of $(B, \vec{\rho})$ is defined in [11, Definition 5.46] as

$$\operatorname{ind}(B, \vec{\rho}) = e(B) + n_{\mathbf{x}}(B) + n_{\mathbf{y}}(B) + |\vec{\rho}| + \iota(\vec{\rho}), \tag{6}$$

where $e(B)$ is the Euler measure of B; $n_{\mathbf{x}}(B)$ (resp. $n_{\mathbf{y}}(B)$) is the sum over points $x_i \in \mathbf{x}$ (resp. $y_i \in \mathbf{y}$) of the average of the multiplicities of the regions incident to x_i (resp. y_i), $|\vec{\rho}|$ is the number of entries in $\vec{\rho}$, and $\iota(\vec{\rho})$ is a combinatorially defined quantity [11, Equation 5.44] that measures the overlapping of the arcs ρ_{I_i}. The index $\operatorname{ind}(B, \vec{\rho})$ is equal to one plus the expected dimension of a certain moduli space $\mathcal{M}^B(\mathbf{x}, \mathbf{y}, \vec{\rho})$ of J-holomorphic curves in $\Sigma \times [0,1] \times \mathbb{R}$ in the homology class B whose asymptotics near $\partial\Sigma \times [0,1] \times \mathbb{R}$ are specified by $\vec{\rho}$. In particular, if $\operatorname{ind}(B, \vec{\rho}) = 1$, then this moduli space contains finitely many points. We do not give the full definition here; see [11, Section 5] for the details.

For each $\mathbf{x}, \mathbf{y} \in \mathfrak{S}(\mathbf{x})$ and $B \in \pi_2(\mathbf{x}, \mathbf{y})$, define

$$a^B_{\mathbf{x},\mathbf{y}} = \sum_{\substack{\{\vec{\rho} = (-\rho_{I_1}, \dots, -\rho_{I_k}) \mid \\ (B, \vec{\rho}) \text{ compatible}, \\ \operatorname{ind}(B, \vec{\rho}) = 1\}}} \#(\mathcal{M}^B(\mathbf{x}, \mathbf{y}, \vec{\rho}))\, \rho_{I_1} \dots \rho_{I_k} \in \mathcal{A},$$

where the count of points in $\mathcal{M}^B(\mathbf{x}, \mathbf{y}, \vec{\rho})$ is taken modulo 2. We define $\delta_1 \colon X(\mathcal{H}) \to \mathcal{A} \underset{\mathcal{I}}{\otimes} X(\mathcal{H})$ by

$$\delta_1(\mathbf{x}) = \sum_{\mathbf{y} \in \mathfrak{S}(\mathcal{H})} \sum_{B \in \pi_2(\mathbf{x}, \mathbf{y})} a^B_{\mathbf{x},\mathbf{y}} \otimes \mathbf{y}. \tag{7}$$

This defines a type D structure, which we denote $\widehat{\mathrm{CFD}}(\mathcal{H})$. The verification of (3) is a version of the standard $\partial^2 = 0$ argument in Floer theory.

Proposition 2.1.

1. *The only sequences of chords that can contribute nonzero terms to* δ_1 *are the empty sequence,* $(-\rho_1)$, $(-\rho_2)$, $(-\rho_3)$, $(-\rho_1, -\rho_2)$, $(-\rho_2, -\rho_3)$, $(-\rho_{123})$, *and* $(-\rho_1, -\rho_2, -\rho_3)$. *Therefore, only classes whose multiplicities in the boundary regions of* Σ *are* 0 *or* 1 *can count for* δ_1.
2. *If* $B \in \pi_2(\mathbf{x}, \mathbf{y})$ *is a positive class whose domain has multiplicity* 1 *in the regions abutting* ρ_1 *and* ρ_2 *(resp.* ρ_2 *and* ρ_3*) and* 0 *in the region abutting* ρ_3 *(resp.* ρ_1*), then* B *may count for the differential only if* $\mathbf{x}$ *and* $\mathbf{y}$ *contain points of* α^a_1 *(resp.* α^a_2*).*

Proof. For the first statement, the only other sequences of chords for which the product of algebra elements in the definition of $a^B_{\mathbf{x},\mathbf{y}}$ is nonzero are $(-\rho_{12})$, $(-\rho_{23})$,

$(-\rho_1, -\rho_{23})$, and $(-\rho_{12}, -\rho_3)$. The two latter sequences are not strongly boundary monotonic. If $B \in \pi_2(\mathbf{x}, \mathbf{y})$ is a positive class compatible with $(-\rho_{12})$, then $\mathbf{x}$ and $\mathbf{y}$ both contain points on α_1^a, since otherwise B would have a boundary component without a β segment. Therefore, $I_D(\mathbf{y}) = \iota_1$. Since the tensor product is taken over the ring of idempotents,

$$\rho_{12} \otimes \mathbf{y} = \rho_{12} \otimes \iota_1 \mathbf{y} = \rho_{12}\iota_1 \otimes \mathbf{y} = 0,$$

so the contribution of B to $\delta_1(\mathbf{x})$ is zero. A similar argument applies for the sequence $(-\rho_{23})$. The second statement follows immediately from the same argument. □

The invariant $\widehat{\mathrm{CFA}}$ is a type A structure associated to a bordered Heegaard diagram whose boundary is identified with $\mathcal{Z}$. We do not give all the details here. The analogue of Proposition 2.1 does not hold for $\widehat{\mathrm{CFA}}$; one must consider domains with arbitrary multiplicities on the boundary and a much larger family of sequences of chords. Therefore, it is generally easier to compute $\widehat{\mathrm{CFD}}$.

We conclude this section with the *gluing theorem*:

Theorem 2.2 (Lipshitz-Ozsváth-Thurston [11]). *Suppose $\mathcal{Y}_1$ and $\mathcal{Y}_2$ are bordered 3-manifolds, and $Y = Y_1 \cup_\phi Y_2$ is the manifold obtained by gluing them together along their boundaries, where $\phi\colon -\partial Y_1 \to \partial Y_2$ is the map induced by the bordered structures. Then*

$$\widehat{\mathrm{CF}}(Y) \simeq \widehat{\mathrm{CFA}}(\mathcal{Y}_1) \boxtimes \widehat{\mathrm{CFD}}(\mathcal{Y}_2),$$

provided that at least one of the modules is bounded (so that the box tensor product is defined).

2.4. **Bimodules.** In [10], Lipshitz, Ozsváth, and Thurston also define invariants for a *bordered manifold with two boundary components*. Essentially, this consists of a manifold Y with two torus boundary components $\partial_L Y$ and $\partial_R Y$, with parametrizations of the two boundary components just like in the single-component case, and a framed arc connecting the two boundary components. (See [10, Chapter 5] for the full definition.)

If both boundary components are parametrized by $-F(\mathcal{Z})$, the associated invariant is a type DD structure over two copies of $\mathcal{A}$, denoted $\widehat{\mathrm{CFDD}}(\mathcal{Y})$; if both are parametrized by $F(\mathcal{Z})$, the invariant is a type AA structure, denoted $\widehat{\mathrm{CFAA}}(\mathcal{Y})$; and similarly there are invariants $\widehat{\mathrm{CFAD}}(\mathcal{Y})$ and $\widehat{\mathrm{CFDA}}(\mathcal{Y})$. We denote the two copies of $\mathcal{A}$ by $\mathcal{A}_\rho$ and $\mathcal{A}_\sigma$; in the latter, the Reeb elements are written σ_1, σ_2, etc.

In fact, we consider only a direct summand of each bimodule, denoted $\widehat{\mathrm{CFDD}}(\mathcal{Y}, 0)$, $\widehat{\mathrm{CFAA}}(\mathcal{Y}, 0)$, etc., which is all that is necessary to compute the Floer complex of a manifold obtained by gluing two separate one-boundary-component manifolds to the two boundary components of Y. The other summands are only necessary if one wishes to glue together the two boundary components of Y.

As in the previous discussion, we describe only the construction of $\widehat{\mathrm{CFDD}}$. A bordered manifold with two toroidal boundary components may be presented by an *arced bordered Heegaard diagram*

$$\mathcal{H} = (\Sigma, \{\alpha_1^c, \dots, \alpha_{g-2}^c, \alpha_1^L, \alpha_2^L, \alpha_1^R, \alpha_2^R\}, \{\beta_1, \dots, \beta_g\}, \mathbf{z}),$$

where now $\partial\Sigma$ has two components $\partial_L\Sigma$ and $\partial_R\Sigma$, on which the arcs α_i^L and α_i^R have their respective boundaries, and $\mathbf{z}$ is an arc in the complement of all the α and β circles and α arcs connecting the two boundary components.

We define $\mathfrak{S}(\mathcal{H})$ and $X(\mathcal{H})$ just in the single-boundary-component case. Let $\mathfrak{S}(\mathcal{H}, 0)$ be the subset of $\mathfrak{S}(\mathcal{H})$ consisting of g-tuples $\mathbf{x}$ containing one point in $\alpha_1^L \cup \alpha_2^L$ and one point in $\alpha_1^R \cup \alpha_2^R$, and let $X(\mathcal{H}, 0)$ be the $\mathbb{F}$-vector space generated by $\mathfrak{S}(\mathcal{H}, 0)$. This is the underlying vector space for the invariants $\widehat{\mathrm{CFDD}}(\mathcal{H}, 0)$, $\widehat{\mathrm{CFAA}}(\mathcal{H}, 0)$, etc.

To define $\widehat{\mathrm{CFDD}}(\mathcal{H}, 0)$, identify both boundary components of Σ with $-\mathcal{Z}$. Each generator of $\widehat{\mathrm{CFDD}}(\mathcal{H}, 0)$ has associated idempotents in $\mathcal{A}_\rho$ and $\mathcal{A}_\sigma$, as in (5). The differential

$$\delta_1 \colon X(\mathcal{H}, 0) \to (\mathcal{A}_\rho \otimes \mathcal{A}_\sigma) \underset{\mathcal{I}_\rho \otimes \mathcal{I}_\sigma}{\otimes} X(\mathcal{H}, 0)$$

is then defined essentially the same way as with $\widehat{\mathrm{CFD}}$ of a single-boundary-component diagram. Specifically, for a homology class $B \in \pi_2(\mathbf{x}, \mathbf{y})$ and sequences of chords $\vec{\rho} = (-\rho_{I_1}, \dots, -\rho_{I_k})$ and $\vec{\sigma} = (-\sigma_{J_1}, \dots, -\sigma_{J_l})$ on the two boundary components, the definitions of compatibility and of the index $\mathrm{ind}(B, \vec{\rho}, \vec{\sigma})$ are as above. Define

$$a_{\mathbf{x},\mathbf{y}}^B = \sum_{\substack{\{(\vec{\rho},\vec{\sigma}) \mid \\ (B,\vec{\rho},\vec{\sigma}) \text{ compatible}, \\ \mathrm{ind}(B,\vec{\rho},\vec{\sigma})=1\}}} \#(\mathcal{M}^B(\mathbf{x}, \mathbf{y}, \vec{\rho}, \vec{\sigma}))\, \rho_{I_1} \dots \rho_{I_k} \otimes \sigma_{J_1} \dots \sigma_{J_l} \in \mathcal{A}_\rho \otimes \mathcal{A}_\sigma.$$

The map δ_1 is then given by (7) just as above. An analogue of Proposition 2.1 also holds in this setting. For further details, see [10, Section 6].

The gluing theorem generalizes naturally to bimodules. For instance, if Y_1 has a single boundary component parametrized by $F(\mathcal{Z})$, Y_2 has two boundary components parametrized by $-F(\mathcal{Z})$, and $\phi\colon -\partial Y_1 \to \partial_L Y_2$ is the map induced by the parametrizations, then

$$\widehat{\mathrm{CFD}}(\mathcal{Y}_1 \cup_\phi \mathcal{Y}_2) \simeq \widehat{\mathrm{CFA}}(\mathcal{Y}_1) \underset{\mathcal{A}_\rho}{\boxtimes} \widehat{\mathrm{CFDD}}(\mathcal{Y}_2, 0).$$

The remaining generalizations are found in [10, Theorems 11, 12].

Finally, we mention the *identity AA bimodule* [10, Subsection 10.1]. Consider the manifold $\mathbb{I} = F(\mathcal{Z}) \times I$. Parametrize $\partial_R Y = F(\mathcal{Z}) \times \{1\}$ by inclusion and $\partial_L Y = F(\mathcal{Z}) \times \{0\}$ (whose boundary-induced orientation is opposite to the standard orientation of $F(\mathcal{Z})$) by the composition $F(\mathcal{Z}) \xrightarrow{r} -F(\mathcal{Z}) \hookrightarrow F(\mathcal{Z}) \times \{0\}$; thus, both boundary components are parametrized by $F(\mathcal{Z})$ as opposed to $-F(\mathcal{Z})$. The bijection between bordered manifolds with boundary $-F(\mathcal{Z})$ and bordered manifolds with boundary $F(\mathcal{Z})$ may be given by $Y \mapsto Y \cup \mathcal{I}$. Thus, if $\mathcal{H}$ is any bordered Heegaard diagram with one boundary component, then the type A module $\widehat{\mathrm{CFA}}(\mathcal{H})$ (where we identify $\partial\Sigma$ with $\mathcal{Z}$) is chain homotopy equivalent to $\widehat{\mathrm{CFAA}}(\mathbb{I}, 0) \boxtimes \widehat{\mathrm{CFD}}(\mathcal{H})$ (where, in the second factor, we identify $\partial\Sigma$ with $-\mathcal{Z}$). As mentioned above, it is

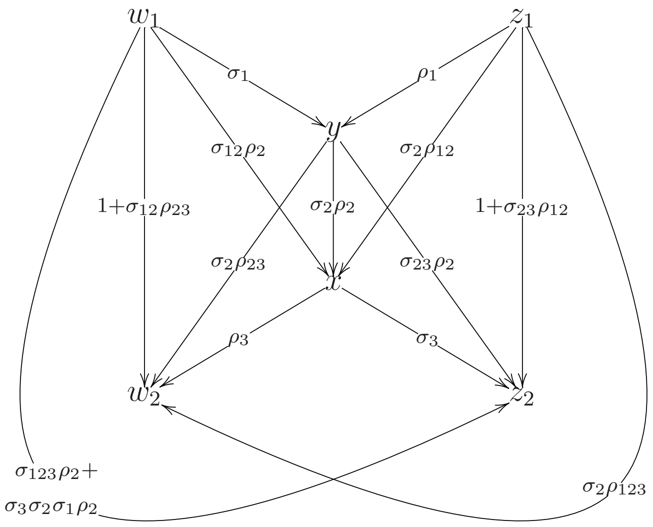

FIGURE 4. The identity AA bimodule, $\widehat{\mathrm{CFAA}}(\mathcal{I}, 0)$.

easier to compute $\widehat{\mathrm{CFD}}$ explicitly from a Heegaard diagram than $\widehat{\mathrm{CFA}}$; by taking a tensor product with $\widehat{\mathrm{CFAA}}(\mathbb{I}, 0)$, we can always avoid the latter.

Theorem 2.3 (Lipshitz-Ozsváth-Thurston)**.** *The type AA module* $\widehat{\mathrm{CFAA}}(\mathbb{I}, 0)$ *has generators* w_1, w_2, x, y, z_1, z_2*, with* $\mathcal{A}_\infty$ *multiplications as illustrated in Figure 4.*

2.5. **Knots in bordered manifolds.** A *doubly-pointed bordered Heegaard diagram* consists of a bordered Heegaard diagram $\mathcal{H} = (\Sigma, \boldsymbol{\alpha}, \boldsymbol{\beta}, z)$ along with an additional basepoint $w \in \Sigma \smallsetminus (\boldsymbol{\alpha} \cup \boldsymbol{\beta})$. As explained in [11, Section 10.4], a doubly-pointed diagram determines a knot $K \subset Y$ with a single point of K meeting the basepoint on ∂Y, invariant up to isotopy fixing this point under Heegaard moves missing w. Lipshitz, Ozsváth, and Thurston define invariants $\mathrm{CFD}^-(Y, K)$ and $\mathrm{CFA}^-(Y, K)$ by working over the algebra $\mathcal{A} \otimes \mathbb{F}[U]$, where the U powers record the multiplicity of w in each domain that counts for the differential or multiplications.

If the knot K is nulhomologous in Y, we prefer the following alternate perspective. Let F be a Seifert surface for K. Just as in ordinary knot Floer homology [15, 19], each generator $\mathbf{x} \in \mathfrak{S}(\mathcal{H})$ has an associated relative spin^c structure $\mathfrak{s}_{z,w}(\mathbf{x}) \in \mathrm{Spin}^c(Y, K)$, and we may define an *Alexander grading* on $\mathfrak{S}(\mathcal{H})$ by

$$A(x) = \frac{1}{2} \left\langle c_1(\mathfrak{s}_{z,w}(\mathbf{x})), [F] \right\rangle, \tag{8}$$

where $c_1(\mathfrak{s}_{z,w}(\mathbf{x})) \in H^2(Y, K)$ and $[F] \in H_2(Y, K)$. The grading difference between two generators is given by

$$A(x) - A(y) = n_w(B) \tag{9}$$

where $B \in \pi_2(\mathbf{x}, \mathbf{y})$ is any domain from $\mathbf{x}$ to $\mathbf{y}$. To verify that the right-hand side of (9) is well-defined, note that for any periodic class $P \in \pi_2(\mathbf{x}, \mathbf{x})$, $n_w(P)$ equals the intersection number of K with the homology class in $H_2(Y, \partial Y)$ corresponding to P, which must be zero since K is nulhomologous. Further details are completely analogous to [15, 19].

The Alexander grading on $X(\mathcal{H})$ determines a filtration on $\widehat{\mathrm{CFA}}(\mathcal{H})$ or $\widehat{\mathrm{CFD}}(\mathcal{H})$, since any domain that counts for the differential or $\mathcal{A}_\infty$ multiplications has nonnegative multiplicity at w. We denote the filtered chain homotopy type by $\widehat{\mathrm{CFA}}(\mathcal{Y}, K)$ or $\widehat{\mathrm{CFD}}(\mathcal{Y}, K)$.

When we evaluate a tensor product $\widehat{\mathrm{CFA}}(\mathcal{Y}_1) \boxtimes \widehat{\mathrm{CFD}}(\mathcal{Y}_2)$, a knot filtration on one factor extends naturally to a filtration on the whole complex, which agrees with the filtration that the knot induces on $\widehat{\mathrm{CF}}(Y_1 \cup Y_2)$.

A nulhomologous knot in a bordered manifold with two boundary components may be handled similarly. For invariance, one point of the knot must be constrained to lie on the arc connecting the two boundary components, and isotopies must be fixed in a neighborhood of that point.

2.6. **The edge reduction algorithm.** We now describe the well-known "edge reduction" procedure for chain complexes and its extension to $\mathcal{A}_\infty$ modules.

Suppose (C, ∂) is a free chain complex with basis $\{x_1, \dots, x_n\}$ over a ring R. For each i, j, let a_{ij} be the coefficient of x_j in ∂x_i with respect to this basis. If some a_{ij} is invertible in R, define a new basis $\{y_1, \dots, y_n\}$ by setting $y_i = x_i$, $y_j = \partial x_i$, and for each $k \neq i, j$, $y_k = x_k - a_{kj} a_{ij}^{-1} x_i$, where a_{kj} is the coefficient of x_j in ∂x_k. With respect to the new basis, the coefficient of y_j in ∂y_k is zero, so the subspace spanned by y_i and y_j is a direct summand subcomplex with trivial homology. Thus, C is chain homotopy equivalent to the subcomplex C' spanned by $\{y_k \mid k \neq i, j\}$, in which the coefficient of y_l in ∂y_k is $a_{kl} - a_{kj} a_{ij}^{-1} a_{il}$.

When $R = \mathbb{F}_2$, a convenient way to represent a chain complex (C, ∂) with basis $\{x_i\}$ is a directed graph $\Gamma_{C, \partial, \{x_i\}}$ with vertices corresponding to basis elements and an edge from x_i to x_j whenever $a_{ij} = 1$. To obtain $\Gamma_{C', \partial, \{y_k\}}$ from $\Gamma_{C, \partial, \{x_i\}}$ as above, we delete the vertices x_i and x_j and any edges going into or out of them. For each k and l with edges $x_k \to x_j$ and $x_i \to x_l$, we either add an edge from x_k to x_l (if there was not one previously) or eliminate the edge from x_k to x_l (if there was one). We call this procedure *canceling the edge from x_i to x_j*. The vertices of the resulting graph should be labeled with $\{y_k \mid k \neq i, j\}$, but by abuse of notation we frequently continue to refer to them with $\{x_k \mid k \neq i, j\}$ instead.

By iterating this procedure until no more edges remain, we compute the homology of C. If the matrix (a_{ij}) is sparse, this tends to be a very efficient algorithm for computing homology. If C is a graded complex and the basis $\{x_1, \dots, x_n\}$ consists of homogeneous elements, then y_k is clearly homogeneous with the same grading as x_k, so we can compute the homology as a graded group.

If C has a filtration $\cdots \subseteq F_p \subseteq F_{p+1} \subseteq \cdots$, the *filtration level* of an element of C is the unique p for which that element is in $F_p \smallsetminus F_{p-1}$. To compute the spectral sequence associated to the filtration, we cancel edges in increasing order of the amount by which they decrease filtration level. At each stage, this guarantees that the filtration level of y_k equals that of x_k. The complex that remains after we delete all edges that decrease filtration level by k is the E^{k+1} page in the spectral sequence, and the vertices that remain after all edges are deleted is the E^∞ page. In particular, when $C = \widehat{\mathrm{CF}}(S^3, K)$, the filtered complex associated to a knot $K \subset S^3$, the total homology of C is $\widehat{\mathrm{HF}}(S^3; \mathbb{F}) \cong \mathbb{F}$, so a unique vertex survives after all cancellations are complete. The filtration level of this vertex is, by definition, the invariant $\tau(K)$.

More generally, over an arbitrary ring R, we may represent (C, ∂) by a labeled, directed graph, where now we label an edge from x_i to x_j by a_{ij}, often omitting the label when $a_{ij} = 1$. When we cancel an unlabeled edge from x_i to x_j, we replace a zigzag

$$x_k \xrightarrow{a_{kj}} x_j \longleftarrow x_i \xrightarrow{a_{il}} x_l$$

with an edge

$$x_k \xrightarrow{-a_{kl}a_{il}} x_l$$

if no such edge existed previously, and either relabel or delete such an edge if it did exist. Of course, when R is not a field, this procedure is not guaranteed to eliminate all edges or to yield a result that is independent of the choice of the order in which the edges are deleted, but it is still often a useful way to simplify a chain complex.

The same procedure works for type D structures over the torus algebra $\mathcal{A}$, as can be seen by looking at the ordinary differential module obtained by taking the tensor product with $\mathcal{A}$ as above.

Edge cancellation for type A structures is slightly more complicated. We work only with bounded modules for simplicity. Suppose M is a bounded type A structure over $\mathcal{A}$ with a basis $\{x_1, \dots, x_n\}$. As above, we may describe the multiplications using a matrix of formal sums of finite sequences of elements of $\mathcal{A}$, and we may represent the nonzero entries using a labeled graph. If there is an unmarked edge from x_i to x_j (and no other edge), then we may cancel x_i and x_j, replacing a zigzag

$$x_k \xrightarrow{(a_1,\dots,a_p)} x_j \longleftarrow x_i \xrightarrow{(b_1,\dots,b_q)} x_l$$

by an edge

$$x_k \xrightarrow{(a_1,\dots,a_p,b_1,\dots,b_q)} x_l$$

(or eliminating such an edge if one already exists). The $\mathcal{A}_\infty$ module M' described by the resulting graph is then $\mathcal{A}_\infty$ chain homotopic to M. If M is a filtered $\mathcal{A}_\infty$-module and the edge being canceled is filtration-preserving (i.e., x_i and x_j have the same filtration level), then M' is filtered $\mathcal{A}_\infty$ chain homotopic to M. Similar techniques may also be used for bimodules.

The author has written a *Mathematica* package that implements these procedures for modules over the torus algebra, as well as the box tensor product. This package is available online at `http://www.math.columbia.edu/~topology/programs.html`.

2.7. $\widehat{\mathrm{CFD}}$ **of knot complements.** For any knot K, let X_K denote the exterior of K. For $t \in \mathbb{Z}$, let $\mathcal{X}_K^t$ denote the bordered structure on X_K determined by a map $\phi : -F(\mathcal{Z}) \to \partial X_K$ sending h_1 to a t-framed longitude (relative to the Seifert framing) and h_2 to a meridian of K. Lipshitz, Ozsváth, and Thurston [11] give a complete computation of $\widehat{\mathrm{CFD}}(\mathcal{X}_K^t)$ in terms of the knot Floer complex of K, which we now describe.

In the computation that follows, we will need to work with two different framed knot complements, $\mathcal{X}_J^s$ and $\mathcal{X}_K^t$. We first state the results for $\widehat{\mathrm{CFD}}(\mathcal{X}_J^s)$ and then indicate how to modify the notation for $\widehat{\mathrm{CFD}}(\mathcal{X}_K^t)$. Define $r = |2\tau(J) - s|$, and say that $\dim \widehat{\mathrm{HFK}}(S^3, J) = 2n+1$.

We may find two distinguished bases for $\mathrm{CFK}^-(S^3, J)$: a "vertically reduced" basis $\{\tilde{\xi}_0, \dots, \tilde{\xi}_{2n}\}$, with "vertical arrows" $\tilde{\xi}_{2j-1} \to \tilde{\xi}_{2j}$ of length $k_j \in \mathbb{N}$, and a "horizontally reduced" basis $\{\tilde{\eta}_0, \dots, \tilde{\eta}_{2n}\}$, with "horizontal arrows" $\tilde{\xi}_{2j-1} \to \tilde{\xi}_{2j}$ of length $l_j \in \mathbb{N}$. (See [11, Chapter 10] for the definitions.) Denote the change-of-basis matrices by $(x_{p,q})$ and $(y_{p,q})$, so that

$$\tilde{\xi}_p = \sum_{q=0}^{2n} x_{p,q} \tilde{\eta}_q \quad \text{and} \quad \tilde{\eta}_p = \sum_{q=0}^{2n} y_{p,q} \tilde{\xi}_q. \tag{10}$$

In all known instances, the two bases may be taken to be equal as sets (up to a permutation), but it has not been proven that this holds in general.

According to [11, Theorems 10.17, 11.7], the structure of $\widehat{\mathrm{CFD}}(\mathcal{X}_J^t)$ is as follows. The part in idempotent ι_0 (i.e., $\iota_0\widehat{\mathrm{CFD}}(\mathcal{X}_J^s)$) has dimension $2n+1$, with designated bases $\{\xi_0, \dots, \xi_{2n}\}$ and $\{\eta_0, \dots, \eta_{2n}\}$ related by (10) without the tildes. The part in idempotent ι_1 (i.e., $\iota_1\widehat{\mathrm{CFD}}(\mathcal{X}_J^s)$) has dimension $r + \sum_{j=1}^n (k_j + l_j)$, with basis

$$\{\gamma_1, \dots, \gamma_r\} \cup \bigcup_{j=1}^n \{\kappa_1^j, \dots, \kappa_{k_j}^j\} \cup \bigcup_{j=1}^n \{\lambda_1^j, \dots, \lambda_{l_j}^j\}.$$

For $j = 1, \dots, n$, corresponding to the vertical arrow $\tilde{\eta}_{2j-1} \to \tilde{\eta}_{2j}$, there are differentials

$$\xi_{2j} \xrightarrow{\rho_{123}} \kappa_1^j \xrightarrow{\rho_{23}} \cdots \xrightarrow{\rho_{23}} \kappa_{k_j}^j \xleftarrow{\rho_1} \xi_{2j-1}. \tag{11}$$

(In other words, $\delta_1(\xi_{2j})$ has a $\rho_{123} \otimes \kappa_1^j$ term, and so on.) We refer to the subspace of $\widehat{\mathrm{CFD}}(\mathcal{X}_J^s)$ spanned by the generators in (11) as a *vertical stable chain.* Similarly, corresponding to the horizontal arrow $\eta_{2j-1} \to \eta_{2j}$ of length l_j, there are differentials

$$\eta_{2j-1} \xrightarrow{\rho_3} \lambda_1^j \xrightarrow{\rho_{23}} \cdots \xrightarrow{\rho_{23}} \lambda_{l_j}^j \xrightarrow{\rho_2} \eta_{2j}, \tag{12}$$

and the generators here span a *horizontal stable chain.* Finally, the generators $\xi_0, \eta_0, \gamma_1, \dots, \gamma_r$ span the *unstable chain*, with differentials depending on s and $\tau(J)$:

$$\begin{cases} \eta_0 \xrightarrow{\rho_3} \gamma_1 \xrightarrow{\rho_{23}} \cdots \xrightarrow{\rho_{23}} \gamma_r \xleftarrow{\rho_1} \xi_0 & s < 2\tau(J) \\ \xi_0 \xrightarrow{\rho_{12}} \eta_0 & s = 2\tau(J) \\ \xi_0 \xrightarrow{\rho_{123}} \gamma_1 \xrightarrow{\rho_{23}} \cdots \xrightarrow{\rho_{23}} \gamma_r \xrightarrow{\rho_2} \eta_0 & s > 2\tau(J). \end{cases} \tag{13}$$

In some instances, as with the unknot and the figure-eight knot, we may have $\xi_0 = \eta_0$.

For $\widehat{\mathrm{CFD}}(\mathcal{X}_K^t)$, we modify the preceding two paragraphs by replacing all lower-case letters with capital letters. Specifically, $\iota_0\widehat{\mathrm{CFD}}(\mathcal{X}_K^t)$ has bases $\{\Xi_0, \dots, \Xi_{2N}\}$

and $\{\mathrm{H}_0, \dots, \mathrm{H}_{2N}\}$ related by change-of-basis matrices $(X_{P,Q})$ and $(Y_{P,Q})$ as in (10); $\iota_1\widehat{\mathrm{CFD}}(\mathcal{X}^t_K)$ has basis

$$\{\Gamma_1, \dots, \Gamma_R\} \cup \bigcup_{J=1}^{N} \{\mathrm{K}^J_1, \dots, \mathrm{K}^J_{K_J}\} \cup \bigcup_{J=1}^{N} \{\Lambda^J_1, \dots, \Lambda^J_{L_J}\};$$

and the differentials are just as in (11), (12), and (13), suitably modified.[2] In the discussion below, we shall treat $\widehat{\mathrm{CFD}}(\mathcal{X}^t_K)$ as a type D structure over a copy of $\mathcal{A}_\sigma$ in which the elements are referred to as σ_1, σ_2, etc., to facilitate taking the double tensor product.

In Section 4, we shall frequently use the following proposition to simplify computations:

Proposition 2.4. *In the matrix entries for the higher maps δ_k for $\widehat{\mathrm{CFD}}(\mathcal{X}^s_J)$, there are no sequences of elements containing $\rho_1 \otimes \rho_2$, $\rho_1 \otimes \rho_{23}$, $\rho_2 \otimes \rho_3$, or $\rho_{12} \otimes \rho_3$.*

Proof. The only instances of ρ_1 in $\widehat{\mathrm{CFK}}(\mathcal{X}^s_J)$ are $\xi_{2j-1} \xrightarrow{\rho_1} \kappa^j_{k_j}$ in the vertical chains and $\xi_0 \xrightarrow{\rho_1} \gamma_r$ in the unstable chain when $s < 2\tau(J)$, and $\delta_1(\kappa^j_{k_j}) = \delta_1(\gamma_r) = 0$. Thus, $\rho_1 \otimes \rho_2$ and $\rho_1 \otimes \rho_{23}$ may not occur in δ_k. Similarly, the only instances of ρ_2 and ρ_{12} are $\lambda^j_{l_j} \xrightarrow{\rho_2} \eta_{2j}$ in the horizontal chains, $\gamma_r \xrightarrow{\rho_2} \eta_0$ in the unstable chain when $s > 2\tau(J)$, and $\xi_0 \xrightarrow{\rho_{12}} \eta_0$ when $s = 2\tau(J)$, and the only instances of ρ_3 are $\eta_{2j-1} \xrightarrow{\rho_3} \lambda^j_1$ in the horizontal chains and $\eta_0 \xrightarrow{\rho_3} \gamma_1$ in the unstable chain when $s < 2\tau(J)$. Thus, no element that is at the head of a ρ_2 or ρ_{12} arrow is also at the tail of a ρ_3 arrow. ☐

3. Direct computation of $\widehat{\mathrm{CFAA}}(Y, B_3)$

As above, let $B = B_1 \cup B_2 \cup B_3 \subset S^3$ denote the Borromean rings. Let Y denote the complement of a neighborhood of $B_1 \cup B_2$; then B_3 is a nulhomologous knot in Y. Let $\partial_L Y$ and $\partial_R Y$ be the boundary components coming from B_1 and B_2, respectively. We define a strongly bordered structure $\mathcal{Y}$ on Y (in the sense of [10, Definition 5.1]) so that the map $\phi_L : F(\mathcal{Z}) \to \partial_L Y$ (resp. $\phi_R : F(\mathcal{Z}) \to \partial_R Y$) takes h_1 to a meridian of B_1 (resp. B_2) and h_2 to a Seifert-framed longitude of B_1 (resp. B_2). It follows that the glued manifold $(\mathcal{Y} \cup_{\partial_L Y} \mathcal{X}^s_J) \cup_{\partial_R Y} \mathcal{X}^t_K$, is S^3, and the image of B_3 is the knot $D_{J,s}(K, t)$.[3] Thus, we must compute the filtered type AA bimodule $\widehat{\mathrm{CFAA}}(\mathcal{Y}, B_3, 0)$. We do this explicitly using a Heegaard diagram.

Proposition 3.1. *The arced Heegaard diagram $\mathcal{H}$ (with extra basepoint w) shown in Figure 5 determines the pair $(\mathcal{Y}, B_3)$.*

---

[2] The reader should take care to distinguish capital eta (H) and kappa (K) from the Roman letters H and K. We find that the mnemonic advantage of using parallel notation for the generators of $\widehat{\mathrm{CFD}}(\mathcal{X}^s_J)$ and $\widehat{\mathrm{CFD}}(\mathcal{X}^t_K)$ outweighs any confusion that may arise.

[3] Because we are gluing the two boundary components of $\mathcal{Y}$ to separate single-boundary-component bordered manifolds, the choice of framed arc connecting $\partial_L Y$ and $\partial_R Y$ does not affect the final computation of the tensor product, so we suppress all reference to it.

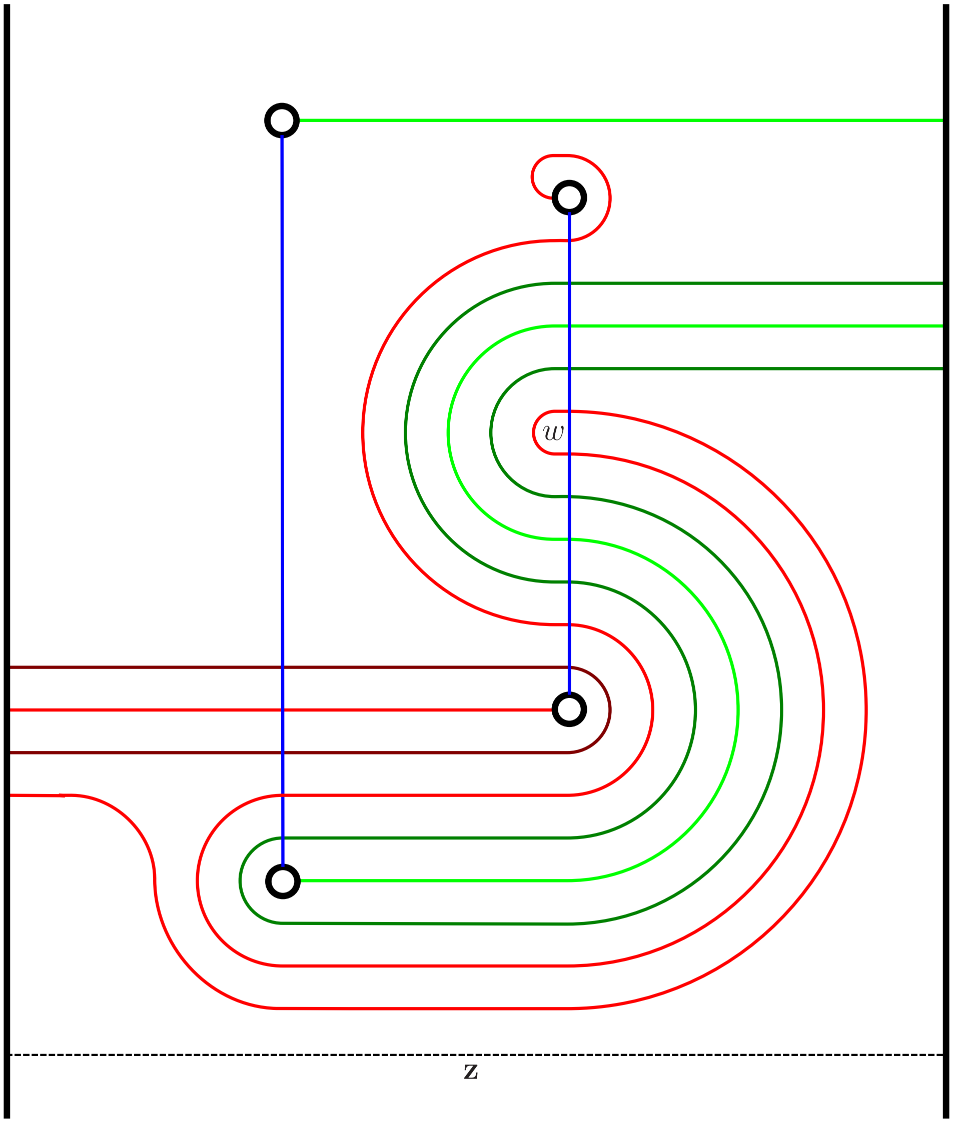

FIGURE 5. The arced Heegaard diagram $\mathcal{H}$.

Proof. As in [10, Construction 5.4], by cutting along the arc $\mathbf{z}$, we obtain a bordered Heegaard diagram with a single boundary component, $\mathcal{H}_{dr}$, which we view as rectangle with two tunnels attached. After attaching 2-handles to $\mathcal{H}_{dr} \times [0,1]$ along $\boldsymbol{\beta} \times \{1\}$ and attaching a single 3-handle, we may view the resulting manifold $Y(\mathcal{H}_{dr})$ as $[-1,1] \times \mathbb{R} \times [0,\infty) \subset \mathbb{R}^3$, minus two tunnels in the upper half-plane, plus the point at infinity (Figure 6). The boundary of $Y(\mathcal{H}_{dr})$ is the union of two embedded copies of $F^\circ(\mathcal{Z})$ that are determined by the α arcs on each side; they intersect along a circle A. The extra basepoint w determines a knot C in $Y(\mathcal{H}_{dr})$ with a single point on the boundary: the union of an arc connecting w to z in the complement of the α arcs and an arc

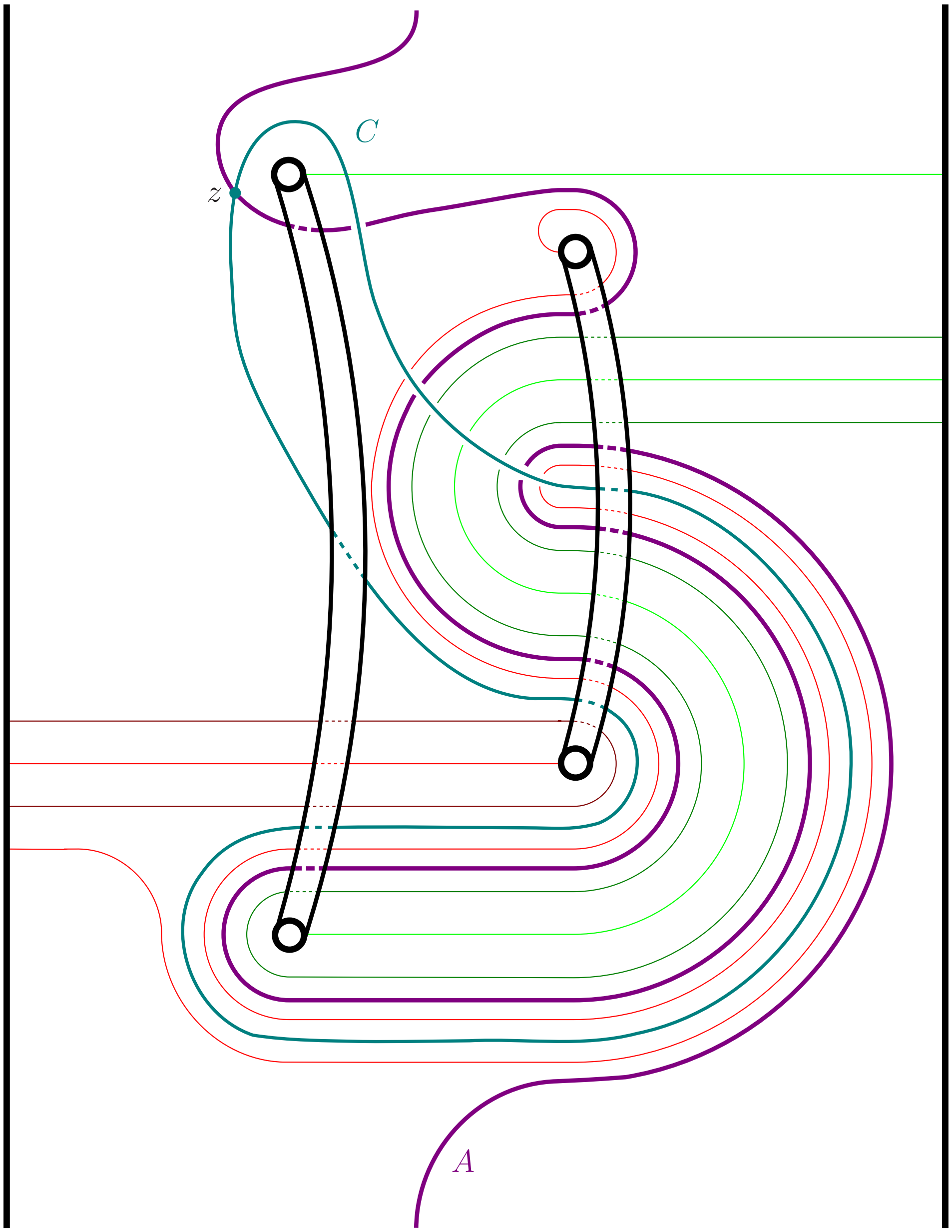

FIGURE 6. The manifold $Y(\mathcal{H}_{dr})$. The α arcs from $\mathcal{H}$ (the thin red and green curves) and the circle A (purple) sit in the xy-plane, while the knot C (turquoise) sits in the interior of $Y(\mathcal{H}_{dr})$ except at the point z.

connecting z to w in the complement of the β circles, pushed into the interior of $Y(\mathcal{H}_{dr})$ except at z. The curves A and C are both shown in Figure 6.

We obtain Figure 7 from Figure 6 by an isotopy that slides the tunnel on the right underneath the tunnel on the left. The circle A can then be identified with the y-axis plus the point at infinity. To obtain $Y(\mathcal{H})$, we attach a three-dimensional two-handle

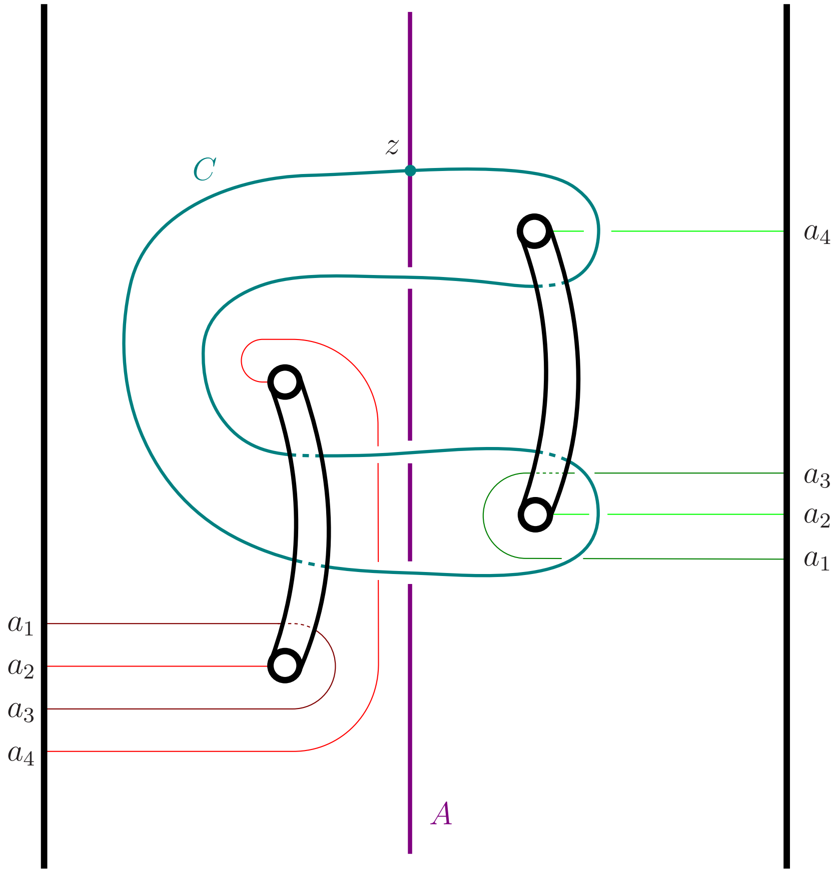

FIGURE 7. The result of isotoping Figure 6. Each boundary component is identified with $\mathcal{Z}$.

along A, which can be seen as $[-\epsilon,\epsilon]\times\mathbb{R}\times(-\infty,0]$ plus the point at infinity. Then $Y(\mathcal{H})$ is the complement of a two-component unlink $(B_1\cup B_2)$ in S^3, and the knot C inside $Y(\mathcal{H})$ is B_3. When we identify each component of $\partial\Sigma$ with $\mathcal{Z}$, we see that the α arc connecting the points a_1 and a_3 is a meridian, and the α arc connecting a_2 and a_4 is a 0-framed longitude, as in the definition of $\mathcal{Y}$. □

If we try to compute $\widehat{\mathrm{CFAA}}(\mathcal{H},0)$ directly, we run into difficulties counting the holomorphic curves, largely because there is a 14-sided region that runs over both handles and shares edges with itself. Instead, it is easier to perform a sequence of isotopies on the α arcs to obtain the diagram $\mathcal{H}'$ shown in Figure 8. While $\mathcal{H}'$ is not a nice diagram in the sense of Sarkar and Wang [23], the analysis needed to count the relevant holomorphic curves is vastly simpler. Of course, the drawback is that the number of generators is much larger.

By Theorem 2.3, it suffices to compute $\widehat{\mathrm{CFDD}}(\mathcal{H}',0)$, as described previously. Thus, we identify each component of $\partial\Sigma$ with $-\mathcal{Z}$. We now describe this computation.

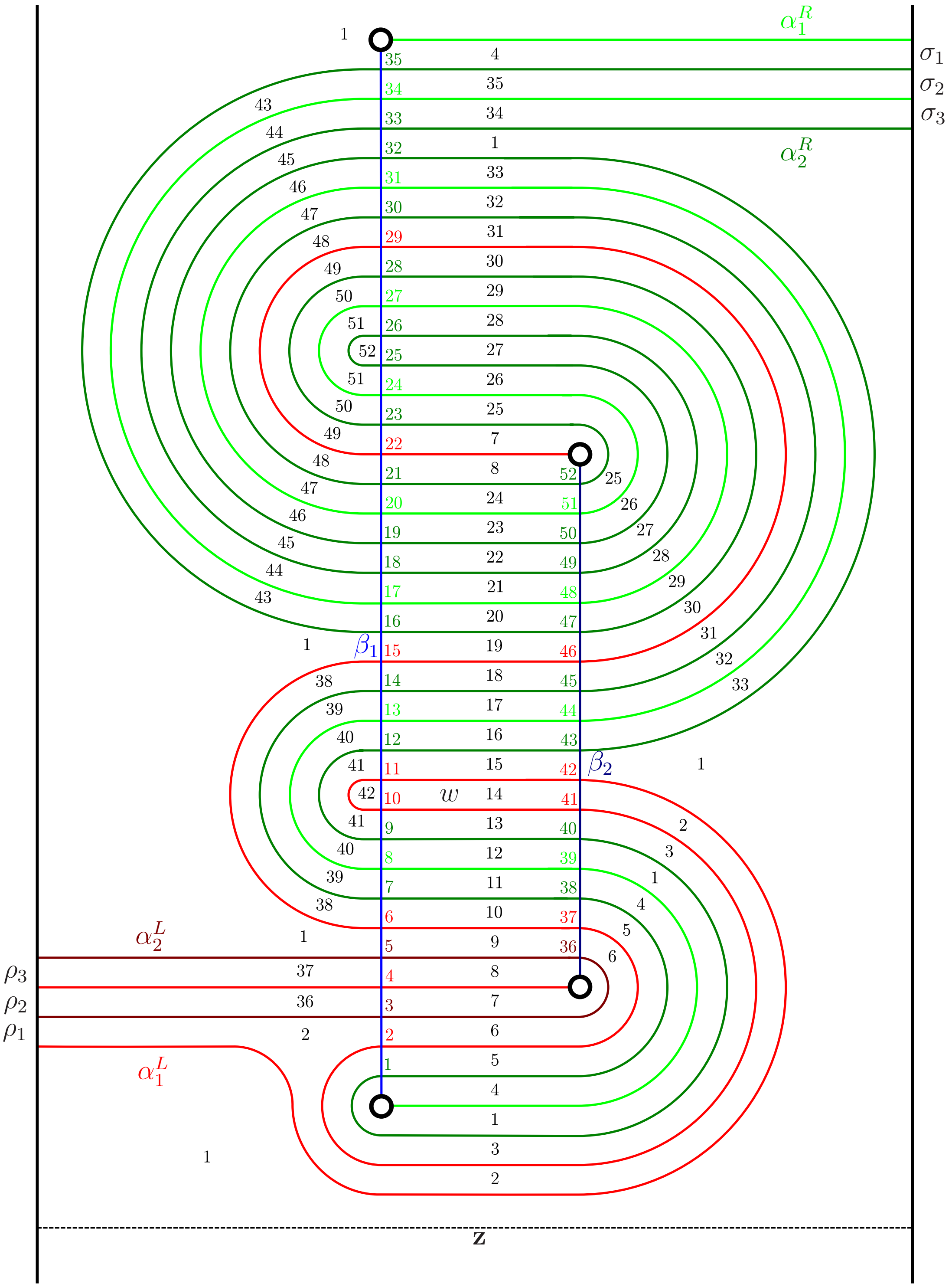

FIGURE 8. The Heegaard diagram $\mathcal{H}'$, with the boundary labeled consistent with the conventions for type D structures.

In $\mathcal{H}'$, we label the intersection points of the α and β curves $x_1, \dots, x_{52}$, as indicated by the colored numbers in Figure 8.[4] These points are distributed among the various α and β circles as follows:

	β_1	β_2
α_1^L	$x_2, x_4, x_6, x_{10}, x_{11}, x_{15}, x_{22}, x_{29}$	$x_{37}, x_{41}, x_{42}, x_{46}$
α_2^L	x_3, x_5	x_{36}
α_1^R	$x_8, x_{13}, x_{17}, x_{20}, x_{24}, x_{27}, x_{31}, x_{34}$	$x_{39}, x_{44}, x_{48}, x_{51}$
α_2^R	$x_1, x_7, x_9, x_{12}, x_{14}, x_{16}, x_{18}, x_{19}$ $x_{21}, x_{25}, x_{26}, x_{28}, x_{32}, x_{33}, x_{35}$	$x_{38}, x_{40}, x_{43}, x_{45}$ $x_{47}, x_{49}, x_{50}, x_{52}$

The underlying vector space for $\widehat{\mathrm{CFDD}}(\mathcal{H}', 0)$ is generated by the set $\mathfrak{S}(\mathcal{H}', 0)$, consisting pairs of intersection points with one point on each β circle, one point on either α_1^L or α_2^L, and one point on either α_1^R or α_2^R. A simple count shows that there are 245 generators.

The bimodule $\widehat{\mathrm{CFDD}}(\mathcal{H}', 0)$ is a type DD structure over two copies of the torus algebra $\mathcal{A}$. We denote these copies by $\mathcal{A}_\rho$ and $\mathcal{A}_\sigma$, corresponding to the left and right boundary components of $\mathcal{H}'$. In $\mathcal{A}_\sigma$, the Reeb elements are denoted σ_1, σ_2, etc. The idempotents in $\mathcal{A}_\rho$ are denoted ι_0^ρ and ι_1^ρ, and those in $\mathcal{A}_\sigma$ are denoted ι_0^σ and ι_1^σ. The idempotent maps $I_D^\rho : \mathfrak{S}(\mathcal{H}', 0) \to \{\iota_0^\rho, \iota_1^\rho\}$ and $I_D^\sigma : \mathfrak{S}(\mathcal{H}', 0) \to \{\iota_0^\sigma, \iota_1^\sigma\}$ are defined just as in (5).

Denote the regions of $\Sigma' \setminus (\boldsymbol{\alpha} \cup \boldsymbol{\beta})$ by $R_1, \dots, R_{52}$, as indicated by the black numbers in Figure 8.

For generators $\mathbf{x}$ and $\mathbf{y}$, we may find all the domains in $\pi_2(\mathbf{x}, \mathbf{y})$ by solving the system of linear equations (4). The multiplicity of each of the boundary regions (R_2, R_4, R_{34}, R_{35}, R_{36}, and R_{37}) must be 0 or 1; each of the 2^6 possible choices for these multiplicities gives a further set of constraints that guarantees a unique solution. We may then list only those solutions which represent positive classes and which have index 1 for some compatible $\vec{\rho}$, subject to the restrictions of Proposition 2.1. Using *Mathematica* to perform these linear algebra computations, we find some 1,051 domains meeting these requirements.

It would not be feasible to list every single domain and whether or not it supports holomorphic representatives, but we shall describe a number of typical examples, and leave further details to the highly motivated reader.

Bigons and quadrilaterals: In the context of closed Heegaard diagrams, Sarkar and Wang [23] showed that in a Heegaard diagram in which every non-basepointed region is either a bigon or a quadrilateral, the domains with Maslov index 1 are precisely the embedded bigons and quadrilaterals that are embedded in the Heegaard diagram, and these all support support a unique holomorphic representatives. Lipshitz, Ozsváth, and Thurston proved an analogous result for bordered diagrams [11, Proposition 8.4], where now we extend the definition of "quadrilateral" to include a region with boundary consisting of one segment of a β circle, two segments of α arcs,

---

[4] While many authors use different letters to distinguish between intersection points on different α or β curves, we use a single indexing set here in order to facilitate computer calculations.

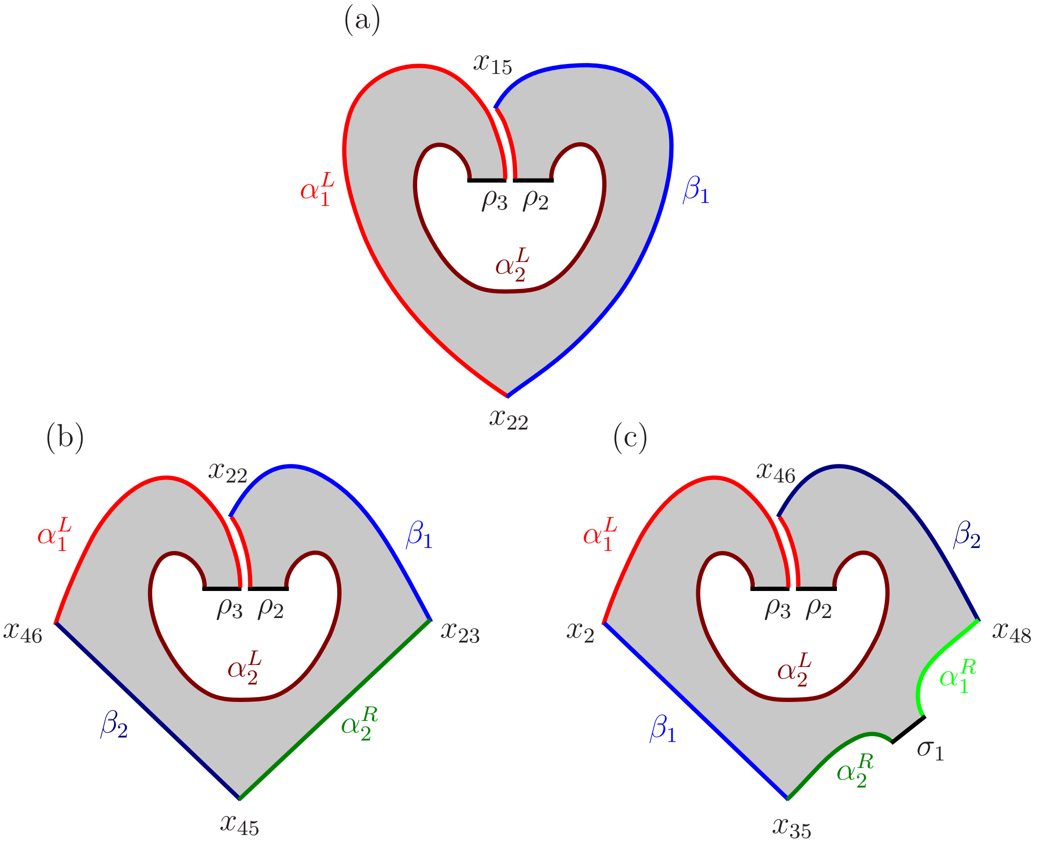

FIGURE 9. The domains D_1 (a), D_2 (b), and D_3 (c).

and one segment of $\partial\Sigma$. The only non-basepointed regions in $\mathcal{H}'$ that are not bigons or quadrilaterals are R_2, R_4, R_7, and R_8, which are hexagons. Therefore, any index-1 domain on our list that does not use one of these four regions automatically supports a unique holomorphic representative.

Domains contributing ρ_{23}: Consider the domains

$$\begin{aligned}
D_1 &= R_7 + R_8 + R_{19} + \cdots + R_{30} + R_{49} + R_{50} + R_{51} + R_{52}\\
D_2 &= R_7 + R_8 + R_{31} + R_{36} + R_{37} + R_{48}\\
D_3 &= D_2 + R_4 + R_5 + R_{10} + R_{11} + R_{17} + R_{18} + R_{24} + R_{25} + R_{29} + R_{30} + R_{32}\\
&\qquad + R_{38} + R_{39} + R_{47} + R_{49} + R_{50},
\end{aligned}$$

which respectively represent index-1 classes in $\pi_2(x_{15}x_i, x_{22}x_i)$, $\pi_2(x_{22}x_{45}, x_{23}x_{46})$, and $\pi_2(x_{35}x_{46}, x_2x_{48})$, where $x_i \in \beta_2 \cap (\alpha_1^R \cup \alpha_2^R)$ and $i < 47$. (If $i \in \{47, \dots, 52\}$, the index of D_1 is too high.) To obtain a representative of each domain compatible with the sequence $(-\rho_2, -\rho_3)$, as required by Proposition 2.1, we cut along α_1^L all the way to the boundary, as shown in Figure 9. The source curve for D_1 is the disjoint union of two bigons: one with two boundary punctures mapped to the Reeb chords $-\rho_2$ and $-\rho_3$, and one mapped trivially to $\{x_i\} \times [0,1] \times \mathbb{R}$. The source curve for D_2 or D_3 is a quadrilateral, with two boundary punctures on one α edge mapping to $-\rho_2$

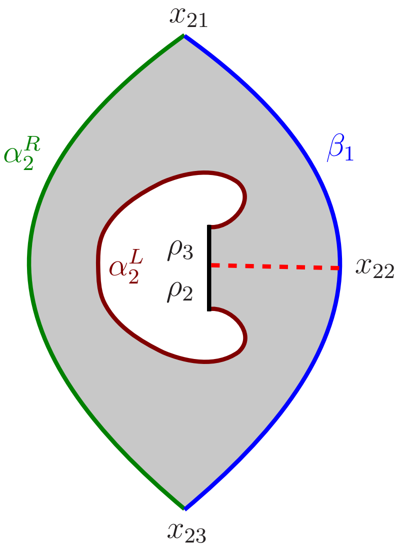

FIGURE 10. The domain D_4.

and $-\rho_3$ and (for D_3) a boundary puncture on the other α edge mapping to σ_1. It is easy to see that these classes all support holomorphic representatives. Thus, we have differentials $x_{15}x_i \xrightarrow{\rho_{23}\otimes\mathbf{1}} x_{22}x_i$, $x_{22}x_{45} \xrightarrow{\rho_{23}\otimes\mathbf{1}} x_{23}x_{46}$, and $x_{35}x_{46} \xrightarrow{\rho_{23}\otimes\sigma_1} x_2x_{48}$.

On the other hand, let $D_4 = R_7 + R_8 + R_{36} + R_{37}$; this domain represents a class in $\pi_2(x_{21}x_j, x_{23}x_j)$, where $x_j \in \beta_2 \cap (\alpha_1^L \cup \alpha_2^L)$. This domain is illustrated in Figure 10. If $x_j \in \alpha_2^L$, then then this class is excluded for idempotent reasons by Proposition 2.1. On the other hand, if $x_j \in \alpha_1^L$, then the index of this class is 0. Therefore, D_4 cannot count for the differential for any choice of x_j.

Decomposable annuli: Let $A = R_7 + R_8 + R_{48} + R_{49} + R_{30} + R_{31}$; this is the domain for an index-0 annulus in $\pi_2(x_3x_{45}, x_5x_{47})$. Consider the index-1 annuli

$$D_5 = A + R_{36} \in \pi_2(x_4x_{45}, x_5x_{47})$$
$$D_6 = A + R_{37} \in \pi_2(x_3x_{45}, x_4x_{47})$$
$$D_7 = A + R_{25} + R_{26} + R_{27} + R_{28} + R_{29} + R_{50} + R_{51} + R_{52} \in \pi_2(x_3x_{45}, x_5x_{52}).$$

each of which is the sum of A with a bigon (possibly with a Reeb chord on the boundary). The mod-2 count of holomorphic representatives of each of these domains depends nontrivially on the choice of complex structure. We claim that either all three domains count for the differential or none of them do. To see this, we use a standard argument in conformal geometry that occurs frequently in computing Heegaard Floer complexes, which we find convenient to state in more generality than is strictly needed for this example. (See, e.g., Ozsváth and Szabó's first paper on Heegaard Floer homology [16].)

Lemma 3.2. *Suppose that a Heegaard diagram contains an annulus A and some or all of the bigons $B_1, \dots, B_8$ shown in Figure 11, where each of the arcs that cuts into A crosses to the opposite boundary component. Let E_i be the domain $A + B_i$, which*

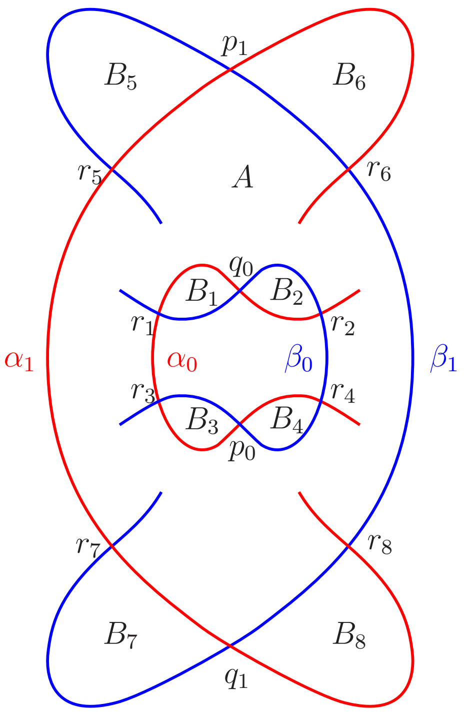

FIGURE 11. Annuli for which the number of holomorphic representatives depends nontrivially on the choice of complex structure as in Lemma 3.2.

has Maslov index 1*. Then either* E_1*,* E_3*,* E_6*, and* E_8 *count for the differential and* E_2*,* E_4*,* E_5*, and* E_7 *do not, or vice versa.*

Proof. Define the *standard annulus* A_0 to be $S^1 \times [0,1]$, with coordinates (s,t), with the complex structure given by $j\partial_s = \partial_t, j\partial_t = -\partial_s$. Up to rotation in the S^1 factor, there is a unique holomorphic map $U : A_0 \to A$ taking $S^1 \times \{0\}$ to the inner boundary $(A \cap (\alpha_0 \cup \beta_0))$ and $S^1 \times \{1\}$ to the outer boundary $(A \cap (\alpha_1 \cup \beta_1))$. For $i \in \{0,1\}$, let a_i and b_i denote the inverse images of α_i and β_i, respectively. Define $\Theta_i = \ell(a_i)/\ell(b_i)$, the ratio of the length of the a_i to the length of b_i. For generic choices of the complex structure on Σ, we may assume that $\Theta_0 \neq \Theta_1$.

We consider $E_1 = A + B_1$; the analysis for the other seven cases is extremely similar. The domain E_1 (going from p_0p_1 to r_1q_1) has a one-parameter family of conformal structures, determined by how far we cut into A at r_1. We specify the length of the cut by $c \in \mathbb{R}$, where $c < 0$ corresponds to cutting along α_0 and $c > 0$ corresponds to cutting along β_0. For each value of c, there is a conformal map $u^c : A_0 \to E_1$, unique up to rotation in the S^1 factor. As above, let $a_i^c, b_i^c \subset S^1 \times \{i\}$ be the preimages of α_i and β_i under u^c, and let $\theta_i^c = \ell(a_i^c)/\ell(b_i^c)$. Whenever $\theta_0^c = \theta_1^c$, there is a holomorphic involution A_0 interchanging a_0^c with a_1^c and b_0^c with b_1^c. Thus, the signed count of the zeroes of the function $f(c) = \theta_0^c - \theta_1^c$ equals the signed number of points in the moduli space $\widehat{\mathcal{M}}(E_1)$. We may assume that f is transverse to zero.

Consider the limiting behavior of $f(c)$. As we cut along β_0, the arcs b_0 and a_1 grow in length, approaching all of $S^1 \times \{0\}$ and $S^1 \times \{1\}$, respectively. Thus $\lim_{c\to\infty} \theta_0^c = 0$ and $\lim_{c\to-\infty} \theta_1^c = \infty$, so $\lim_{c\to\infty} f(c) = -\infty$. In the opposite direction, as we cut along α_0, Gromov compactness implies that the maps u^c limit to a broken flowline consisting of holomorphic representatives for B_1 and A, so the limiting values of θ_0^c and θ_1^c are equal the corresponding values for $U : A_0 \to A$. That is, $\lim_{c\to-\infty} f(c) = \Theta_0 - \Theta_1$. By transversality and the intermediate value theorem, we thus see that $\#\widehat{\mathcal{M}}(E_1)$ is odd if and only if $\Theta_0 < \Theta_1$.

For the remaining domains $E_2, \dots, E_8$, we apply the same sort of analysis. As before, we parametrize the cut by $c \in \mathbb{R}$, with $c < 0$ corresponding to cutting along the α circle and $c > 0$ corresponding to cutting along the β circle. The limits are in the following table:

	$\lim_{c\to-\infty} f(c)$ (cutting along α)	$\lim_{c\to\infty} f(c)$ (cutting along β)
E_1, E_3	$\Theta_0 - \Theta_1$	$-\infty$
E_2, E_4	∞	$\Theta_0 - \Theta_1$
E_5, E_7	$\Theta_0 - \Theta_1$	∞
E_6, E_8	$-\infty$	$\Theta_0 - \Theta_1$

Thus, E_1, E_3, E_6, and E_8 count for the differential if and only if $\Theta_0 < \Theta_1$, and E_2, E_4, E_5, and E_7 count otherwise. □

In our Heegaard diagram $\mathcal{H}'$, we identify α_0, β_0, α_1, and β_1 in Figure 11 with α_2^L, β_1, α_2^R, and β_2 in Figure 8, respectively. For the bigons, we may take $B_2 = R_{37}$, $B_4 = R_{36}$, and $B_7 = R_{25} + R_{26} + R_{27} + R_{28} + R_{29} + R_{50} + R_{51} + R_{52}$, so that the domains D_5, D_6, and D_7 have the forms of E_4, E_2, and E_7, respectively. (For D_5 and D_6, the source surface should actually be $A_0' = A_0 \smallsetminus (p, 0)$, where p is some point in S^1, and the puncture is sent to the Reeb chord ρ_2 or ρ_3. The analysis is exactly the same, however.) By Lemma 3.2, either all three of these domains count for the differential or none of them do, depending on the value of $\Theta_0 - \Theta_1$. If we arrange that $\Theta_0 < \Theta_1$, we see that none of these domains count.

Moreover, the other annuli in $\mathcal{H}'$ with Maslov index 0 are obtained by adding rectangular strips (e.g., $R_6 + R_9$ or $R_{24} + R_{25} + R_{47} + R_{50} + R_{29} + R_{32}$) to this one, and we may easily arrange that the values of $\Theta_0 - \Theta_1$ for all of these annuli are arbitrarily close together. Therefore, the annuli obtained by adding rectangular strips to D_5, D_6, and D_7 also do not count for the differential.

More annuli: Let $D_8 = R_2 + R_6 + R_7 + R_8 + R_{14} + R_{36} + R_{37} + R_{42}$, which determines an annulus in $\pi_2(x_{21}x_{36}, x_{23}x_{37})$ with a single ρ_{123} chord on one boundary component (Figure 12(a)). Let $c \in \mathbb{R}$ represent the cut parameter at x_{36}, where $c < 0$ corresponds to cutting along α_2^L and $c > 0$ corresponds to cutting along β_2. As above, for each value of c there is a unique holomorphic map u^c from the source annulus A_0' taking $(S^1 \smallsetminus p) \times \{0\}$ to $\alpha_1^L \cup \alpha_2^L \cup \beta_2$, the puncture $(p, 0)$ to the Reeb chord ρ_{123}, and $(S^1 \times \{1\})$ to $\alpha_2^R \cup \beta_1$. With notation as in the proof of Lemma 3.2, we must consider the limits of $f(c) = \theta_0^c - \theta_1^c$ as $c \to \pm\infty$. As we cut along β_2, the arcs $b_0^c = (u^c)^{-1}(\beta_2)$

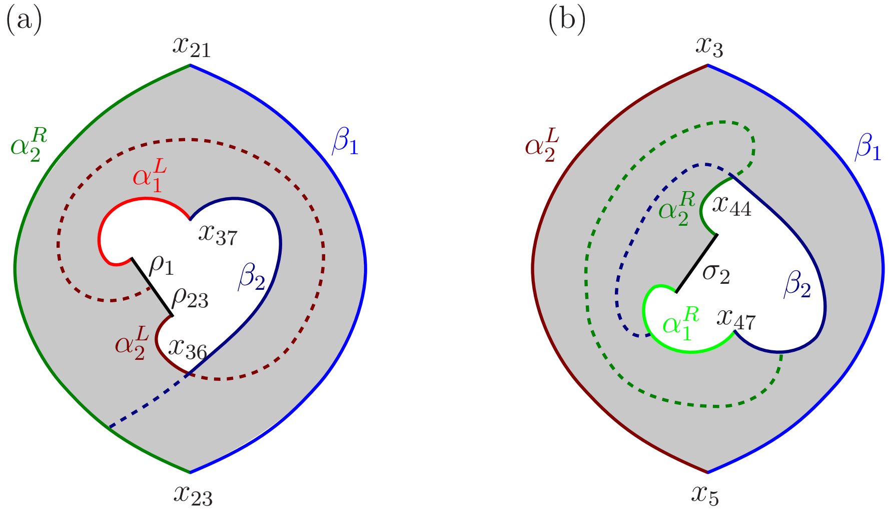

FIGURE 12. The domains D_9 (a) and D_9 (b).

and $a_1^c = (u^c)^{-1}(\alpha_2^R)$ become arbitrarily long relative to their complements, so

$$\lim_{c\to\infty} f(c) = \lim_{c\to\infty} \theta_0^c - \lim_{c\to\infty} \theta_1^c = 0 - \infty = -\infty.$$

As we cut along α_2^L out toward the puncture, the arc a_0^c becomes arbitrarily long relative to b_0^c, while the ratio of the lengths of a_1^c and b_1^c approaches some finite value Θ, so

$$\lim_{c\to-\infty} f(c) = \lim_{c\to-\infty} \theta_0^c - \lim_{c\to-\infty} \theta_1^c = \infty - \Theta = \infty.$$

By transversality, we see that f always has an odd number of zeroes, so the class given by D_8 always counts for the differential.

Next, consider the domain

$$\begin{aligned} D_9 = R_7 + R_8 + R_{20} + R_{24} + R_{25} + R_{29} + R_{30} \\ + R_{31} + R_{32} + R_{35} + R_{43} + R_{47} + R_{48} + R_{49} + R_{50}, \end{aligned}$$

which represents an annulus in $\pi_2(x_3x_{44}, x_5x_{47})$ with a single σ_2 Reeb chord (Figure 12(b)). Once again, we specify the cut parameter at x_{47} by $c \in \mathbb{R}$ and consider the limiting behavior of a function $f(c)$ defined as in previous examples. In the as $c \to \pm\infty$, the domain decomposes into a bigon $B_\pm$ with a single boundary puncture and an annulus $A_\pm$ with Maslov index 0, so by Gromov compactness, $\lim_{c\to\pm\infty} f(c) = \Theta_0^\pm - \Theta_1^\pm$, where $\Theta_0^\pm$ and $\Theta_1^\pm$ are the conformal angle ratios of $A_\pm$ as in the proof of Lemma 3.2. As mentioned previously, we may assume that $\Theta_0^+ - \Theta_1^+$ and $\Theta_0^- - \Theta_1^-$ are arbitrarily close together; in particular, they have the same sign. Thus, D_9 does not count for the differential. A similar argument applies for

$$D_{10} = R_2 + R_6 + R_7 + R_8 + R_9 + R_{14} + R_{30} + R_{31} + R_{42} + R_{48} + R_{49}.$$

Genus-1 classes: Let $D_{11} = R_7 + R_8 + \cdots + R_{24}$ (Figure 13(a)), which determines a class in $\pi_2(x_3x_{52}, x_{23}x_{36})$ represented by an embedded punctured torus. Determining whether domains with positive genus support holomorphic representatives is often one

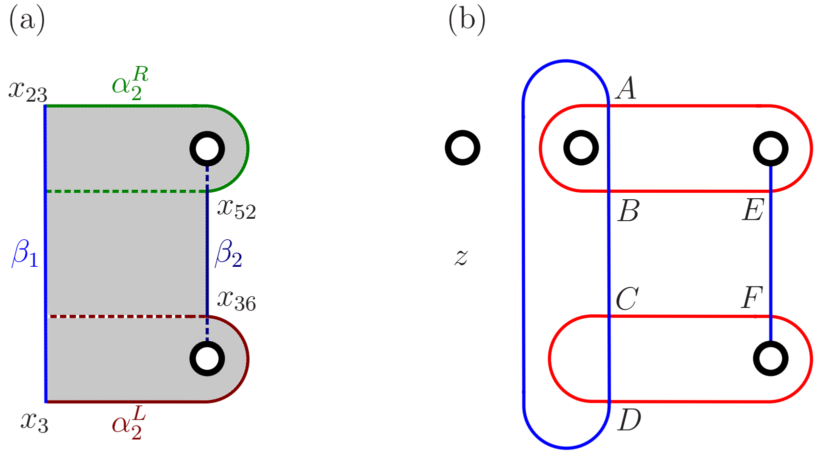

FIGURE 13. (a) The genus-1 domain D_{11}. (b) A Heegaard diagram for $S^1 \times S^2$ containing a domain biholomorphic to D_{11}.

of the biggest difficulties in computing Heegaard Floer homology directly. In this case, the trick is to notice that the genus-2 Heegaard diagram for $S^1 \times S^2$ shown in Figure 13(b) has a domain (connecting the generators DE and AF) that is biholomorphic to D_{11}. By counting the remaining disks in this diagram, it is easy to see that the toroidal domain must count in order for the homology to be correct. Therefore, D_5 must also support a holomorphic representative. The same analysis applies to any domain of the form $\sum_{i=a}^{b} R_i$, where $4 \leq a \leq 7$ and $24 \leq b \leq 33$, provided that a and b are chosen such that the two α segments of the boundary do not lie on the same α curve. A similar analysis also works for the domain

$$D_{12} = R_5 + R_6 + R_7 + R_8 + R_9 + R_{10} + R_{18} + R_{30} + R_{31} + R_{48} + R_{49}$$

and others like it.

Next, consider the domains

$$\begin{aligned} D_{13} &= R_8 + \cdots + R_{24} \in \pi_2(x_4x_{47}, x_{22}x_{47}) \\ D_{14} &= R_7 + \cdots + R_{19} + R_{30} + R_{31} + R_{48} + R_{49} \in \pi_2(x_3x_{45}, x_{16}x_{36}) \\ D_{15} &= R_8 + R_{20} + R_{21} + R_{22} + R_{23} + R_{24} + R_{37} \in \pi_2(x_{16}x_{36}, x_{22}x_{47}). \end{aligned}$$

The domains D_{13} and D_{15} obviously do count for the differential: D_{13} is an annulus that always has a holomorphic representative (by a standard argument), and D_{15} is a rectangle with a single Reeb chord. The domain D_{14}, however, is a punctured torus. Notice that $D_6 + D_{13}$ and $D_{14} + D_{15}$ both determine the same homology class in $\pi_2(x_3x_{45}, x_{22}x_{47})$, with index 2. More precisely, we there is a one-parameter family of disks limiting in one direction to the broken flowline $D_6 * D_{13}$ and in the other direction to $D_{14} * D_{15}$, which can be seen explicitly by varying the cut parameter at x_{47}. It follows that D_{14} counts for the differential if and only if D_6 does. By our assumption above, D_{14} does not count.

Miscellaneous domains: Let $D_{16} = R_7 + 2R_8 + R_9 + R_{10} + \cdots + R_{24} + R_{31} + R_{37} + R_{48}$; this is a domain from x_3x_{45} to $x_{23}x_{46}$. Because the region R_8, which as drawn in Figure

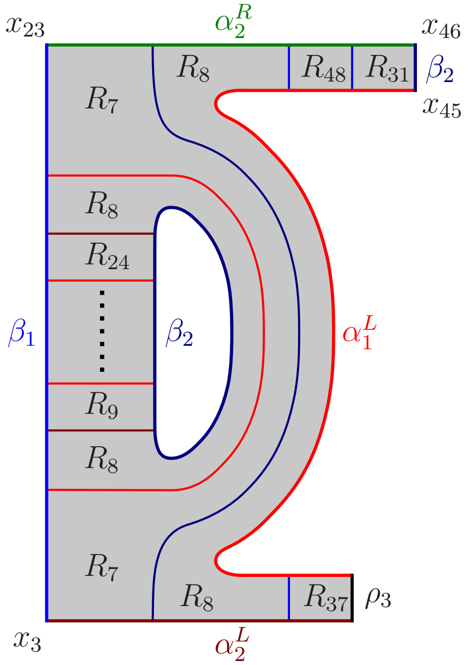

FIGURE 14. The only possible source surface for the domain D_{16}, which does not satisfy the correct boundary conditions.

8 goes over one of the handles, is used twice, it is a little bit tricky to see what the source surface should be; the only possibility is indicated in Figure 14. Topologically, this is an immersed annulus with one boundary component having two α and two β segments (and a single Reeb chord), and the other component consisting of all of β_2, so it does not satisfy the necessary boundary conditions. Thus, D_{16} cannot count for the differential.

By inspecting the long list of the index-1 domains in $\mathcal{H}'$, we see that they all fall into one of the classes just described. We may thus sort the list into those that support holomorphic representatives and those that do not. Using this list, we may then record the differential on $\widehat{\mathrm{CFDD}}(\mathcal{H}', 0)$ as a 245×245 matrix with entries in $\mathcal{A}_\rho \otimes \mathcal{A}_\sigma$, although for obvious reasons we do not record this matrix here.

By counting the multiplicity of w in each domain (whether it counts for the differential or not), we can determine the relative Alexander gradings of all of the generators. We find that the generators of $\widehat{\mathrm{CFDD}}(\mathcal{H}', 0)$ all fall into three consecutive gradings, which for now we arbitrarily declare to be -1, 0, and 1. In the end, after we evaluate all tensor products, the symmetry of $\widehat{\mathrm{CFK}}(S^3, D_{J,s}(K,t))$ will show that this was the correct choice. We do not explicitly list all of the gradings here, however.

We may then use the edge cancellation algorithm explained in Subsection 2.6 to simplify $\widehat{\mathrm{CFDD}}(\mathcal{H}', 0)$, canceling only edges that preserve the filtration level. By abuse of notation, we denote the resulting module by $\widehat{\mathrm{CFDD}}(\mathcal{Y}, B_3, 0)$.

Theorem 3.3. *The type DD structure* $\widehat{\mathrm{CFDD}}(\mathcal{Y}, B_3, 0)$ *has a basis* $\{y_1, \dots, y_{19}\}$ *with the following properties:*

(1) The Alexander gradings of the basis elements are:

$$A(y_i) = \begin{cases} -1 & i = 1 \\ 0 & i = 2, \dots, 10 \\ 1 & i = 11, \dots, 19. \end{cases}$$

(2) The associated idempotents in $\mathcal{A}_\rho$ *and* $\mathcal{A}_\sigma$ *of the generators are:*

	ι_0^ρ	ι_1^ρ
ι_0^σ	$y_4, y_5, y_7, y_{11}, y_{13}, y_{17}, y_{19}$	$y_8, y_{10}, y_{14}, y_{16}$
ι_1^σ	y_3, y_6, y_{12}, y_{18}	y_1, y_2, y_9, y_{15}

(3) The differential is given by

$$\delta_1(y_i) = \sum_{j=1}^{19} a_{ij} \otimes y_j,$$

where (a_{ij}) *is the following matrix:*

$$\left(\begin{array}{c|ccccccccc|ccccccccc}
0 & 0 & 0 & 0 & 0 & 0 & 0 & 0 & 0 & 0 & 0 & 0 & 0 & 0 & 0 & 0 & 0 & 0 & 0 \\
\hline
1 & 0 & 0 & 0 & 0 & 0 & \sigma_2 & 0 & 0 & 0 & 0 & 0 & 0 & 0 & 0 & 0 & 0 & 0 & 0 \\
\rho_1 & 0 & 0 & 0 & 0 & 0 & 0 & 0 & 0 & 0 & 0 & 0 & 0 & 0 & 0 & 0 & 0 & 0 & 0 \\
\rho_1\sigma_{123} & \rho_1\sigma_3 & \sigma_3 & 0 & 0 & 0 & 0 & 0 & 0 & 0 & 0 & 0 & 0 & 0 & 0 & 0 & 0 & 0 & 0 \\
0 & \rho_3\sigma_{123} + \rho_{123}\sigma_3 & 0 & 0 & 0 & \sigma_3 & 0 & 0 & \rho_3\sigma_{123} & \rho_3 & 0 & 0 & 0 & 0 & 0 & 0 & 0 & 0 & 0 \\
\rho_{123} & 0 & 0 & 0 & 0 & 0 & \sigma_2 & 0 & \rho_3 & 0 & 0 & 0 & 0 & 0 & 0 & 0 & 0 & 0 & 0 \\
0 & 0 & 0 & 0 & 0 & 0 & 0 & \rho_3 & 0 & 0 & 0 & 0 & 0 & 0 & 0 & 0 & 0 & 0 & 0 \\
0 & 0 & \rho_2\sigma_1 & 0 & 0 & 0 & 0 & 0 & 0 & 0 & 0 & 0 & 0 & 0 & 0 & 0 & 0 & 0 & 0 \\
0 & 0 & \rho_2 & 0 & 0 & 0 & 0 & \sigma_2 & 0 & 0 & 0 & 0 & 0 & 0 & 0 & 0 & 0 & 0 & 0 \\
\sigma_{123} & 0 & 0 & \rho_2 & 0 & 0 & 0 & 0 & \sigma_3 & 0 & 0 & 0 & 0 & 0 & 0 & 0 & 0 & 0 & 0 \\
\hline
0 & \rho_1\sigma_1 & \sigma_1 & 0 & 0 & 0 & 0 & \rho_1 & \rho_1\sigma_1 & 0 & 0 & 0 & 0 & 0 & 0 & 0 & 0 & 0 & 0 \\
0 & \rho_1 & 1 & 0 & 0 & 0 & 0 & 0 & 0 & 0 & \sigma_2 & 0 & 0 & 0 & 0 & 0 & 0 & 0 & 0 \\
0 & 0 & \sigma_{123} & 1 & 0 & 0 & 0 & 0 & 0 & 0 & 0 & \sigma_3 & 0 & 0 & 0 & 0 & 0 & 0 & 0 \\
0 & 0 & 0 & 0 & 1 & 0 & 0 & 0 & 0 & 0 & 0 & 0 & 0 & 0 & \sigma_3 & 0 & 0 & 0 & \rho_3 \\
0 & \rho_{123} & 0 & 0 & 0 & 1 & 0 & 0 & 0 & 0 & 0 & 0 & 0 & 0 & 0 & \sigma_2 & 0 & \rho_3 & 0 \\
0 & 0 & 0 & 0 & 0 & 0 & 1 & \rho_{123} & 0 & 0 & 0 & 0 & 0 & 0 & 0 & 0 & \rho_3 & 0 & 0 \\
0 & 0 & 0 & 0 & 0 & 0 & 0 & 1 & 0 & 0 & \rho_2 & 0 & 0 & 0 & 0 & 0 & 0 & 0 & 0 \\
0 & 0 & 0 & 0 & 0 & 0 & 0 & 0 & 1 & 0 & 0 & \rho_2 & 0 & 0 & 0 & 0 & \sigma_2 & 0 & 0 \\
0 & \sigma_{123} & 0 & 0 & 0 & 0 & 0 & 0 & \sigma_{123} & 1 & 0 & 0 & \rho_2 & 0 & 0 & 0 & 0 & \sigma_3 & 0
\end{array}\right)$$

The block decomposition indicates the filtration levels.

Finally, to compute $\widehat{\mathrm{CFAA}}(\mathcal{Y}, B_3, 0)$, we use the AA identity bimodule described in Theorem 2.3:

$$\widehat{\mathrm{CFAA}}(\mathcal{Y}, B_3, 0) \simeq \widehat{\mathrm{CFAA}}(\mathbb{I}, 0) \underset{\mathcal{A}_\sigma}{\boxtimes} (\widehat{\mathrm{CFAA}}(\mathbb{I}, 0) \underset{\mathcal{A}_\rho}{\boxtimes} \widehat{\mathrm{CFDD}}(\mathcal{Y}, B_3, 0)).$$

We evaluate this tensor product using our *Mathematica* package. The filtration on $\widehat{\mathrm{CFDD}}(\mathcal{Y}, B_3, 0)$ induces a filtration on $\widehat{\mathrm{CFAA}}(\mathcal{Y}, B_3, 0)$, and we again use the edge cancellation procedure to reduce the number of generators.

Theorem 3.4. *The filtered AA-module* $\widehat{\mathrm{CFAA}}(\mathcal{Y}, B_3, 0)$ *has a basis*

$$\{a_1, \ldots, a_5, b_1, \ldots, b_6, c_1, d_1, \ldots, d_4, e_1, e_2, e_3\}$$

with the following properties:

(1) *The Alexander gradings of the basis elements are:*

$$\begin{aligned} A(c_1) &= -1 \\ A(a_i) = A(d_i) &= 0 \\ A(b_i) = A(e_i) &= 1. \end{aligned}$$

(2) *The associated idempotents in* $\mathcal{A}_\rho$ *and* $\mathcal{A}_\sigma$ *of the generators are:*

	ι_0^ρ	ι_1^ρ
ι_0^σ	$a_1, a_3, a_4, b_1, b_3, b_4, b_6$	d_1, d_3, e_1, e_3
ι_1^σ	a_2, a_5, b_2, b_5	c_1, d_2, d_4, e_2

(3) *The* A_∞ *multiplications are presented in the matrices that follow. For* $x, y \in \{a, b, c, d, e\}$, *the entry in the* i^{th} *row and* j^{th} *column of the matrix* M_{xy} *records the multiplications taking* x_i *to* y_j, *as described in Subsection 2.1. The matrices* M_{ab}, M_{cb}, M_{cd}, M_{ce}, M_{db}, *and* M_{de} *are necessarily zero because of the Alexander grading.*

$$M_{aa} = \begin{pmatrix} 0 & \sigma_1 & \sigma_{12} & \rho_{12} & \sigma_{123}\rho_{12} + \sigma_1\rho_3\rho_2\rho_{12} \\ 0 & 0 & \sigma_2 & 0 & \sigma_{23}\rho_{12} + \rho_{12} \\ 0 & 0 & 0 & 0 & \sigma_3\rho_{12} \\ 0 & 0 & 0 & 0 & \sigma_1 \\ 0 & 0 & 0 & 0 & 0 \end{pmatrix}$$

$$M_{ac} = \begin{pmatrix} \begin{array}{l} \sigma_{123}\rho_{123} + \sigma_{123}\sigma_{23}\rho_{123} + \sigma_3\sigma_2\sigma_1\rho_{123} + \sigma_1\sigma_{23}\rho_3\rho_2\rho_{123} \\ \qquad + \sigma_{123}\sigma_{23}\rho_3\rho_2\rho_1 + \sigma_3\sigma_2\sigma_1\rho_3\rho_2\rho_1 + \sigma_1\sigma_{23}\rho_3\rho_2\rho_3\rho_2\rho_1 \end{array} \\ \sigma_{23}\rho_{123} + \rho_3\rho_2\rho_1 + \sigma_{23}\sigma_{23}\rho_{123} + \sigma_{23}\sigma_{23}\rho_3\rho_2\rho_1 \\ \sigma_3\sigma_{23}\rho_{123} + \sigma_3\rho_3\rho_2\rho_1 + \sigma_3\sigma_{23}\rho_3\rho_2\rho_1 \\ \sigma_{123}\rho_3 + \sigma_3\sigma_2\sigma_1\rho_3 \\ \sigma_{23}\rho_3 \end{pmatrix}$$

$$M_{ad} = \begin{pmatrix} \rho_1 & 0 & \begin{array}{l} \sigma_{12}\rho_{123} + \sigma_{123}\sigma_2\rho_{123} + \sigma_{12}\rho_3\rho_2\rho_1 + \sigma_1\sigma_2\rho_3\rho_2\rho_{123} \\ \qquad + \sigma_{123}\sigma_2\rho_3\rho_2\rho_1 + \sigma_1\sigma_2\rho_3\rho_2\rho_3\rho_2\rho_1 \end{array} & \sigma_{123}\rho_1 + \sigma_1\rho_3\rho_2\rho_1 \\ 0 & \rho_1 & \sigma_2\rho_{123} + \sigma_{23}\sigma_2\rho_{123} + \sigma_2\rho_3\rho_2\rho_1 + \sigma_{23}\sigma_2\rho_3\rho_2\rho_1 & \sigma_{23}\rho_1 \\ 0 & 0 & \sigma_3\sigma_2\rho_{123} + \sigma_3\sigma_2\rho_3\rho_2\rho_1 + \rho_1 & \sigma_3\rho_1 \\ 0 & 0 & \sigma_{12}\rho_3 & 0 \\ 0 & 0 & \sigma_2\rho_3 & 0 \end{pmatrix}$$

$$M_{ba} = \begin{pmatrix} 1 & 0 & 0 & \sigma_3\sigma_2\rho_{123}\rho_2 + \sigma_3\sigma_2\rho_3\rho_2\rho_1\rho_2 & \sigma_{123}\rho_3\rho_2\rho_{12} + \sigma_1\rho_3\rho_2\rho_3\rho_2\rho_{12} \\ 0 & 1 & 0 & 0 & \rho_3\rho_2\rho_{12} + \sigma_{23}\rho_3\rho_2\rho_{12} \\ 0 & 0 & 1 & 0 & \sigma_3\rho_3\rho_2\rho_{12} \\ 0 & 0 & 0 & 1 + \sigma_3\sigma_2\rho_3\rho_2 & \sigma_{123} \\ 0 & 0 & 0 & 0 & 1 + \sigma_{23} \\ 0 & 0 & 0 & 0 & \sigma_3 \end{pmatrix}$$

$$M_{bb} = \begin{pmatrix} 0 & \sigma_1 & \sigma_{12} & \rho_{12} & 0 & 0 \\ 0 & 0 & \sigma_2 & 0 & \rho_{12} & 0 \\ 0 & 0 & 0 & 0 & 0 & \rho_{12} \\ 0 & 0 & 0 & 0 & \sigma_1 & \sigma_{12} \\ 0 & 0 & 0 & 0 & 0 & \sigma_2 \\ 0 & 0 & 0 & 0 & 0 & 0 \end{pmatrix}$$

$$M_{bc} = \begin{pmatrix} \begin{array}{l} \sigma_3\sigma_2\sigma_{123}\rho_{123}\rho_{23} + \sigma_{123}\sigma_{23}\rho_3\rho_2\rho_{123} + \sigma_{123}\rho_3\rho_2\rho_3\rho_2\rho_1 + \sigma_1\sigma_{23}\rho_3\rho_2\rho_3\rho_2\rho_{123} \\ \qquad + \sigma_3\sigma_2\sigma_3\sigma_2\sigma_1\rho_{123}\rho_{23} + \sigma_3\sigma_2\sigma_{123}\rho_3\rho_2\rho_1\rho_{23} + \sigma_{123}\sigma_{23}\rho_3\rho_2\rho_3\rho_2\rho_1 \\ \qquad + \sigma_1\sigma_{23}\rho_3\rho_2\rho_3\rho_2\rho_3\rho_2\rho_1 + \sigma_3\sigma_2\sigma_3\sigma_2\sigma_1\rho_3\rho_2\rho_1\rho_{23} \end{array} \\ \sigma_{23}\rho_3\rho_2\rho_{123} + \rho_3\rho_2\rho_3\rho_2\rho_1 + \sigma_{23}\sigma_{23}\rho_3\rho_2\rho_{123} + \sigma_{23}\sigma_{23}\rho_3\rho_2\rho_3\rho_2\rho_1 \\ \sigma_3\sigma_{23}\rho_3\rho_2\rho_{123} + \sigma_3\rho_3\rho_2\rho_3\rho_2\rho_1 + \sigma_3\sigma_{23}\rho_3\rho_2\rho_3\rho_2\rho_1 \\ \sigma_3\sigma_2\sigma_{123}\rho_3\rho_{23} + \sigma_3\sigma_2\sigma_3\sigma_2\sigma_1\rho_3\rho_{23} \\ 0 \\ 0 \end{pmatrix}$$

$$M_{bd} = \begin{pmatrix} 0 & \sigma_{123}\rho_{123} + \sigma_{123}\rho_3\rho_2\rho_1 & \begin{array}{l} \sigma_3\sigma_2\sigma_{12}\rho_{123}\rho_{23} + \sigma_{123}\sigma_2\rho_3\rho_2\rho_{123} \\ \quad + \sigma_1\sigma_2\rho_3\rho_2\rho_3\rho_2\rho_{123} + \sigma_3\sigma_2\sigma_{12}\rho_3\rho_2\rho_1\rho_{23} \\ \quad + \sigma_{123}\sigma_2\rho_3\rho_2\rho_3\rho_2\rho_1 + \sigma_1\sigma_2\rho_3\rho_2\rho_3\rho_2\rho_3\rho_2\rho_1 \end{array} & \begin{array}{l} \sigma_{123}\rho_{123} + \sigma_3\sigma_2\sigma_1\rho_{123} \\ \quad + \sigma_1\rho_3\rho_2\rho_3\rho_2\rho_1 \\ \quad + \sigma_3\sigma_2\sigma_1\rho_3\rho_2\rho_1 \end{array} \\ 0 & \sigma_{23}\rho_{123} + \sigma_{23}\rho_3\rho_2\rho_1 & \begin{array}{l} \sigma_2\rho_3\rho_2\rho_{123} + \sigma_{23}\sigma_2\rho_3\rho_2\rho_{123} + \sigma_2\rho_3\rho_2\rho_3\rho_2\rho_1 \\ \quad + \sigma_{23}\sigma_2\rho_3\rho_2\rho_3\rho_2\rho_1 \end{array} & \sigma_{23}\rho_{123} + \rho_3\rho_2\rho_1 \\ 0 & \sigma_3\rho_{123} + \sigma_3\rho_3\rho_2\rho_1 & \begin{array}{l} \rho_3\rho_2\rho_1 + \sigma_3\sigma_2\rho_3\rho_2\rho_{123} \\ \quad + \sigma_3\sigma_2\rho_3\rho_2\rho_3\rho_2\rho_1 + \rho_{123} \end{array} & \sigma_3\rho_{123} \\ 0 & \sigma_{123}\rho_3 & \sigma_3\sigma_2\sigma_{12}\rho_3\rho_{23} & \sigma_{123}\rho_3 + \sigma_3\sigma_2\sigma_1\rho_3 \\ 0 & \sigma_{23}\rho_3 & 0 & \sigma_{23}\rho_3 \\ 0 & \sigma_3\rho_3 & \rho_3 & \sigma_3\rho_3 \end{pmatrix}$$

$$M_{be} = \begin{pmatrix} \rho_1 & 0 & 0 \\ 0 & \rho_1 & 0 \\ 0 & 0 & \rho_1 \\ 0 & 0 & 0 \\ 0 & 0 & 0 \\ 0 & 0 & 0 \end{pmatrix}$$

$$M_{cc} = (0)$$

$$M_{da} = \begin{pmatrix} 0 & 0 & 0 & \rho_2 & 0 \\ 0 & 0 & 0 & 0 & \rho_2 \\ 0 & 0 & 0 & 0 & 0 \\ 0 & 0 & 0 & 0 & \rho_2 \end{pmatrix}$$

$$M_{dc} = \begin{pmatrix} \sigma_{123}\rho_{23} + \sigma_3\sigma_2\sigma_1\rho_{23} + \sigma_{123} \\ \sigma_{23}\rho_{23} + \sigma_{23} \\ \sigma_3 \\ 1 + \sigma_{23}\rho_{23} \end{pmatrix}$$

$$M_{dd} = \begin{pmatrix} 0 & \sigma_1 & \sigma_{12}\rho_{23} + \sigma_{12} & 0 \\ 0 & 0 & \sigma_2\rho_{23} + \sigma_2 & 0 \\ 0 & 0 & 0 & 0 \\ 0 & 0 & \sigma_2\rho_{23} & 0 \end{pmatrix}$$

$$M_{ea} = \begin{pmatrix} 0 & 0 & 0 & \sigma_3\sigma_2\rho_{23}\rho_2 & 0 \\ 0 & 0 & 0 & 0 & 0 \\ 0 & 0 & 0 & 0 & 0 \end{pmatrix}$$

$$M_{eb} = \begin{pmatrix} 0 & 0 & 0 & \rho_2 & 0 & 0 \\ 0 & 0 & 0 & 0 & \rho_2 & 0 \\ 0 & 0 & 0 & 0 & 0 & \rho_2 \end{pmatrix}$$

$$M_{ec} = \begin{pmatrix} \sigma_3\sigma_2\sigma_{123}\rho_{23}\rho_{23} \\ 0 \\ 0 \end{pmatrix}$$

$$M_{ed} = \begin{pmatrix} 1 & \sigma_{123}\rho_{23} & \sigma_3\sigma_2\sigma_{12}\rho_{23}\rho_{23} & \sigma_{123}\rho_{23} + \sigma_3\sigma_2\sigma_1\rho_{23} + \sigma_{123} \\ 0 & 1 + \sigma_{23}\rho_{23} & 0 & \sigma_{23}\rho_{23} + \sigma_{23} \\ 0 & \sigma_3\rho_{23} & 1 + \rho_{23} & \sigma_3\rho_{23} + \sigma_3 \end{pmatrix}$$

$$M_{ee} = \begin{pmatrix} 0 & \sigma_1 & \sigma_{12} \\ 0 & 0 & \sigma_2 \\ 0 & 0 & 0 \end{pmatrix}$$

Because we are ultimately interested in the tensor product of $\widehat{\mathrm{CFAA}}(\mathcal{Y}, B_3, 0)$ with $\widehat{\mathrm{CFD}}(\mathcal{X}_J^s)$ and $\widehat{\mathrm{CFD}}(\mathcal{X}_K^t)$, we may disregard any higher multiplication that uses sequences of algebra elements that cannot occur in these type D structures. Specifically, by Proposition 2.4, we may disregard any sequence containing $\rho_2\rho_3$, $\rho_1\rho_2$, $\rho_1\rho_{23}$, $\sigma_2\sigma_3$, $\sigma_1\sigma_2$, or $\sigma_1\sigma_{23}$. Accordingly, for the discussion that follows, we may replace M_{ac}, M_{ad}, M_{ba}, M_{bc}, and M_{bd} with the following:

$$M'_{ac} = \begin{pmatrix} \sigma_{123}\rho_{123} + \sigma_{123}\sigma_{23}\rho_{123} + \sigma_3\sigma_2\sigma_1\rho_{123} + \sigma_{123}\sigma_{23}\rho_3\rho_2\rho_1 + \sigma_3\sigma_2\sigma_1\rho_3\rho_2\rho_1 \\ \sigma_{23}\rho_{123} + \rho_3\rho_2\rho_1 + \sigma_{23}\sigma_{23}\rho_{123} + \sigma_{23}\sigma_{23}\rho_3\rho_2\rho_1 \\ \sigma_3\sigma_{23}\rho_{123} + \sigma_3\rho_3\rho_2\rho_1 + \sigma_3\sigma_{23}\rho_3\rho_2\rho_1 \\ \sigma_{123}\rho_3 + \sigma_3\sigma_2\sigma_1\rho_3 \\ \sigma_{23}\rho_3 \end{pmatrix}$$

$$M'_{ad} = \begin{pmatrix} \rho_1 & 0 & \sigma_{12}\rho_{123} + \sigma_{123}\sigma_2\rho_{123} + \sigma_{12}\rho_3\rho_2\rho_1 + \sigma_{123}\sigma_2\rho_3\rho_2\rho_1 & \sigma_{123}\rho_1 + \sigma_1\rho_3\rho_2\rho_1 \\ 0 & \rho_1 & \sigma_2\rho_{123} + \sigma_{23}\sigma_2\rho_{123} + \sigma_2\rho_3\rho_2\rho_1 + \sigma_{23}\sigma_2\rho_3\rho_2\rho_1 & \sigma_{23}\rho_1 \\ 0 & 0 & \sigma_3\sigma_2\rho_{123} + \sigma_3\sigma_2\rho_3\rho_2\rho_1 + \rho_1 & \sigma_3\rho_1 \\ 0 & 0 & \sigma_{12}\rho_3 & 0 \\ 0 & 0 & \sigma_2\rho_3 & 0 \end{pmatrix}$$

$$M'_{ba} = \begin{pmatrix} 1 & 0 & 0 & \sigma_3\sigma_2\rho_{123}\rho_2 & \sigma_{123}\rho_3\rho_2\rho_{12} \\ 0 & 1 & 0 & 0 & \rho_3\rho_2\rho_{12} + \sigma_{23}\rho_3\rho_2\rho_{12} \\ 0 & 0 & 1 & 0 & \sigma_3\rho_3\rho_2\rho_{12} \\ 0 & 0 & 0 & 1 + \sigma_3\sigma_2\rho_3\rho_2 & \sigma_{123} \\ 0 & 0 & 0 & 0 & 1 + \sigma_{23} \\ 0 & 0 & 0 & 0 & \sigma_3 \end{pmatrix}$$

$$M'_{bc} = \begin{pmatrix} \sigma_3\sigma_2\sigma_{123}\rho_{123}\rho_{23} + \sigma_{123}\sigma_{23}\rho_3\rho_2\rho_{123} \\ \sigma_{23}\rho_3\rho_2\rho_{123} + \sigma_{23}\sigma_{23}\rho_3\rho_2\rho_{123} \\ \sigma_3\sigma_{23}\rho_3\rho_2\rho_{123} \\ \sigma_3\sigma_2\sigma_{123}\rho_3\rho_{23} \\ 0 \\ 0 \end{pmatrix}$$

$$M'_{bd} = \begin{pmatrix} 0 & \sigma_{123}\rho_{123} + \sigma_{123}\rho_3\rho_2\rho_1 & \sigma_3\sigma_2\sigma_{12}\rho_{123}\rho_{23} + \sigma_{123}\sigma_2\rho_3\rho_2\rho_{123} & \begin{matrix} \sigma_{123}\rho_{123} + \sigma_3\sigma_2\sigma_1\rho_{123} \\ + \sigma_3\sigma_2\sigma_1\rho_3\rho_2\rho_1 \end{matrix} \\ 0 & \sigma_{23}\rho_{123} + \sigma_{23}\rho_3\rho_2\rho_1 & \sigma_2\rho_3\rho_2\rho_{123} + \sigma_{23}\sigma_2\rho_3\rho_2\rho_{123} & \sigma_{23}\rho_{123} + \rho_3\rho_2\rho_1 \\ 0 & \sigma_3\rho_{123} + \sigma_3\rho_3\rho_2\rho_1 & \rho_3\rho_2\rho_1 + \sigma_3\sigma_2\rho_3\rho_2\rho_{123} + \rho_{123} & \sigma_3\rho_{123} \\ 0 & \sigma_{123}\rho_3 & \sigma_3\sigma_2\sigma_{12}\rho_3\rho_{23} & \sigma_{123}\rho_3 + \sigma_3\sigma_2\sigma_1\rho_3 \\ 0 & \sigma_{23}\rho_3 & 0 & \sigma_{23}\rho_3 \\ 0 & \sigma_3\rho_3 & \rho_3 & \sigma_3\rho_3 \end{pmatrix}$$

4. Evaluation of the tensor product

Using the computation of $\widehat{\mathrm{CFAA}}(\mathcal{Y}, B_3, 0)$ given in the previous section, we may now compute the double tensor product

$$(\widehat{\mathrm{CFAA}}(\mathcal{Y}, B_3, 0) \underset{\mathcal{A}_\rho}{\boxtimes} \widehat{\mathrm{CFD}}(\mathcal{X}_J^s)) \underset{\mathcal{A}_\sigma}{\boxtimes} \widehat{\mathrm{CFD}}(\mathcal{X}_K^t).$$

In what follows, we evaluate the tensor product over $\mathcal{A}_\rho$ and simplify the resulting filtered type A module before evaluating the tensor product over $\mathcal{A}_\sigma$. Then we use the edge cancellation algorithm to compute $\tau(D_{J,s}(K,t))$. As a reminder, we restate the main theorem:

$$\tau(D_{J,s}(K,t)) = \begin{cases} 1 & s < 2\tau(J) \text{ and } t < 2\tau(K) \\ -1 & s > 2\tau(J) \text{ and } t > 2\tau(K) \\ 0 & \text{otherwise.} \end{cases}$$

Notice that it suffices to consider only the cases where $s \le 2\tau(J)$, since if $s > 2\tau(J)$, the behavior of τ under mirroring implies:

$$\begin{aligned} \tau(D_{J,s}(K,t)) &= -\tau\left(\overline{D_{J,s}(K,t)}\right) \\ &= -\tau(D_{\bar{J},-s}(\bar{K},-t)) \\ &= \begin{cases} -1 & -t < 2\tau(\bar{K}) \\ 0 & -t \ge 2\tau(\bar{K}) \end{cases} \\ &= \begin{cases} -1 & t > -2\tau(K) \\ 0 & t \le -2\tau(K) \end{cases} \end{aligned}$$

With only slightly more bookkeeping, we could also write down a formula for the knot Floer homology groups $\widehat{\mathrm{HFK}}(D_{J,s}(K,t))$, but since we are primarily interested in the value of τ and its applications to knot and link concordance, we do not bother to do that here.[5]

4.1. Tensor product over $\mathcal{A}_\rho$.

Let $\mathcal{V}$ denote the bordered solid torus obtained by gluing together $\mathcal{Y}$ and $\mathcal{X}_J^s$, and let $D_{J,s}$ denote the image of the knot B_3 in the union. By the gluing theorem, $\widehat{\mathrm{CFA}}(\mathcal{V}, D_{J,s}) \simeq \widehat{\mathrm{CFAA}}(\mathcal{Y}, B_3, 0) \underset{\mathcal{A}_\rho}{\boxtimes} \widehat{\mathrm{CFD}}(\mathcal{X}_J^s)$. We shall describe this tensor product as a direct sum of subspaces corresponding to the stable and unstable chains in $\widehat{\mathrm{CFD}}(\mathcal{X}_J^s)$. This decomposition will not be a direct sum of $\mathcal{A}_\infty$ modules, but we will be able to keep track of the few multiplications that do not respect the decomposition, and ultimately they will not affect the computation of $\tau(D_{J,s}(K,t))$.

The generators of $\iota_1\widehat{\mathrm{CFD}}(\mathcal{X}_J^s)$ all lie in the interiors of the chains, so the corresponding generators of the tensor product can be grouped in a natural way, but it is not obvious *a priori* how to divide up the generators coming from $\iota_0\widehat{\mathrm{CFD}}(\mathcal{X}^s_J)$. Consider the two specified bases for $\iota_0\widehat{\mathrm{CFD}}(\mathcal{X}^s_J)$: $\{\eta_0,\dots,\eta_{2n}\}$ and $\{\xi_0,\dots,\xi_{2n}\}$. Depending on the structure of the unstable chain, the generators ξ_i have outgoing arrows labeled ρ_1, ρ_{12}, or ρ_{123}, while the η_i have outgoing arrows labeled ρ_3 and incoming arrows labeled ρ_2 or ρ_{12}. Accordingly, we should try to pair the generators of $\widehat{\mathrm{CFAA}}(\mathcal{Y},B_3,0)\iota_0$ with the ξ_i or η_i depending on which of these two conditions they satisfy. If we consider only the $\mathcal{A}_\infty$ maps in $\widehat{\mathrm{CFAA}}(\mathcal{Y},B_3,0)$ that use a single element of $\mathcal{A}_\rho$, we notice that each of the generators $a_1,\dots,a_5$ and $b_1,\dots,b_6$ satisfies exactly one such condition. Specifically, define the following subspaces of $\widehat{\mathrm{CFAA}}(\mathcal{Y},B_3,0)\underset{\mathcal{A}_\rho}{\boxtimes}\widehat{\mathrm{CFD}}(\mathcal{X}^s_J)$:

---

[5] A simplified computation in which the knot J is assumed to be the unknot can be found in a previous version of [9], available online at arXiv:0912.5222v1.

$$\begin{aligned} P^j_{\mathrm{vert}} &= \langle a_4,a_5,b_4,b_5,b_6\rangle \boxtimes \langle \xi_{2j-1},\xi_{2j}\rangle \\ &\quad + \langle c_1,d_1,d_2,d_3,d_4,e_1,e_2,e_3\rangle \boxtimes \left\langle \kappa^j_i \mid 1\le i\le k_j\right\rangle \\ P^j_{\mathrm{hor}} &= \langle a_1,a_2,a_3,b_1,b_2,b_3\rangle \boxtimes \langle \eta_{2j-1},\eta_{2j}\rangle \\ &\quad + \langle c_1,d_1,d_2,d_3,d_4,e_1,e_2,e_3\rangle \boxtimes \left\langle \lambda^j_i \mid 1\le i\le l_j\right\rangle \\ P_{\mathrm{unst}} &= \langle a_4,a_5,b_4,b_5,b_6\rangle \boxtimes \langle \xi_0\rangle \\ &\quad + \langle a_1,a_2,a_3,b_1,b_2,b_3\rangle \boxtimes \langle \eta_0\rangle \\ &\quad + \langle c_1,d_1,d_2,d_3,d_4,e_1,e_2,e_3\rangle \boxtimes \langle \lambda_i \mid 1\le i\le r\rangle\,. \end{aligned} \tag{14}$$

We thus obtain a direct sum decomposition of $\widehat{\mathrm{CFAA}}(\mathcal{Y},B_3,0)\underset{\mathcal{A}_\rho}{\boxtimes}\widehat{\mathrm{CFD}}(\mathcal{X}^s_J)$ as a vector space:

$$\widehat{\mathrm{CFAA}}(\mathcal{Y},B_3,0)\underset{\mathcal{A}_\rho}{\boxtimes}\widehat{\mathrm{CFD}}(\mathcal{X}^s_J) = \bigoplus_{j=1}^n P^j_{\mathrm{vert}} \oplus \bigoplus_{j=1}^n P^j_{\mathrm{hor}} \oplus P_{\mathrm{unst}}. \tag{15}$$

By inspecting the matrices M_{xy}, we see that any $\mathcal{A}_\infty$ multiplication on the tensor product that comes from a multiplication in $\widehat{\mathrm{CFAA}}(\mathcal{Y},B_3,0)$ that uses at most one element of $\mathcal{A}_\rho$ preserves this decomposition. These multiplications are illustrated in Figures 15 through 18. In these and subsequent figures, the dashed arrows represent repeated sections. For instance, the dashed arrow from $e_1\kappa^j_1$ to $d_2\kappa^j_{k_j}$ in Figure 15 means that there are multiplications $e_1\kappa^j_i \xrightarrow{\sigma_{123}} d_2\kappa^j_{i+1}$ for each $i=1,\dots,k_j-1$. The Alexander grading is indicated by horizontal position, increasing from left to right.

In addition, there are a few more multiplications that preserve the splitting, coming from multiplications in $\widehat{\mathrm{CFAA}}(\mathcal{Y},B_3,0)$ that use sequences like $\rho_3\rho_2$, $\rho_3\rho_{23}$, or $\rho_{23}\rho_{23}$. These multiplications are not shown in Figures 15 through 18. They are as follows:

- In P^j_{vert}, when $k_j>1$, there are multiplications

$$\begin{aligned} &b_1\xi_{2j} \xrightarrow{\sigma_3\sigma_2\sigma_{12}} d_3\kappa^j_2 && b_1\xi_{2j} \xrightarrow{\sigma_3\sigma_2\sigma_{123}} c_1\kappa^j_2 \\ &e_1\kappa^j_i \xrightarrow{\sigma_3\sigma_2\sigma_{12}} d_3\kappa^j_{i+2} && e_1\kappa^j_i \xrightarrow{\sigma_3\sigma_2\sigma_{123}} c_1\kappa^j_{i+2} \quad (i=1,\dots,k_j-2). \end{aligned} \tag{16}$$

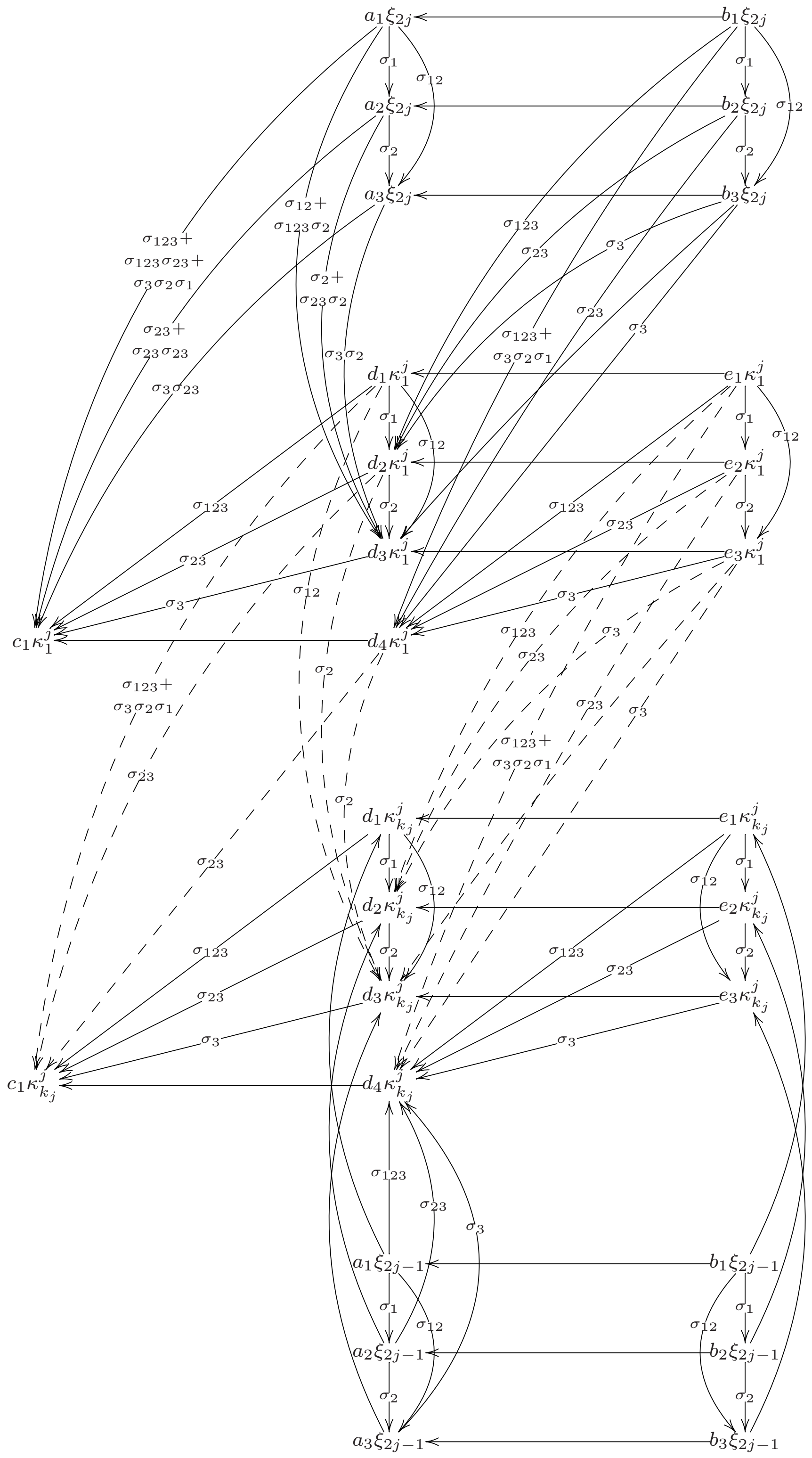

FIGURE 15. The subspace P^j_{vert}, corresponding to a vertical stable chain $\xi_{2j} \xrightarrow{\rho_{123}} \kappa^j_1 \xrightarrow{\rho_{23}} \cdots \xrightarrow{\rho_{23}} \kappa^j_{k_j} \xleftarrow{\rho_1} \xi_{2j-1}$.

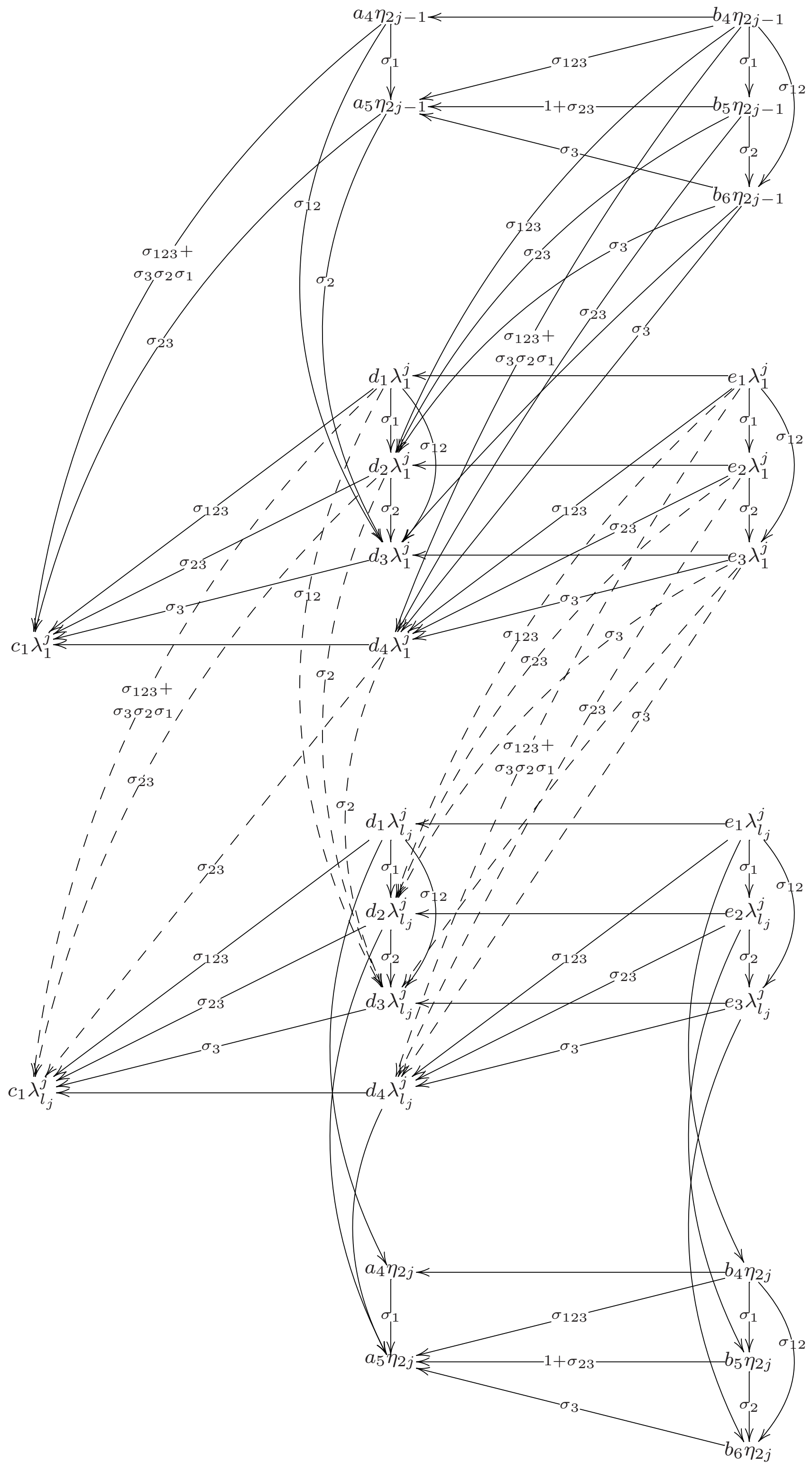

FIGURE 16. The subspace P^j_{hor}, corresponding to a horizontal stable chain $\eta_{2j-1} \xrightarrow{\rho_3} \lambda_1^j \xrightarrow{\rho_{23}} \cdots \xrightarrow{\rho_{23}} \lambda_{l_j}^j \xrightarrow{\rho_2} \eta_{2j}$.

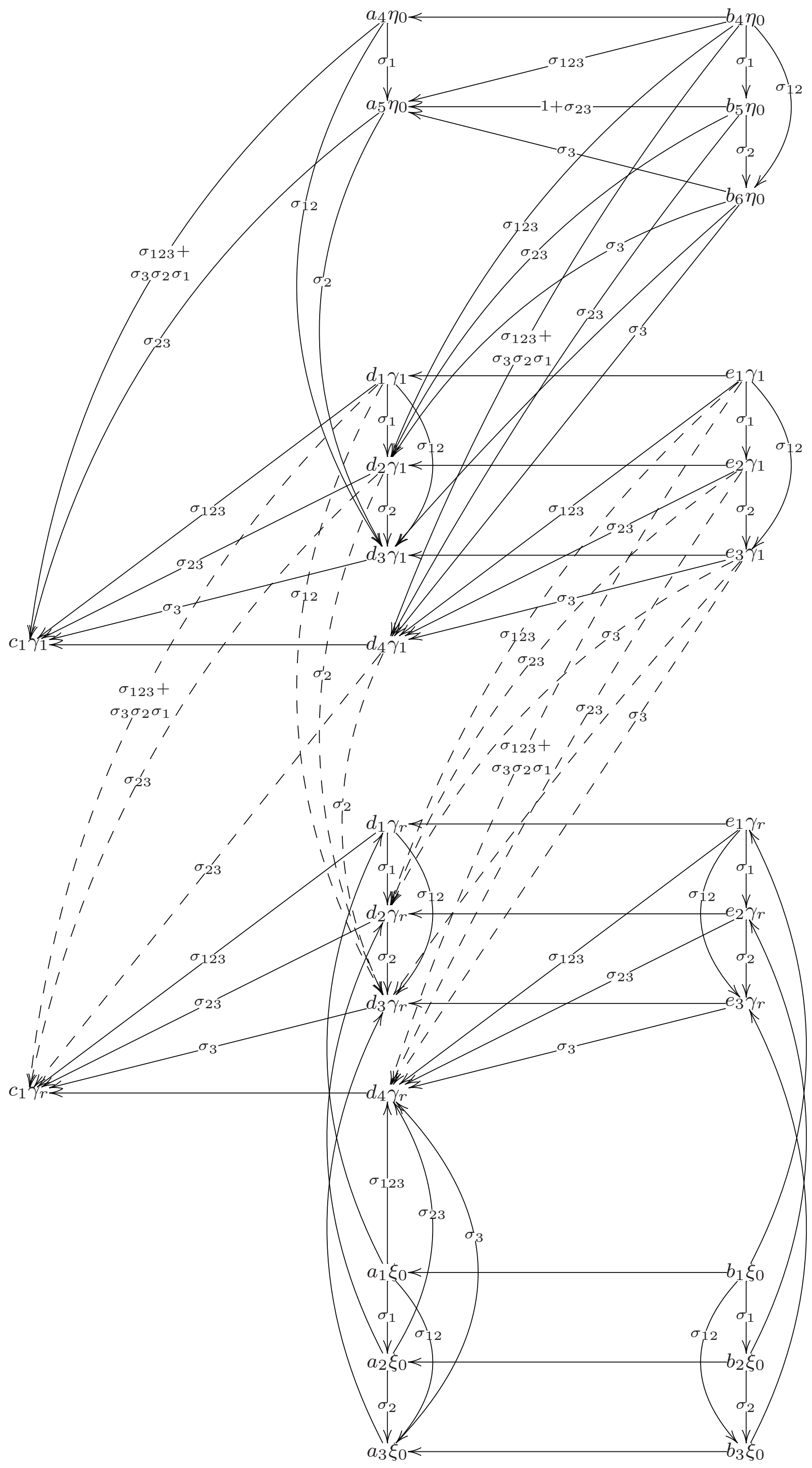

Figure 17. The subspace P_{unst} when $s < 2\tau(J)$, corresponding to the unstable chain $\eta_0 \xrightarrow{\rho_3} \gamma_1 \xrightarrow{\rho_{23}} \cdots \xrightarrow{\rho_{23}} \gamma_s \xleftarrow{\rho_1} \xi_0$.

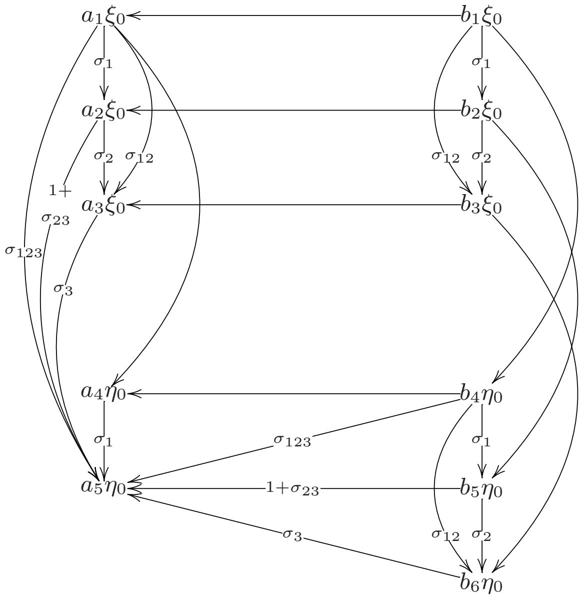

FIGURE 18. The subspace P_{unst} when $s = 2\tau(J)$, corresponding to the unstable chain $\xi_0 \xrightarrow{\rho_{12}} \eta_0$.

- In P^j_{hor}, when $l_j = 1$, there is a multiplication $b_4\eta_{2j-1} \xrightarrow{\sigma_3\sigma_2} a_4\eta_{2j}$. When $l_j > 1$, there are multiplications

$$\begin{aligned} &b_4\eta_{2j-1} \xrightarrow{\sigma_3\sigma_2\sigma_{12}} d_3\lambda^j_2 \qquad && b_4\eta_{2j-1} \xrightarrow{\sigma_3\sigma_2\sigma_{123}} c_1\lambda^j_2 \\ &e_1\lambda^j_{l_j-1} \xrightarrow{\sigma_3\sigma_2} a_4\eta_{2j} && \\ &e_1\lambda^j_i \xrightarrow{\sigma_3\sigma_2\sigma_{12}} d_3\lambda^j_{i+2} && e_1\lambda^j_i \xrightarrow{\sigma_3\sigma_2\sigma_{123}} c_1\lambda^j_{i+2} \quad (i = 1, \dots, l_j - 2). \end{aligned} \tag{17}$$

- In P_{unst} in the case when $s < 2\tau(J) - 1$, there are multiplications

$$\begin{aligned} &b_4\eta_0 \xrightarrow{\sigma_3\sigma_2\sigma_{12}} d_3\gamma_2 \qquad && b_4\eta_0 \xrightarrow{\sigma_3\sigma_2\sigma_{123}} c_1\gamma_2 \\ &e_1\gamma_i \xrightarrow{\sigma_3\sigma_2\sigma_{12}} d_3\gamma_{i+2} && e_1\gamma_i \xrightarrow{\sigma_3\sigma_2\sigma_{123}} c_1\gamma_{i+2} \quad (i = 1, \dots, r - 2). \end{aligned} \tag{18}$$

Finally, we must consider the multiplications in the tensor product that do not respect the splitting in (15). These arise from sequences of arrows in $\widehat{\mathrm{CFD}}(\mathcal{X}^s_J)$ that involve multiple stable or unstable chains, and they depend on the change-of-basis coefficients relating $\{\eta_0, \dots, \eta_{2n}\}$ and $\{\xi_0, \dots, \xi_{2n}\}$.

For instance, if $\eta_{2j} = \xi_{2h}$ (where $j, h \in \{1, \dots, n\}$), then $\widehat{\mathrm{CFD}}(\mathcal{X}^s_J)$ contains a string of arrows of the form

$$\eta_{2j-1} \xrightarrow{\rho_3} \lambda^j_1 \xrightarrow{\rho_{23}} \cdots \xrightarrow{\rho_{23}} \lambda^j_{l_j} \xrightarrow{\rho_2} \eta_{2j} \xrightarrow{\rho_{123}} \kappa^h_1 \xrightarrow{\rho_{23}} \cdots \xrightarrow{\rho_{23}} \kappa^h_{k_h}.$$

Any multiplication in $\widehat{\mathrm{CFAA}}(\mathcal{Y}, B_3, 0)$ that uses a contiguous subsequence of

$$\rho_3, \underbrace{\rho_{23}, \dots, \rho_{23}}_{l_j - 1 \text{ times}}, \rho_2, \rho_{123}, \underbrace{\rho_{23}, \dots, \rho_{23}}_{k_h - 1 \text{ times}}$$

contributes a nonzero multiplication in the tensor product that need not respect the splitting. Similarly, if $\eta_{2j} = \xi_{2h-1}$, then the same is true for contiguous subsequences of

$$\rho_3, \underbrace{\rho_{23}, \dots, \rho_{23}}_{l_j - 1 \text{ times}}, \rho_2, \rho_1.$$

Similar sequences may also occur near the unstable chain, where we take ξ_0 instead of ξ_{2h-1} or ξ_{2h}. By Proposition 2.4, these are the only such sequences that occur. More generally, if the coefficient of ξ_p in η_{2j} is nonzero, we obtain multiplications that do not respect the splitting in (15). We make this notion more precise below.

By inspecting the matrices M_{xy}, we see that the only sequences of this form that actually occur in $\widehat{\mathrm{CFAA}}(\mathcal{Y}, B_3, 0)$ are $\rho_3\rho_2\rho_{123}$, $\rho_3\rho_2\rho_{12}$, and $\rho_3\rho_2\rho_1$, which occur in the first three rows of M_{ac}, M_{ad}, M_{ba}, M_{bc}, and M_{bd}. Accordingly, the only multiplications that do not preserve the splitting arise when there is a horizontal edge $\eta_{2j-1} \to \eta_{2j}$ of length 1, and they act on the elements $a_i \boxtimes \eta_{2j-1}$ and $b_i \boxtimes \eta_{2j-1}$ $(i = 1, 2, 3)$.

Notice that there are no multiplications into or out of any of the subspaces P^j_{hor}. Therefore, each P^j_{hor} is actually a direct summand of $\widehat{\mathrm{CFA}}(\mathcal{V}, D_{J,s})$ as an $\mathcal{A}_\infty$ submodule, as is $P = \bigoplus_{j=1}^n P^j_{\mathrm{vert}} \oplus P_{\mathrm{unst}}$. This implies that the tensor product $\widehat{\mathrm{CFA}}(\mathcal{V}, D_{J,s}) \boxtimes \widehat{\mathrm{CFD}}(\mathcal{X}^t_K)$ (whose total homology, ignoring the filtration, is $\widehat{\mathrm{HF}}(S^3) \cong \mathbb{F}$) will also split as a direct sum. We shall eventually see that the direct summand coming from P contributes $\mathbb{F}$ to the total homology, which means that each summand coming from P^j_{hor} is acyclic and thus does not affect the computation of $\tau(D_{J,s}(K,t))$. Therefore, we shall henceforth ignore the submodules P^j_{hor}.

It is preferable to describe all of the multiplications that do not respect the splitting in terms of the bases specified in (14). Recall that $(x_{p,q})$ and $(y_{p,q})$ are the change-of-basis matrices, so that $\xi_p = \sum_{q=0}^{2n} x_{p,q}\eta_q$ and $\eta_p = \sum_{q=0}^{2n} y_{p,q}\xi_q$. Let $\mathfrak{j}$ denote the set $\{j \in \{1, \dots, n\} \mid l_j = 1\}$. For each $p \in \{0, \dots, 2n\}$ and $h \in \{1, \dots, n\}$, each $j \in \mathfrak{j}$ for which $x_{p,2j-1} = 1$ and $y_{2j,2h-1} = 1$ contributes multiplications (which we will specify shortly) from $a_i\xi_p$ and/or $b_i\xi_p$ $(i = 1, 2, 3)$ into P^h_{vert} via the sequence $\rho_3\rho_2\rho_{123}$. Of course, multiple values of j may satisfy this criterion, but they all contribute the same multiplications, so we really only care about the count of such j modulo 2. That is, define $u_{p,h} = \sum_{j \in \mathfrak{j}} x_{p,2j-1}y_{2j,2h-1}$; there are multiplications from $a_i\xi_p$ and $b_i\xi_p$ into P^h_{vert} iff $u_{p,h} = 1$.

Similarly, each j for which $x_{p,2j-1} = 1$ and $y_{2j,2h}$ $(h = 1, \dots, n)$ contributes multiplications via $\rho_3\rho_2\rho_1$, so define $v_{p,h} = \sum_{j \in \mathfrak{j}} x_{p,2j-1}y_{2j,2h}$. Finally, we set $w_p = \sum_{j \in \mathfrak{j}} x_{p,2j-1}y_{2h,0}$; this determines whether there are additional multiplications from $a_i\xi_p$ and $b_i\xi_p$ into the unstable chain via $\rho_3\rho_2\rho_1$, $\rho_3\rho_2\rho_{12}$, or $\rho_3\rho_2\rho_{123}$, according to whether $s < 2\tau(J)$, $s = 2\tau(J)$ or $s > 2\tau(K)$, respectively (although we are ignoring the third case).

We now specify these multiplications:

- If $u_{p,h} = 1$, the sequence $\rho_3\rho_2\rho_{123}$ provides the multiplications shown in Figure 19.

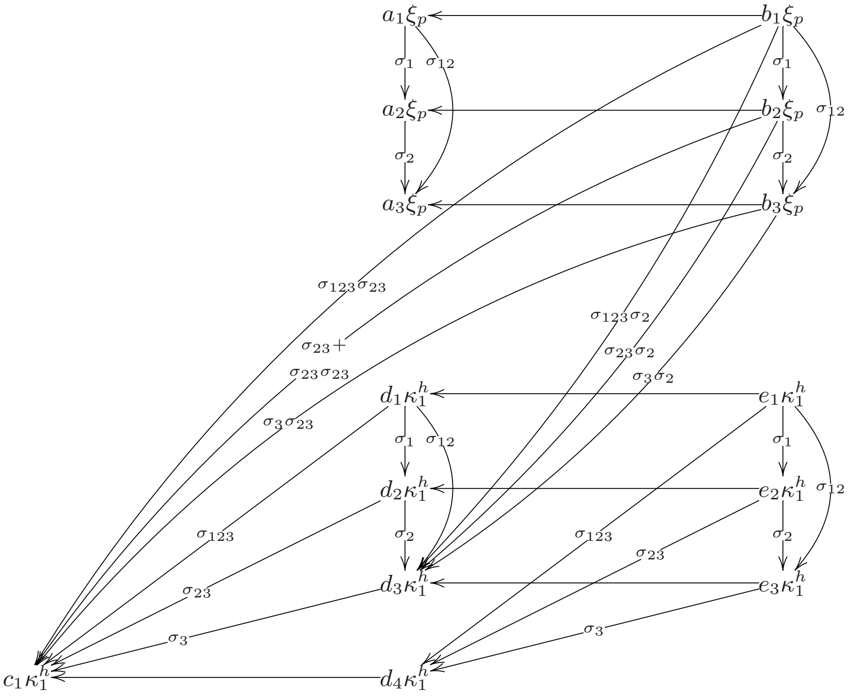

Figure 19. Multiplications coming from a sequence $\rho_3\rho_2\rho_{123}$ when $u_{p,h} = 1$.

- If $v_{p,h} = 1$, the sequence $\rho_3\rho_2\rho_1$ provides the multiplications shown in Figure 20.
- If $s < 2\tau(J)$ and $w_p = 1$, the sequence $\rho_3\rho_2\rho_1$ provides the multiplications shown in Figure 20, where we replace $\kappa^h_{k_h}$ by γ_r.
- Finally, if $s = 2\tau(K)$ and $w_p = 1$, the sequence $\rho_3\rho_2\rho_{12}$ provides the following multiplications:

$$\begin{gathered} a_1\xi_p \xrightarrow{\sigma_1} a_5\eta_0 \\ b_1\xi_p \xrightarrow{\sigma_{123}} a_5\eta_0 \\ b_2\xi_p \xrightarrow{1+\sigma_{23}} a_5\eta_0 \\ b_3\xi_p \xrightarrow{\sigma_3} a_5\eta_0. \end{gathered} \tag{19}$$

4.2. **Simplification of $\widehat{\mathrm{CFA}}(\mathcal{V}, D_{J,s})$.** Next, we may simplify $\widehat{\mathrm{CFA}}(\mathcal{V}, D_{J,s})$ by canceling unmarked edges that preserve the filtration level. In order to keep track of additional edges that may appear, we must look carefully at the order of cancellation. As mentioned above, we ignore the direct summands P^j_{hor}. Define $P^0 = P_{\mathrm{unst}}$ and $P^j = P^j_{\mathrm{vert}}$.

Assume first that $s < 2\tau(J)$.

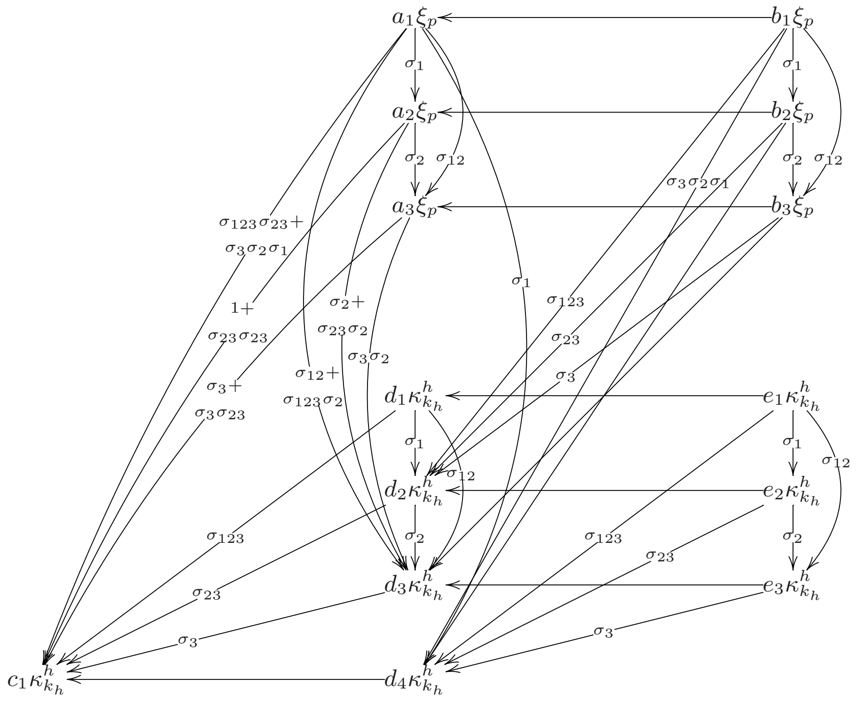

FIGURE 20. Multiplications coming from a sequence $\rho_3\rho_2\rho_1$ when $v_{p,h} = 1$. If $w_p = 1$ and $s < 2\tau(K)$, we obtain the same multiplications by replacing $\kappa^h_{k_h}$ by γ_r.

For each $j \in \{1, \dots, n\}$, in P^j, we may cancel the differentials $b_1\xi_{2j-1} \to e_1\kappa^j_{k_j}$, $b_2\xi_{2j-1} \to e_2\kappa^j_{k_j}$, $b_2\xi_{2j-1} \to e_2\kappa^j_{k_j}$, and $a_1\xi_{2j-1} \to d_1\kappa^j_{k_j}$. Since the targets of those arrows do not lie at the heads of any other arrows, no additional arrows are introduced. Similarly, in P^0, cancel $b_1\xi_0 \to e_1\gamma_r$, $b_2\xi_0 \to e_2\gamma_r$, $b_2\xi_0 \to e_2\gamma_r$, and $a_1\xi_0 \to d_1\gamma_r$.

Next, we cancel the differentials $a_2\xi_{2j-1} \to d_2\kappa^j_{k_j}$ and $a_2\xi_0 \to d_2\gamma_r$. Because of the edge $a_2\xi_{2j-1} \xrightarrow{\sigma_{23}} d_4\kappa^j_{k_j}$, canceling $a_2\xi_{2j-1} \to d_2\kappa^j_{k_j}$ introduces new multiplications:

$$\begin{aligned}
&e_1\kappa^j_{k_j-1} \xrightarrow{\sigma_{123}\sigma_2} a_3\xi_{2j-1} \qquad && e_1\kappa^j_{k_j-1} \xrightarrow{\sigma_{123}\sigma_{23}} d_4\kappa^j_{k_j} \\
&e_2\kappa^j_{k_j-1} \xrightarrow{\sigma_{23}\sigma_2} a_3\xi_{2j-1} && e_2\kappa^j_{k_j-1} \xrightarrow{\sigma_{23}\sigma_{23}} d_4\kappa^j_{k_j} \\
&e_3\kappa^j_{k_j-1} \xrightarrow{\sigma_3\sigma_2} a_3\xi_{2j-1} && e_3\kappa^j_{k_j-1} \xrightarrow{\sigma_3\sigma_{23}} d_4\kappa^j_{k_j}.
\end{aligned} \tag{20}$$

(If $k_j = 1$, then replace $e_i\kappa^j_{k_j-1}$ by $b_i\xi_{2j}$ in (20).) We shall examine the effects of these cancellations on the edges that do not respect the splitting momentarily.

Next, because of the edge $a_3\xi_{2j-1} \xrightarrow{\sigma_3} d_4\kappa^j_{k_j}$, canceling $a_3\xi_{2j-1} \to d_3\kappa^j_{k_j}$ removes the edge $e_3\kappa^j_{k_j-1} \xrightarrow{\sigma_3} d_4\kappa^j_{k_j}$ and adds edges

$$\begin{aligned} &d_1\kappa^j_{k_j-1} \xrightarrow{\sigma_{12}\sigma_3} d_4\kappa^j_{k_j} \\ &d_2\kappa^j_{k_j-1} \xrightarrow{\sigma_2\sigma_3} d_4\kappa^j_{k_j} \\ &d_4\kappa^j_{k_j-1} \xrightarrow{\sigma_2\sigma_3} d_4\kappa^j_{k_j} \\ &e_1\kappa^j_{k_j-2} \xrightarrow{\sigma_3\sigma_2\sigma_{12}\sigma_3} d_4\kappa^j_{k_j}. \end{aligned} \tag{21}$$

Because we will ultimately tensor with $\widehat{\mathrm{CFD}}(X^t_K)$, in which the sequences $\sigma_2\sigma_3$ and $\sigma_{12}\sigma_3$ do not appear, we may disregard these four edges. We also eliminate the edge $e_3\kappa^j_{k_j-1} \xrightarrow{\sigma_3} d_4\kappa^j_{k_j-1}$. The same thing occurs in P^0 when we cancel $a_3\xi_0 \to d_3\gamma_r$.

Let Q^j denote the module resulting from P^j after the cancellations just described. The multiplications on Q^j are shown in Figures 21 and 22 and equations (16) and (18).

Now we keep track of what these cancellations do to the edges that do not respect the splitting, as shown in Figures 19 and 20.

If $u_{p,j} = 1$, then there are edges from $b_i\xi_p$ to $d_3\kappa^j_1$, as shown in Figure 19. If $k_j = 1$, then canceling $a_3\xi_{2j-1} \to d_3\kappa^j_1$ will introduce new multiplications coming from $b_i\xi_p$, but all of these multiplications involve $\sigma_2\sigma_3$ or $\sigma_{12}\sigma_3$ and may thus be disregarded. Also, when $p = 2m+1$ or $p = 0$ these edges are eliminated when we cancel $b_i\xi_{2m+1} \to e_i\kappa^m_{k_m}$ or $b_i\xi_0 \to e_i\gamma_r$, respectively.

If $v_{p,j} = 1$, when we cancel $a_2\xi_{2j-1} \to d_2\kappa^j_{k_j}$, we obtain multiplications

$$\begin{aligned} &b_1\xi_p \xrightarrow{\sigma_{123}\sigma_2} a_3\xi_{2j-1} && b_1\xi_p \xrightarrow{\sigma_{123}\sigma_{23}} d_4\kappa^j_{k_j} \\ &b_2\xi_p \xrightarrow{\sigma_{23}\sigma_2} a_3\xi_{2j-1} && b_2\xi_p \xrightarrow{\sigma_{23}\sigma_{23}} d_4\kappa^j_{k_j} \\ &b_3\xi_p \xrightarrow{\sigma_3\sigma_{23}} d_4\kappa^j_{k_j} && b_3\xi_p \xrightarrow{\sigma_3\sigma_2} a_3\xi_{2j-1} \end{aligned} \tag{22}$$

in addition to the ones already appearing in Figure 20. When we then cancel $a_3\xi_{2j-1} \to d_3\kappa^j_{k_j}$, we obtain new multiplications:

$$\begin{aligned} &a_1\xi_p \xrightarrow{\sigma_{12}\sigma_3+\sigma_{123}\sigma_2\sigma_3} d_4\kappa^j_{k_j} \\ &a_2\xi_p \xrightarrow{\sigma_2\sigma_3+\sigma_{23}\sigma_2\sigma_3} d_4\kappa^j_{k_j} \\ &a_3\xi_p \xrightarrow{\sigma_3\sigma_2\sigma_3} d_4\kappa^j_{k_j} \\ &b_3\xi_p \xrightarrow{\sigma_3} d_4\kappa^j_{k_j} \end{aligned} \tag{23}$$

Most of these may be disregarded by Proposition 2.4. If $p = 2m$ for $m > 0$, the resulting reduced form of Figure 20 is shown in Figure 23. On the other hand, if $p = 2m+1$, we also cancel the edges $a_i\xi_{2m+1} \to d_i\kappa^m_{k_m}$ and $b_i\xi_{2m+1} \to e_i\kappa^m_{k_m}$, introducing the multiplications shown in Figure 24. Similarly, if $p = 0$, we cancel the edges $a_i\xi_0 \to d_i\gamma_r$ and $b_i\xi_0 \to e_i\gamma_r$, introducing similar multiplications.

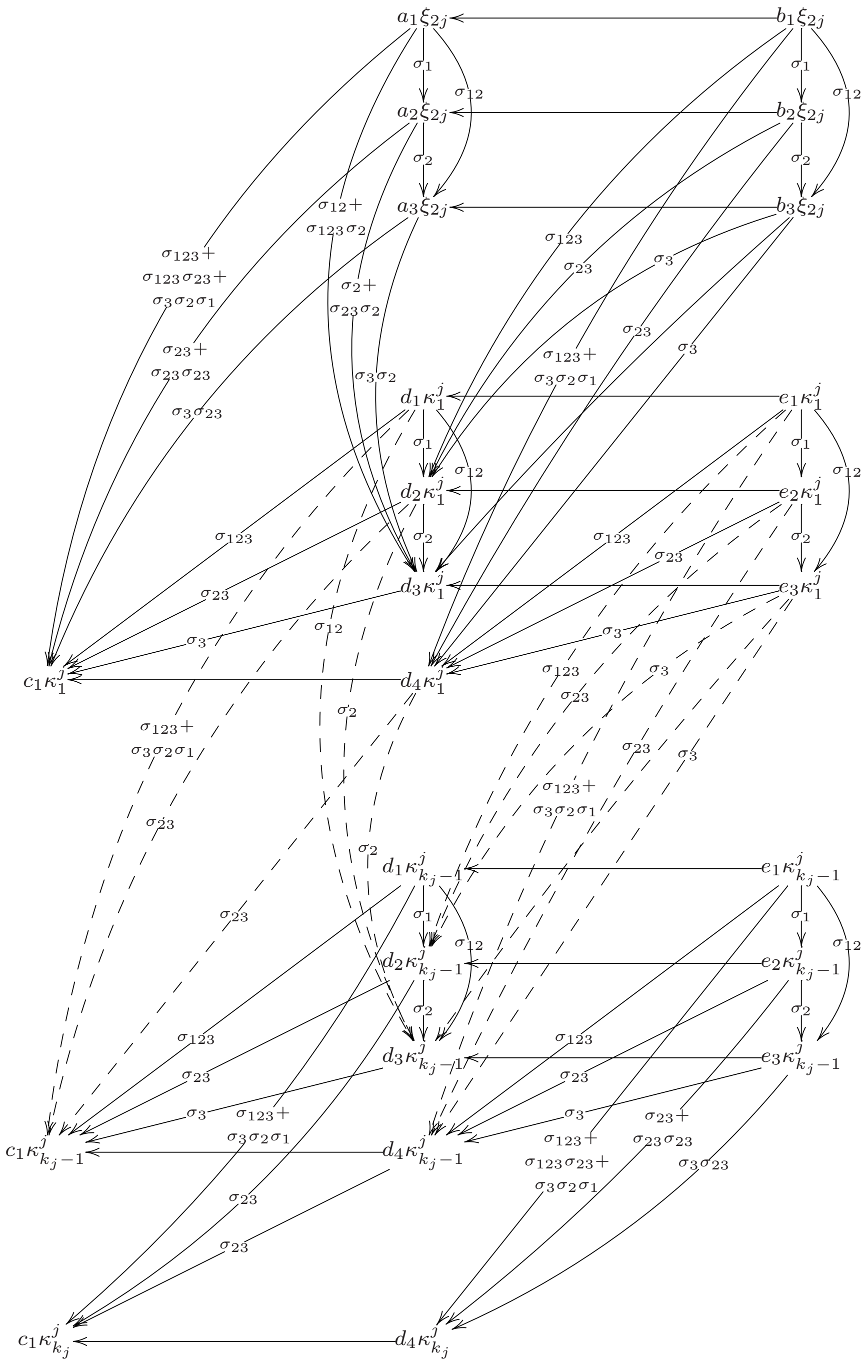

FIGURE 21. The subspace Q^j ($j > 0$) obtained from P^j_{vert} by canceling edges.

We now return to the case where $s = 2\tau(J)$. In P_{unst}, the edges $a_1\xi_0 \to a_4\eta_0$, $b_1\xi_0 \to b_4\eta_0$, $b_2\xi_0 \to b_5\eta_0$, and $b_3\xi_0 \to b_6\eta_0$ cancel, and since their targets do not have any other incoming edges, no new multiplications are introduced. The only

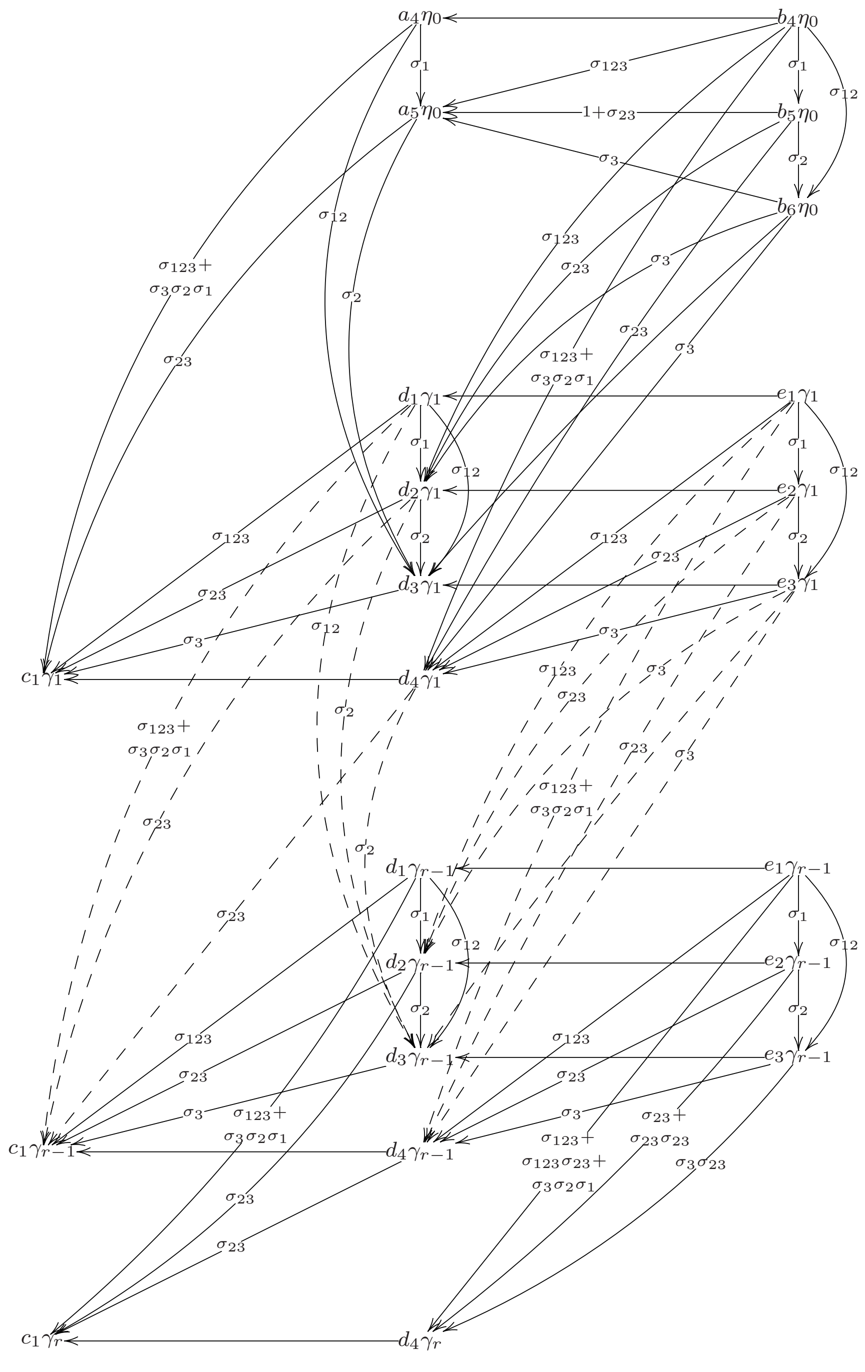

FIGURE 22. The subspace Q^0 obtained from P_{unst} by canceling edges, when $s < 2\tau(J)$.

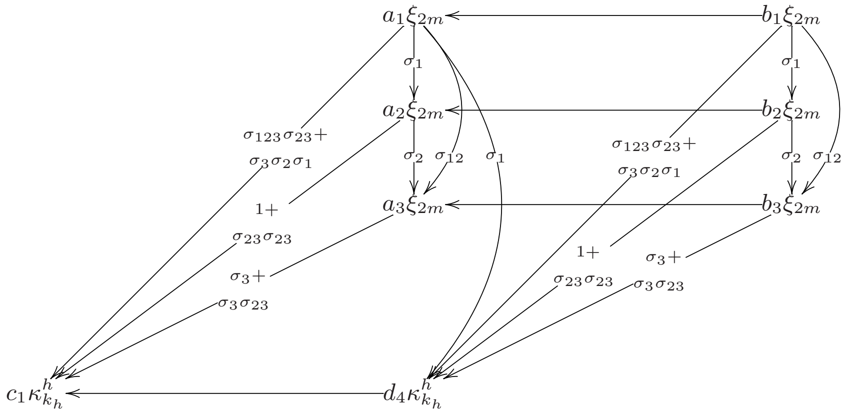

Figure 23. Reduced form of Figure 20 when $p = 2m$, $m > 0$.

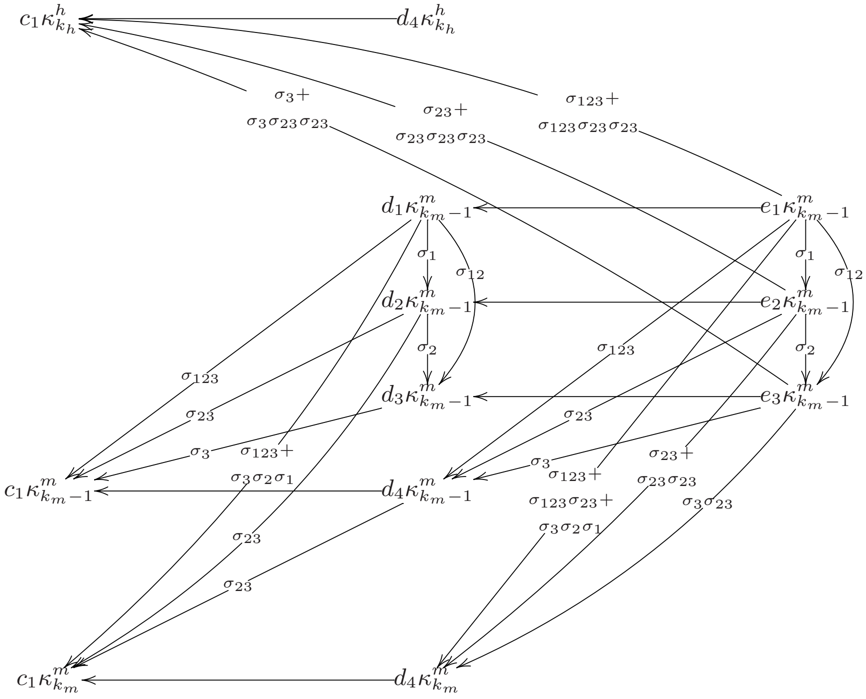

Figure 24. Reduced form of Figure 20 in the case where $p = 2m + 1$ (or $p = 0$, replacing $\kappa^m_{k_m-1}$ by γ_{r-1} and $\kappa^m_{k_m}$ by γ_r).

three remaining generators are $a_2\xi_0$, $a_3\xi_0$, and $a_5\eta_0$, all in filtration level 0, with the following multiplications:

$$\begin{tikzcd} & a_3\xi_0 \arrow[dr, "\sigma_3"] & \\ a_2\xi_0 \arrow[ur, "\sigma_2"] \arrow[rr, "1+\sigma_{23}"] & & a_5\eta_0 \end{tikzcd} \tag{24}$$

As above, $a_2\xi_0$ and $a_3\xi_0$ may have some outgoing edges, and $a_5\eta_0$ may have some incoming ones. The rest of the argument goes through unchanged.

4.3. Tensor product over $\mathcal{A}_\sigma$.

Let $Q = \bigoplus_{j=0}^{n} Q^j$, with multiplications as described in the previous subsection. We consider the tensor product $Q \underset{\mathcal{A}_\sigma}{\boxtimes} \widehat{\mathrm{CFD}}(\mathcal{X}_K^t)$. Again, the goal is to obtain a decomposition of the tensor product according to the stable and unstable chains in $\widehat{\mathrm{CFD}}(\mathcal{X}_K^t)$.

It is convenient to give the generators of Q^j new names. For $j = 1, \dots, n$ and $i = 1, \dots, k_j - 1$, define:

$$\begin{array}{llll} A^j = a_1\xi_{2j} & A'^j = b_1\xi_{2j} & E_i^j = d_1\kappa_i^j & E_i'^j = e_1\kappa_i^j \\ B^j = a_2\xi_{2j} & B'^j = b_2\xi_{2j} & F_i^j = d_2\kappa_i^j & F_i'^j = e_2\kappa_i^j \\ C^j = a_3\xi_{2j} & C'^j = b_3\xi_{2j} & G_i^j = d_3\kappa_i^j & G_i'^j = e_3\kappa_i^j \\ D^j = c_1\kappa_{k_j}^j & D'^j = d_4\kappa_{k_j}^j & H_i^j = c_1\kappa_i^j & H_i'^j = d_4\kappa_i^j \end{array}$$

When $s < 2\tau(J)$, for $i = 1, \dots, r-1$, define:

$$\begin{array}{llll} A^0 = a_4\eta_0 & A'^0 = b_4\eta_0 & E_i^0 = d_1\gamma_i & E_i'^0 = e_1\gamma_i \\ B^0 = a_5\eta_0 & B'^0 = b_5\eta_0 & F_i^0 = d_2\gamma_i & F_i'^0 = e_2\gamma_i \\ & C'^0 = b_6\eta_0 & G_i^0 = d_3\gamma_i & G_i'^0 = e_3\gamma_i \\ D^0 = c_1\gamma_r & D'^0 = d_4\gamma_r & H_i^0 = c_1\gamma_i & H_i'^0 = d_4\gamma_i \end{array}$$

Also, for notational convenience, define $k_0 = r$.

We divide up the generators of the subspaces Q^j by Alexander grading and idempotent:

	$A = -1$	$A = 0$	$A = 1$
ι_0^σ		A^j, C^j, E_i^j, G_i^j	$A'^j, C'^j, E_i'^j, G_i'^j$
ι_1^σ	D^j, H_i^j	$B^j, D'^j, F_i^j, H_i'^j$	$B'^j, F_i'^j$

In Figures 21 and 22, notice that of the generators in idempotent ι_0, A^j, A'^j, E_i^j, and $E_i'^j$ have outgoing edges labeled σ_1, σ_{12}, and σ_{123}, while C^j, C'^j, G_i^j, and $G_i'^j$ have outgoing edges labeled σ_3 and incoming edges labeled σ_2 and σ_{12}. Accordingly, it makes sense to associate the former with the vertical chains and the latter with the horizontal chains. That is, for each $J \in \{1, \dots, N\}$ and $j \in \{0, \dots, n\}$, define:

$$
\begin{aligned}
Z^{J,j}_{\text{vert}} &= \left\langle A^j, A'^j, E^j_i, E'^j_i \right\rangle \boxtimes \langle \Xi_{2J-1}, \Xi_{2J} \rangle \\
&\quad + \left\langle B^j, B'^j, D^j, D'^j, F^j_i, F'^j_i, H^j_i, H'^j_i \right\rangle \boxtimes \left\langle \mathrm{K}^J_I \mid 1 \le I \le K_J \right\rangle \\
Z^{J,j}_{\text{hor}} &= \left\langle C^j, C'^j, G^j_i, G'^j_i \right\rangle \boxtimes \langle \mathrm{H}_{2J-1}, \mathrm{H}_{2J} \rangle \\
&\quad + \left\langle B^j, B'^j, D^j, D'^j, F^j_i, F'^j_i, H^j_i, H'^j_i \right\rangle \boxtimes \left\langle \Lambda^J_I \mid 1 \le I \le L_J \right\rangle \\
Z^{j}_{\text{unst}} &= \left\langle A^j, A'^j, E^j_i, E'^j_i \right\rangle \boxtimes \langle \Xi_0 \rangle \\
&\quad + \left\langle C^j, C'^j, G^j_i, G'^j_i \right\rangle \boxtimes \langle \mathrm{H}_0 \rangle \\
&\quad + \left\langle B^j, B'^j, D^j, D'^j, F^j_i, F'^j_i, H^j_i, H'^j_i \right\rangle \boxtimes \langle \Gamma_i \mid 1 \le I \le R \rangle .
\end{aligned}
\tag{25}
$$

Then, as a vector space,

$$
Q \boxtimes \widehat{\mathrm{CFD}}(\mathcal{X}^t_K) = \bigoplus_{\substack{J=1,\dots,N \\ j=0,\dots,n}} Z^{J,j}_{\text{vert}} \oplus \bigoplus_{\substack{J=1,\dots,N \\ j=0,\dots,n}} Z^{J,j}_{\text{hor}} \oplus \bigoplus_{j=0}^{n} Z^{j}_{\text{unst}}. \tag{26}
$$

For fixed J, we write $Z^{J,*}_{\text{vert}} = \bigoplus_{j=0}^n Z^{J,j}_{\text{vert}}$, and so on.

As before, it is easy to verify that the differentials on the tensor product coming from m_1 and m_2 multiplications in Figures 21 and 22 respect the splitting (26). These differentials are illustrated in Figures 25 through 29. Note that we obtain slightly different differentials depending on whether $j = 0$ or $j > 0$. The double-dotted arrows correspond to the dashed arrows in Figures 15 through 18: for instance, in Figure 25, the double-dotted arrow from $E'^j_1 \Xi_{2J}$ to $H'^j_{k_j-1} \mathrm{K}^J_1$ really means that there are differentials $E'^j_i \Xi_{2J} \to H'^j_{i+1} \mathrm{K}^J_1$ for $i = 1, \dots, k_j - 2$.

Next, we must consider the differentials coming from the remaining multiplications on Q. First, we look at differentials that respect the splitting. If $k_j > 1$, the relevant multiplications on Q^j are:

$$
\begin{array}{llll}
A^j \xrightarrow{\sigma_{123}\sigma_2} G^j_1 & B^j \xrightarrow{\sigma_{23}\sigma_2} G^j_1 & C^j \xrightarrow{\sigma_3\sigma_2} G^j_1 & \text{if } j > 0 \\
A'^j \xrightarrow{\sigma_{123}\sigma_{23}} D'^j & B'^j \xrightarrow{\sigma_{23}\sigma_{23}} D'^j & C'^j \xrightarrow{\sigma_3\sigma_{23}} D'^j & \text{if } k_j = 1 \\
E'^j_{k_j-1} \xrightarrow{\sigma_{123}\sigma_{23}} D'^j & F'^j_{k_j-1} \xrightarrow{\sigma_{23}\sigma_{23}} D'^j & G'^j_{k_j-1} \xrightarrow{\sigma_3\sigma_{23}} D'^j & \text{if } k_j > 1.
\end{array}
$$

Therefore:

- In $Z^{J,j}_{\text{vert}}$, if $K_J > 1$, there are differentials $E'^j_{k_j-1} \Xi_{2J} \to D'^j \mathrm{K}^J_2$ and $F'^j_{k_j-1} \mathrm{K}^J_I \to D'^j \mathrm{K}^J_{I+2}$.
- In $Z^{J,j}_{\text{hor}}$, if $K_J > 1$, there are differentials $G'^j_{k_j-1} \mathrm{H}_{2J-1} \to D'^j \Lambda^J_2$ and $F'^j_{k_j-1} \Lambda^J_I \to D'^j \Lambda^J_{I+2}$. Additionally, when $j > 0$, there are differentials $C^j \mathrm{H}_{2J-1} \to G^j_1 \mathrm{H}_{2J}$ if $K_J = 1$, and $B^j \Lambda^J_{K_J-1} \to G^j_1 \mathrm{H}_{2J}$ if $K_J > 1$.
- In Z^j_{unst}, if $t < 2\tau(K) - 1$, there are differentials $G'^j_{k_j-1} \mathrm{H}_0 \to D'^j \Gamma_2$ and $F'^j_{k_j-1} \Gamma_I \to D'^j \Gamma_{I+2}$. If $t = 2\tau(K) + 1$, there are differentials $A^j \Xi_0 \to G^j_1 \mathrm{H}_0$

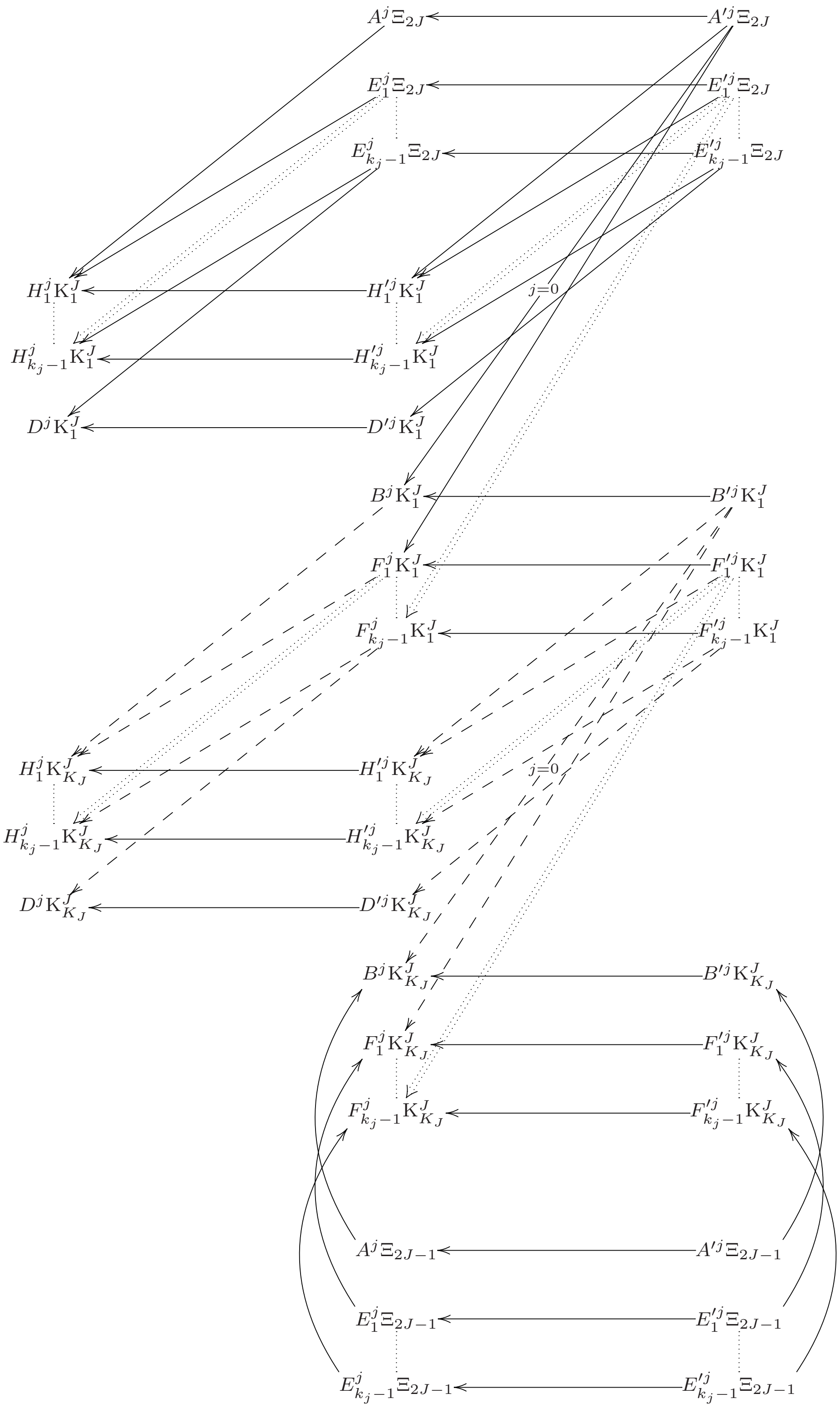

FIGURE 25. The subspace $Z^{J,j}_{\text{vert}}$, corresponding to a vertical stable chain $\Xi_{2J}\xrightarrow{\sigma_{123}}\mathrm{K}^J_1\xrightarrow{\sigma_{23}}\cdots\xrightarrow{\sigma_{23}}\mathrm{K}^J_{K_J}\xleftarrow{\sigma_1}\Xi_{2J-1}$.

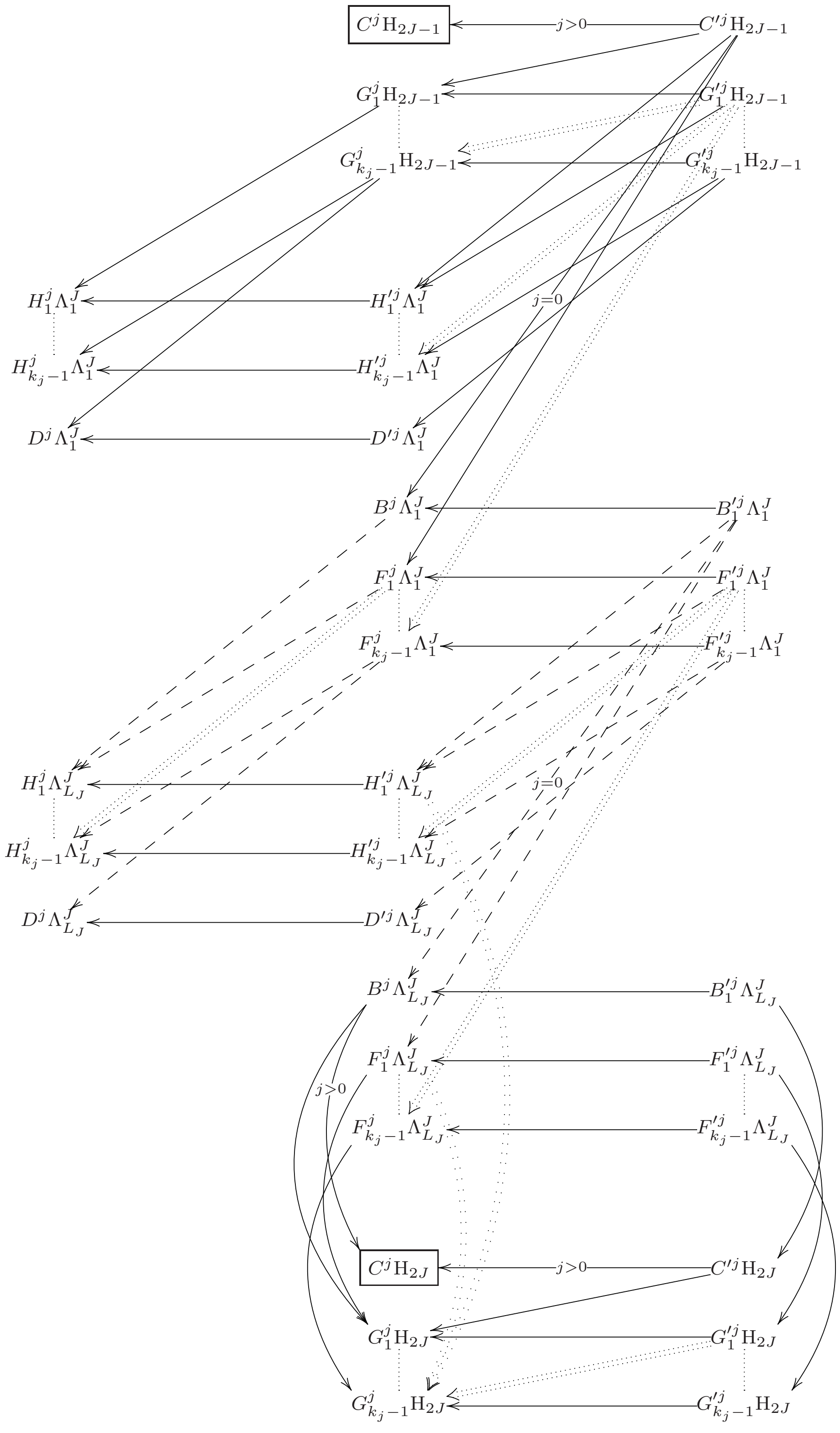

FIGURE 26. The subspace $Z_{\mathrm{hor}}^{J,j}$, corresponding to a horizontal stable chain $\mathrm{H}_{2J-1} \xrightarrow{\sigma_3} \Lambda_1^J \xrightarrow{\sigma_{23}} \cdots \xrightarrow{\sigma_{23}} \Lambda_{L_J}^J \xrightarrow{\sigma_2} \mathrm{H}_{2J}$.

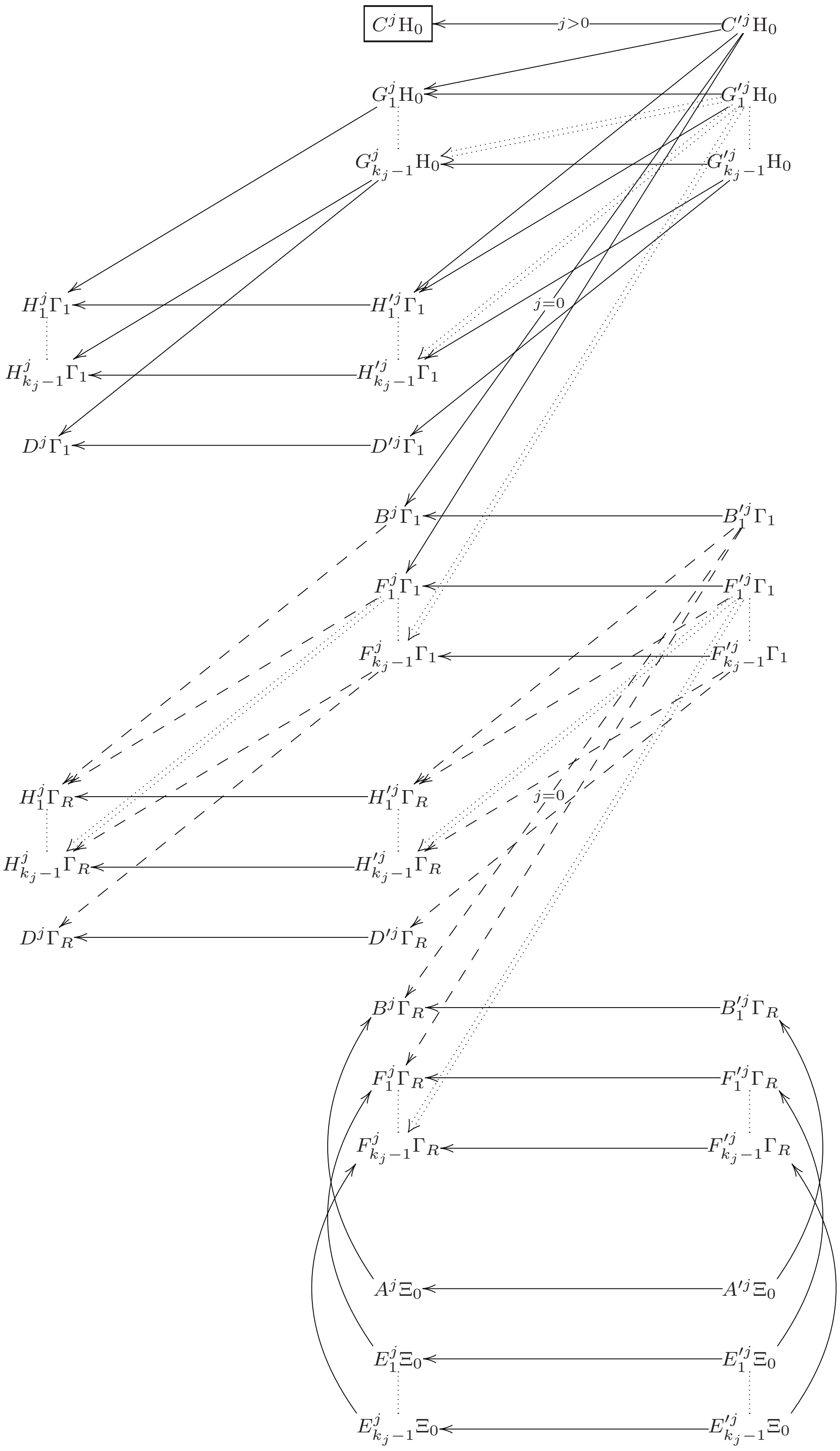

FIGURE 27. The subspace Z^j_{unst} when $t < 2\tau(K)$, corresponding to the unstable chain $\mathrm{H}_0 \xrightarrow{\sigma_3} \Gamma_1 \xrightarrow{\sigma_{23}} \cdots \xrightarrow{\sigma_{23}} \Gamma_R \xleftarrow{\sigma_1} \Xi_0$.

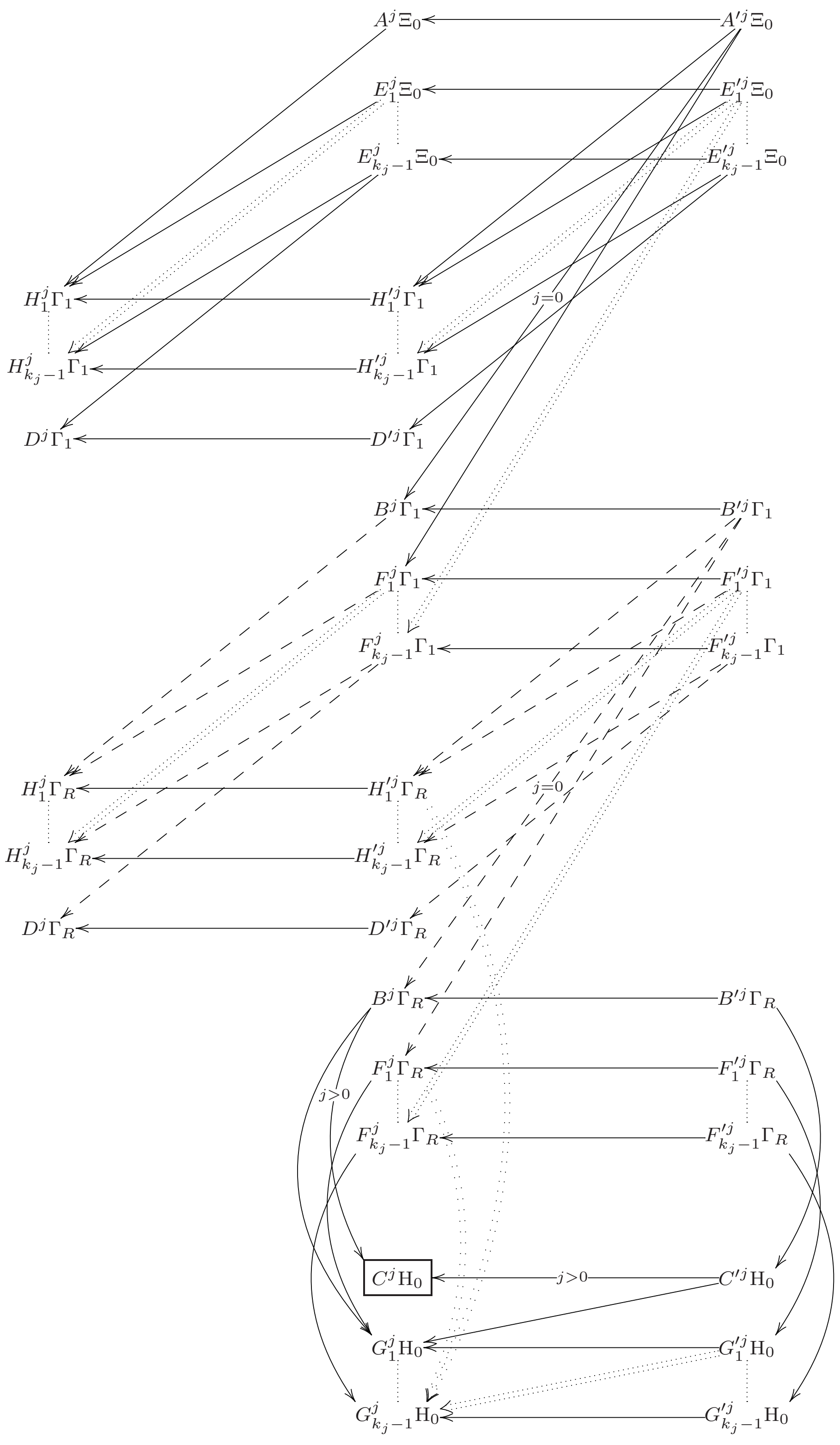

FIGURE 28. The subspace Z^j_{unst} when $t > 2\tau(K)$, corresponding to the unstable chain $\Xi_0 \xrightarrow{\sigma_{123}} \Gamma_1 \xrightarrow{\sigma_{23}} \cdots \xrightarrow{\sigma_{23}} \Gamma_R \xrightarrow{\sigma_2} \mathrm{H}_0$.

$$\begin{tikzcd}
A^j\Xi_0 \arrow[ddd, bend right, "j>0"'] & A'^j\Xi_0 \arrow[l] \arrow[ddd, bend left] \\
E^j_1\Xi_0 \arrow[ddd, bend right] \arrow[d, dotted, no head] & E'^j_1\Xi_0 \arrow[l] \arrow[ddd, bend left] \arrow[d, dotted, no head] \\
E^j_{k_j-1}\Xi_0 \arrow[ddd, bend right] & E'^j_{k_j-1}\Xi_0 \arrow[l] \arrow[ddd, bend left] \\
\boxed{C^j\mathrm{H}_0} & C'^j\mathrm{H}_0 \arrow[l, "j>0"] \arrow[dl] \\
G^j_1\mathrm{H}_0 \arrow[d, dotted, no head] & G'^j_1\mathrm{H}_0 \arrow[l] \arrow[d, dotted, no head] \arrow[dl, Rightarrow, dotted] \\
G^j_{k_j-1}\mathrm{H}_0 & G'^j_{k_j-1}\mathrm{H}_0 \arrow[l]
\end{tikzcd}$$

FIGURE 29. The subspace Z^j_{unst} when $t = 2\tau(K)$, corresponding to the unstable chain $\Xi_0 \xrightarrow{\sigma_{12}} \mathrm{H}_0$.

for $j > 0$. If $t > 2\tau(K) + 1$, there are differentials $E'^j_{k_{j-1}}\Xi_0 \to D'^j\Gamma_2$ and $F'^j_{k_{j-1}}\Gamma_I \to D'^j\Gamma_{I+2}$ for all j, and $B^j\Gamma_{R-1} \to G^j_1\mathrm{H}_0$ for $j > 0$.

Next, we may have some differentials that preserve the decomposition

$$\bigoplus_J Z^{J,*}_{\mathrm{vert}} \oplus \bigoplus_J Z^{J,*}_{\mathrm{hor}} \oplus Z^*_{\mathrm{unst}}$$

but which come from the multiplications on Q that do not preserve the splitting $Q = \bigoplus_{j=0}^n Q^j$, shown in Figures 19, 23, and 24. The resulting differentials are shown in Table 1. In each line that involves expressions like K^J_I, Λ^J_I, and Γ_I, we assume that K_J, L_J, or R is sufficiently large for the indices to make sense and that I ranges over appropriate bounds. The symbol * denotes both primed and unprimed symbols; thus, for instance, the notation $A^{*j}\Xi_{2J} \to D^{*h}\mathrm{K}^J_2$ means that there are differentials $A^j\Xi_{2J} \to D^h\mathrm{K}^J_2$ and $A'^j\Xi_{2J} \to D'^h\mathrm{K}^J_2$. Additionally, note that if $k_h = 1$, then we replace H^h_1 by D^h where it appears; if $k_j = 1$, we replace $E'^j_{k_j-1}$, $F'^j_{k_j-1}$, and $G'^j_{k_j-1}$ by A'^j, B'^j, and C'^j, respectively.

Notice that almost all of the differentials in Table 1 drop the filtration level by a nonzero amount. The two exceptions are $A^j\Xi_{2J-1} \to D'^h\mathrm{K}^J_{K_J}$ and $A^j\Xi_0 \to D'^h\Gamma_R$ in the second column.

Finally, we must look at differentials that do not respect the splitting at all. Notice that the sequence $\sigma_3\sigma_2\sigma_1$ occurs several times in Figures 21 and 22, and the sequences $\sigma_3\sigma_2\sigma_{12}$ and $\sigma_3\sigma_2\sigma_{123}$ occur in Equations (16) and (18), and these are the only such sequences that appear. More precisely, in Q^j with $k_j > 1$, we have the following

	$u_{2j,h} = 1,\ j,h > 0$	$v_{2j,h} = 1,\ j > 0$	$v_{2j-1,h} = 1$ or $w_h = 1$
Z^J_{vert}	$A'^j \Xi_{2J} \to H^h_1 \mathrm{K}^J_2$ $B'^j \mathrm{K}^J_I \to H^h_1 \mathrm{K}^J_{I+1}$ $B'^j \mathrm{K}^J_I \to H^h_1 \mathrm{K}^J_{I+2}$	$A^{*j} \Xi_{2J} \to D^{*h} \mathrm{K}^J_2$ $B^{*j} \mathrm{K}^J_I \to D^{*h} \mathrm{K}^J_I$ $B^{*j} \mathrm{K}^J_I \to D^{*h} \mathrm{K}^J_{I+2}$ $A^j \Xi_{2J-1} \to D'^h \mathrm{K}^J_{K_J}$	$E'^j_{k_j-1} \Xi_{2J} \to D^h \mathrm{K}^J_1$ $E'^j_{k_j-1} \Xi_{2J} \to D^h \mathrm{K}^J_3$ $F'^j_{k_j-1} \mathrm{K}^J_I \to D^h \mathrm{K}^J_{I+1}$ $F'^j_{k_j-1} \mathrm{K}^J_I \to D^h \mathrm{K}^J_{I+3}$
Z^J_{hor}	If $L_J = 1:$ $C'^j \mathrm{H}_{2J-1} \to G^h_1 \mathrm{H}_{2J-1}$ If $L_J > 1:$ $C'^j \mathrm{H}_{2J-1} \to H^h_1 \Lambda^J_2$ $B'^j \Lambda^J_I \to H^h_1 \Lambda^J_{I+1}$ $B'^j \Lambda^J_I \to H^h_1 \Lambda^J_{I+2}$ $B'^j \Lambda^J_{K_J-1} \to G^h_1 \mathrm{H}_{2J-1}$	$C^{*j} \mathrm{H}_{2J-1} \to D^{*J} \Lambda^J_1$ $C^{*j} \mathrm{H}_{2J-1} \to D^{*J} \Lambda^J_2$ $B^{*j} \Lambda^J_I \to D^{*h} \Lambda^J_I$ $B^{*j} \Lambda^J_I \to D^{*h} \Lambda^J_{I+2}$	$G'^j_{k_j-1} \mathrm{H}_{2J-1} \to D^h \Lambda^J_1$ $G'^j_{k_j-1} \mathrm{H}_{2J-1} \to D^h \Lambda^J_3$ $F'^j_{k_j-1} \Lambda^J_I \to D^h \Lambda^J_{I+1}$ $F'^j_{k_j-1} \Lambda^J_I \to D^h \Lambda^J_{I+3}$
Z_{unst}, $t < 2\tau(K)$	$C'^j \mathrm{H}_0 \to H^h_1 \Gamma_2$ $B'^j \Gamma_I \to H^h_1 \Gamma_{I+1}$ $B'^j \Gamma_I \to H^h_1 \Gamma_{I+2}$	$C^{*j} \mathrm{H}_0 \to D^{*J} \Gamma_1$ $C^{*j} \mathrm{H}_0 \to D^{*J} \Gamma_2$ $B^{*j} \Gamma_I \to D^{*h} \Gamma_I$ $B^{*j} \Gamma_I \to D^{*h} \Gamma_{I+2}$ $A^j \Xi_0 \to D'^h \Gamma_R$	$G'^j_{k_j-1} \mathrm{H}_0 \to D^h \Gamma_1$ $G'^j_{k_j-1} \mathrm{H}_0 \to D^h \Gamma_3$ $F'^j_{k_j-1} \Gamma_I \to D^h \Gamma_{I+1}$ $F'^j_{k_j-1} \Gamma_I \to D^h \Gamma_{I+3}$
Z_{unst}, $t > 2\tau(K)$	If $R = 1:$ $A'^j \Xi_0 \to G^h_1 \mathrm{H}_0$ If $R > 1:$ $A'^j \Xi_0 \to H^h_1 \Gamma_2$ $B'^j \Gamma_I \to H^h_1 \Gamma_{I+1}$ $B'^j \Gamma_I \to H^h_1 \Gamma_{I+2}$ $B'^j \Gamma_{R-1} \to G^h_1 \mathrm{H}_0$	$A^{*j} \Xi_0 \to D^{*h} \Gamma_2$ $B^{*j} \Gamma_I \to D^{*h} \Gamma_I$ $B^{*j} \Gamma_I \to D^{*h} \Gamma_{I+2}$	$E'^j_{k_j-1} \Xi_0 \to D^h \Gamma_1$ $E'^j_{k_j-1} \Xi_0 \to D^h \Gamma_3$ $F'^j_{k_j-1} \Gamma_I \to D^h \Gamma_{I+1}$ $F'^j_{k_j-1} \Gamma_I \to D^h \Gamma_{I+3}$

Table 1. Differentials arising from the multiplications in Figures 19, 23, and 24.

multiplications:

$$\begin{array}{rlrll}
A^j & \xrightarrow{\sigma_3\sigma_2\sigma_1} H^j_1 & A'^j & \xrightarrow{\sigma_3\sigma_2\sigma_1} H'^j_1 & \\
E^j_i & \xrightarrow{\sigma_3\sigma_2\sigma_1} H^j_{i+1} & E'^j_i & \xrightarrow{\sigma_3\sigma_2\sigma_1} H'^j_{i+1} & (i = 1, \dots, k_j - 2) \\
E^j_{k_j-1} & \xrightarrow{\sigma_3\sigma_2\sigma_1} D^j & E'^j_{k_j-1} & \xrightarrow{\sigma_3\sigma_2\sigma_1} D'^j & \\
A'^j & \xrightarrow{\sigma_3\sigma_2\sigma_{12}} G^j_2 & A'^j & \xrightarrow{\sigma_3\sigma_2\sigma_{123}} H^j_2 & \\
E'^j_i & \xrightarrow{\sigma_3\sigma_2\sigma_{12}} G^j_{i+2} & E'^j_i & \xrightarrow{\sigma_3\sigma_2\sigma_{123}} H^j_{i+2} & (i = 1, \dots, k_j - 3) \\
 & & E'^j_{k_j-2} & \xrightarrow{\sigma_3\sigma_2\sigma_{123}} D^j &
\end{array} \tag{27}$$

If $k_j = 1$, then we simply have $A^j \xrightarrow{\sigma_3\sigma_2\sigma_1} D^j$ and $A'^j \xrightarrow{\sigma_3\sigma_2\sigma_1} D'^j$. Finally, from Figure 23, if $v_{2j,h} = 1$, then there are multiplications $A^j \xrightarrow{\sigma_3\sigma_2\sigma_1} D^h$ and $A'^j \xrightarrow{\sigma_3\sigma_2\sigma_1} D'^h$.

Notice that all of these multiplications come out of A^j, A'^j, E^j_i, or E'^j_i, all of which are paired with $\{\Xi_0, \dots, \Xi_{2N}\}$ rather than $\{\mathrm{H}_0, \dots, \mathrm{H}_{2N}\}$ in (25). It follows that each group $Z^{J,*}_{\mathrm{hor}}$ is actually a direct summand as a chain complex. We shall see that the generator of the total homology comes from $\bigoplus_J Z^{J,*}_{\mathrm{vert}} \oplus Z^*_{\mathrm{unst}}$, so we may ignore each of these summands. Furthermore, if we define $U_{P,M}$, $V_{P,M}$, and W_P analogously to $u_{p,h}$, $v_{p,m}$, and w_p above, then we obtain differentials from $A^j\Xi_P$, $A'^j\Xi_P$, $E^j_i\Xi_P$, and/or $E'^j_i\Xi_P$ to elements of Z^M_{vert} and Z_{unst} whenever $U_{P,M}$, $V_{P,M}$, or W_P is nonzero. Specifically:

- If $V_{P,M} = 1$, then there are differentials

$$\begin{aligned} A^j\Xi_P &\to H^j_1\mathrm{K}^M_{K_M} & A'^j\Xi_P &\to H'^j_1\mathrm{K}^M_{K_M} & \\ E^j_i\Xi_P &\to H^j_{i+1}\mathrm{K}^M_{K_M} & E'^j_i\Xi_P &\to H'^j_{i+1}\mathrm{K}^M_{K_M} & (i = 1, \dots, k_j - 2) \\ E^j_{k_j-1}\Xi_P &\to D^j\mathrm{K}^M_{K_M} & E'^j_{k_j-1}\Xi_P &\to D'^j\mathrm{K}^M_{K_M} & \end{aligned} \tag{28}$$

  if $k_j > 1$, and $A^j\Xi_P \to D^j\mathrm{K}^M_{K_M}$ and $A'^j\Xi_P \to D'^j\mathrm{K}^M_{K_M}$ if $k_j = 1$. Also, if $v_{2j,h} = 1$, then there are differentials $A^j\Xi_P \to D^h\mathrm{K}^M_{K_M}$ and $A'^j\Xi_P \to D'^h\mathrm{K}^M_{K_M}$.

  Similarly, if $W_P = 1$ and $t < 2\tau(K)$, then we obtain similar differentials going into Z_{unst}, replacing $\mathrm{K}^M_{K_M}$ by Γ_R.

- If $U_{P,M} = 1$, then there are differentials

$$\begin{aligned} A'^j\Xi_P &\to H^j_2\mathrm{K}^M_1 \\ E'^j_i\Xi_P &\to H^j_{i+2}\mathrm{K}^M_1 \ (i = 1, \dots, k_j - 3) \\ E'^j_{k_j-2}\Xi_P &\to D^j\mathrm{K}^M_1. \end{aligned} \tag{29}$$

  Similarly, if $W_P = 1$ and $t > 2\tau(K)$, then we obtain similar differentials going into Z_{unst}, replacing K^M_1 by Γ_1.

- Finally, if $W_P = 1$ and $t = 2\tau(K)$, there are differentials

$$\begin{aligned} A'^j\Xi_P &\to G^j_2\mathrm{H}_0 \\ E'^j_i\Xi_P &\to G^j_{i+2}\mathrm{H}_0 \ (i = 1, \dots, k_j - 3) \end{aligned} \tag{30}$$

4.4. **Computation of $\tau(D_{J,s}(K,t))$.** We now describe the edge cancellations that occur in each of the pieces. Recall that we must cancel edges in increasing order of the amount by which they drop filtration level. We shall see that a single generator survives. The filtration level of this generator, by definition, is $\tau(D_{J,s}(K,t))$.

We start by canceling the filtration-preserving edges in $Z^{J,j}_{\mathrm{vert}}$. Note that there are are no other edges into $B'^j\mathrm{K}^J_{K_J}$ or $F'^j_i\mathrm{K}^J_{K_J}$, so eliminating the edges coming from these does not introduce any new edges. If $V_{2J-1}, M = 1$, or if $W_{2J-1} = 1$ and $t < 2\tau(K)$, then canceling the edges $A^j\Xi_{2J-1} \to B^j\mathrm{K}^J_{K_J}$ and $E^j_i \to F^j_k\mathrm{K}^J_{K_J}$ introduces some new edges, which all reduce filtration level by 2. Note also that the filtration-preserving edges $A^j\Xi_{2j-1} \to D'^h\mathrm{K}^J_{K_J}$ $(j > 0)$ in Table 1 are eliminated, since $B^j\mathrm{K}^J_{K_j}$ has no other incoming edges when $j > 0$.

In Z^j_{unst}, when $t < 2\tau(K)$, we perform the same cancellations as in $Z^{J,j}_{\mathrm{vert}}$, *mutatis mutandis.* When $t > 2\tau(K)$, there are $2k_j$ filtration-preserving edges to cancel when $j > 0$ (namely, $B^{*j}\Gamma^R \to C'^{*j}\mathrm{H}_0$ and $F^{*j}_i\Gamma^R \to G^{*j}_i\mathrm{H}_0$ for $i = 1, \dots, k_j - 1$), but only $2k_0 - 1$ such edges in Z^0_{unst}, since the generator $C_0\mathrm{H}_0$ does not exist. Thus, the generator $B^0\Gamma^R$ survives after these cancellations. Also, note that canceling $B^j\Gamma^R \to C^j\mathrm{H}_0$ and $F^j_i\Gamma^R \to G^j_i\mathrm{H}_0$ may introduce some new differentials using the arrows in Table 1, but they all filtration level by 2.

When $t = 2\tau(K)$, the only generator in Z^0_{unst} that survives is $A^0\Xi_0$. Notice, however, that by (28), there is a differential $A^0\Xi_0 \to H^0_1\mathrm{K}^M_{K_M}$ for any M with $V_{0,M} = 1$. All the generators of Z^j_{unst} for $j > 0$ are canceled.

We have now canceled all edges that preserve the filtration level, so we now begin canceling differentials that drop filtration level by 1. Specifically, in $Z^{J,j}_{\mathrm{vert}}$, cancel every horizontal edge $X' \to X$, starting at the top of Figure 25 and working down. We use the following key observations:

- If X is in filtration level 0 and X' is in level 1, then X has no other incoming edges, since by induction we have already eliminated everything above X and X', and Table 1 and Equations (28) and (29) contain no differentials that go into $A^j\Xi_{2J}$, $E^j_i\Xi_{2J}$, $B^j\mathrm{K}^J_I$, or $F^j_i\mathrm{K}^J_I$ from elsewhere.
- If X is in filtration level -1 and X' is in level 0, then X' has no other outgoing edges, since Table 1 and Equations (28) and (29) contain no differentials that go out of $H'^j_i\mathrm{K}^J_I$ or $D'^j\mathrm{K}^J_I$.

Thus, we can completely cancel $Z^{J,j}_{\mathrm{vert}}$.

If $t = 2\tau(K)$, we have now eliminated all generators except $A^0\Xi_0$, which is in filtration level 0, so $\tau(D_{J_s}(K,t)) = 0$ when $s < 2\tau(J)$ and $t = 2\tau(K)$.

If $t > 2\tau(K)$, we proceed with Z^j_{unst} just as with $Z^{J,j}_{\mathrm{vert}}$. When $j > 0$, all generators in cancel; when $j = 0$, the one surviving generator is $B^0\Gamma_R$, which is in filtration level 0. Thus, $\tau(D_{J_s}(K,t)) = 0$ when $s < 2\tau(J)$ and $t > 2\tau(K)$.

If $t < 2\tau(K)$, when $j > 0$, we start by canceling $C'^j\mathrm{H}_0 \to C^j\mathrm{H}_0$ and proceeding downward in Figure 27, as before, eliminating all generators. When $j = 0$, we start by canceling $G'^j_1\mathrm{H}_0 \to G^j_1\mathrm{H}_0$ and proceed downward, and we thus see that the only surviving generator is $C'^j\mathrm{H}_0$, which is in filtration level 1. Thus, $\tau(D_{J_s}(K,t)) = 1$ when $s < 2\tau(J)$ and $t < 2\tau(K)$.

Finally, we must return to the case where $s = 2\tau(J)$. Recall that Q_0 in this case consists of three generators, all in filtration level 0, as in (24). For $j > 0$, the definitions of $Z^{J,j}_{\mathrm{vert}}$, $Z^{J,j}_{\mathrm{hor}}$, and Z^j_{unst} go through the same way, and we see again that all of the resulting generators eventually cancel. It follows that the surviving generator must be in filtration level 0, so $\tau(D_{J,s}(K,t)) = 0$ whenever $s = 2\tau(K)$. □

5. Other results regarding $D_{J,s}(K,t)$

Prior to Hedden's complete computation of $\widehat{\mathrm{HFK}}$ and τ of all twisted Whitehead doubles [4], Livingston and Naik [13] used the formal properties of τ to understand the asymptotic behavior of τ for large values of the twisting parameter:

Theorem 5.1. *Suppose ν is any homomorphism from the smooth knot concordance group to $\mathbb{Z}$ with the properties that $|\nu(K)| \leq g_4(K)$ and $\nu(T_{p,q}) = (p-1)(q-1)/2$, where $p,q > 0$ and $T_{p,q}$ denotes the (p,q) torus knot. Then for any knot K, there exists $t_\nu(K) \in \mathbb{Z}$ such that*

$$\nu(Wh_+(K,t)) = \begin{cases} 1 & t \leq t_\nu(K) \\ 0 & t > t_\nu(K) \end{cases}$$

and $TB(K) \leq t_\nu(K) < -TB(-K)$ (where $TB(K)$ denotes the maximal Thurston-Bennequin number of K).

Two invariants satisfying the hypotheses of Theorem 5.1 are $\tau(K)$ and $-s(K)/2$, a renormalization of Rasmussen's concordance invariant $s(K)$ [18]. Around the same time, Hedden and Ording [5] proved that these two invariants are not equal by showing that $\tau(Wh_+(T_{2,3},2)) = 0$ while $s(Wh_+(T_{2,3},2)) = -2$, disproving a conjecture of Rasmussen. Later, Hedden [4] showed that $t_\tau(K) = 2\tau(K) - 1$ for any knot K. Finding a general formula for the s invariant of Whitehead doubles remains an open question.

We may extend the techniques of Livingston and Naik to study knots of the form $D_{J,s}(K,t)$ as well.

Proposition 5.2. *Let ν be an invariant satisfying the hypotheses of Theorem 5.1, and fix knots J and K.*

1. *If $s \leq TB(J)$ and $t \leq TB(K)$, then $\nu(D_{J,s}(K,t)) = 1$. If $s \geq -TB(-J)$ and $t \geq -TB(-K)$, then $\nu(D_{J,s}(K,t)) = -1$.*
2. *For fixed s (resp. t), the function $t \mapsto \nu(D_{J,s}(K,t))$ (resp. $s \mapsto \nu(D_{J,s}(K,t))$) is non-increasing and has as its image either $\{-1,0\}$, $\{0\}$, or $\{0,1\}$.*

Proof. The proof is very similar to that of [13, Theorem 2].

Let $A(J,s)$ denote an annulus in S^3, embedded along J with framing s, and define $A(K,t)$ analogously. We may obtain a Seifert surface for $D_{J,s}(K,t)$ as a plumbing $A(J,s) * A(K,t)$. By results of Rudolph [20, 22], when $s \leq TB(J)$ and $t \leq TB(K)$, the annuli $A(J,s)$ and $A(K,t)$ are *quasipositive surfaces*, so $A(J,s) * A(K,t)$ is also a quasipositive surface. Thus, $D_{J,s}(K,t)$ is a strongly quasipositive knot with genus 1, and hence $\nu(D_{J,s}(K,t)) = 1$ as in [12]. Mirroring gives the second half of (1).

The non-increasing statement in (2) follows from the fact that $D_{J,s}(K,t)$ is obtained from $D_{J,s-1}(K,t)$ or $D_{J,s}(K,t-1)$ by changing a positive crossing to a negative crossing, which can only preserve or decrease ν [12]. Also, since $D_{J,s}(K,t)$ is related to $D_{J,s'}(K,t)$ or $D_{J,s}(K,t')$ (for any s' or t') by a *band modification*, each of the two functions can assume at most two values, either $\{-1,0\}$ or $\{0,1\}$. Finally, we rule out the possibility that either of the functions in (1) is constant and nonzero. Suppose,

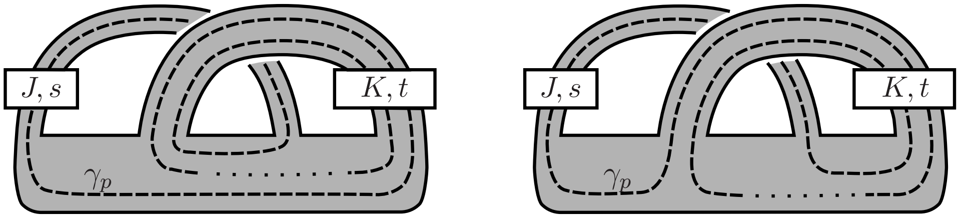

FIGURE 30. The Seifert surface F with the curve γ_p, in the cases where $p < 0$ (left) and $p > 0$ (right).

without loss of generality, that $\nu(D_{J,s}(K,t)) = 1$ for a fixed s and all t. In particular, $\nu(D_{J,s}(K, -TB(-K))) = 1$. On the other hand, $\nu(D_{J,-TB(-J)}(K, -TB(-K))) = -1$, which contradicts the fact that the image of the function $s \mapsto \nu(D_{J,s}(K, -TB(-K)))$ contains at most two consecutive integers. ☐

It follows that if $s \leq TB(J)$ and $t \geq -TB(-K)$, or $s \geq -TB(-J)$ and $t \leq TB(K)$, then $\nu(D_{J,s}(K,t)) = 0$. Thus, for large absolute values of s and t, $\nu(D_{J,s}(K,t)) = \tau(D_{J,s}(K,t))$. On the other hand, the behavior of $\nu(D_{J,s}(K,t)$ for small s and t (specifically, when $TB(J) < s < -TB(-J)$ or $TB(K) < t < -TB(-K)$) may be more complicated than the simple behavior of τ given by Theorem 1.1.

In another direction, we may also look for instances when $D_{J,s}(K,t)$ is actually smoothly slice. The following proposition generalizes Casson's argument [7, page 227] that the $p(p+1)$-twisted positive Whitehead double of the $(p, p+1)$ torus knot is smoothly slice. For an oriented knot K and relatively prime integers p, q, let $C_{p,q}(K)$ denote the (p,q)-cable of K. (Note that $C_{p,q}(K)^r = C_{-p,-q}(K) = C_{p,q}(K^r)$ and $\overline{C_{p,q}(K)} = C_{p,-q}(\bar{K})$.)

Proposition 5.3. *Let K be any knot, and let $p, t \in \mathbb{Z}$. If J is any knot that is smoothly concordant to $-C_{p,pt\pm1}(K)$, then $D_{J,-p(pt\pm1)}(K,t)$ is smoothly slice.*

Proof. Let F be the Seifert surface for $D_{J,s}(K,t)$ shown in Figure 30, and let γ_p be a curve that winds once around the band tied into J and p times around the band tied into K, as indicated. The knot type of γ_p is $C_{p,pt+1}(K)$, and the surface framing on γ_p is $s + p + p^2 t$. Thus, if J is smoothly concordant to $-C_{p,pt+1}(K)$ and $s = -p(pt+1)$, we may surger F along γ_p in D^4 along a smooth slice disk for $J \# C_{p,pt+1}(K)$, resulting in a smooth slice disk for $D_{J,s}(K,t)$.

If we reverse the crossing between the two bands of F, we obtain the result with the opposite signs. ☐

Proposition 5.3 is quite interesting in light of very recent work of Hom [6], who found a general formula for the τ invariant of all cable knots in terms of p, q, $\tau(K)$, and an invariant $\epsilon(K) \in \{-1, 0, 1\}$ that depends solely on the knot Floer complex of K. She proved:

Theorem 5.4. *Let K be a knot, and let $p > 0$. Then:*

- *If $\epsilon(K) = 1$, then $\tau(C_{p,q}(K)) = p\tau(K) + \frac{1}{2}(p-1)(q-1)$ for all q.*
- *If $\epsilon(K) = -1$, then $\tau(C_{p,q}(K)) = p\tau(K) + \frac{1}{2}(p-1)(q+1)$ for all q.*

- *If* $\epsilon(K) = 0$, *then* $\tau(K) = 0$, *and*
$$\tau(C_{p,q}(K)) = \begin{cases} \frac{1}{2}(p-1)(q+1) & q < 0 \\ \frac{1}{2}(p-1)(q-1) & q > 0. \end{cases}$$

We may use Theorem 5.4 to compute the value of τ for the cable knots appearing in Proposition 5.3, where we take $t = 2\tau(K)$.

Corollary 5.5. *For any knot* K, *if either* $\epsilon(K) \geq 0$ *and* $p > 0$, *or* $\epsilon(K) \leq 0$ *and* $p < 0$, *there exists a knot* J *such that* $D_{J,2\tau(J)-p}(K, 2\tau(K))$ *is smoothly slice, while* $\tau(D_{J,2\tau(J)-p}(K, 2\tau(K) - \frac{p}{|p|})) \neq 0$.

Proof. Suppose that $\epsilon(K) = 1$ and $p > 0$. Set $J = -C_{p,2p\tau(K)+1}(K)$, so that:
$$\begin{aligned} 2\tau(J) - p &= -2\tau(C_{p,2p\tau(K)+1}(K)) - p \\ &= -2p\tau(K) - (p-1)(2p\tau(K)) - p \\ &= -2p^2\tau(K) - p \\ &= -p(2p\tau(K) + 1). \end{aligned}$$
By Proposition 5.3, $D_{J,2\tau(J)-p}(K, 2\tau(K))$ is smoothly slice. On the other hand, $\tau(D_{J,2\tau(J)-p}(K, 2\tau(K) - 1) = 1$ by Theorem 1.1. The case where $\epsilon(K) = -1$ and $p < 0$ follows by mirroring, since $\epsilon(\bar{K}) = -\epsilon(K)$. Finally, if $\epsilon(K) = 0$, we set $J = -C_{p,1}(K)$ if $p > 0$ and $J = -C_{-p,-1}$ if $p < 0$. □

Theorem 1.1 says that the set $\{(s,t) \in \mathbb{Z}^2 \mid D_{J,s}(K,t) = 0\}$ always has the same shape for any J and K, up to translation: the union of the second and fourth quadrants of the $\mathbb{Z}^2$ lattice, including both axes. Corollary 5.5 implies that any point on the boundary of this region may be realized by a smoothly slice knot $D_{J,s}(K,t)$ for suitable choices of J and K.

Finally, recall that the main idea of the proof of Theorem 1.1 is that only the form of the unstable chains in $\widehat{\mathrm{CFD}}(\mathcal{X}_J^s)$ and $\widehat{\mathrm{CFD}}(\mathcal{X}_K^t)$ matters for the computation of of $\tau(D_{J,s}(K,t))$. Petkova [17] and Hom [6] have observed similar behavior in using bordered Heegaard Floer homology to compute $\tau(C_{p,q}(K))$. The invariant $\epsilon(K)$ defined by Hom describes the structure of the part of $\widehat{\mathrm{CFD}}(\mathcal{X}_K^t)$ "near" the unstable chain. Specifically, when we take vertically and horizontally reduced bases $\{\tilde{\xi}_0, \dots, \tilde{\xi}_{2n}\}$ and $\{\tilde{\eta}_0, \dots, \tilde{\eta}_{2n}\}$ for $\mathrm{CFK}^-(K)$, we may arrange that $\tilde{\xi}_0 = \tilde{\eta}_i$ for some i. The cases $\epsilon(K) = 1$, $\epsilon(K) = -1$, and $\epsilon(K) = 0$ correspond, respectively, to whether i is even and positive, odd and positive, or zero. Within each case, Hom showed that only the form of the unstable chain matters for computing $\tau(C_{p,q}(K))$. It is an interesting question whether the behavior of τ for more general classes of satellite knots can be described in this way.

References

[1] Žarko Bižaca, *An explicit family of exotic Casson handles*, Proc. Amer. Math. Soc. **123** (1995), no. 4, 1297–1302.

[2] Michael H. Freedman, Whitehead$_3$ *is a "slice" link*, Invent. Math. **94** (1988), no. 1, 175–182.

[3] Michael H. Freedman and Frank Quinn, *Topology of 4-manifolds*, Princeton Mathematical Series, vol. 39, Princeton University Press, Princeton, NJ, 1990.

[4] Matthew Hedden, *Knot Floer homology of Whitehead doubles*, Geom. Topol. **11** (2007), 2277–2338.

[5] Matthew Hedden and Philip Ording, *The Ozsváth-Szabó and Rasmussen concordance invariants are not equal*, Amer. J. Math. **130** (2008), no. 2, 441–453.

[6] Jennifer Hom, *Bordered Heegaard Floer homology and the τ invariant of cable knots*, in preparation.

[7] Louis H. Kauffman, *On knots*, Annals of Mathematics Studies, vol. 115, Princeton University Press, Princeton, NJ, 1987.

[8] Rob Kirby (ed.), *Problems in low-dimensional topology*, AMS/IP Stud. Adv. Math., vol. 2, Amer. Math. Soc., Providence, RI, 1997.

[9] Adam S. Levine, *Slicing mixed Bing-Whitehead doubles*, preprint (2009), arXiv:0912.5222.

[10] Robert Lipshitz, Peter Ozsváth, and Dylan Thurston, *Bimodules in bordered Heegaard Floer homology*, preprint (2010), arXiv:1003.0598.

[11] ———, *Bordered Heegaard Floer homology: invariance and pairing*, preprint (2009), arXiv:0810.0687.

[12] Charles Livingston, *Computations of the Ozsváth-Szabó knot concordance invariant*, Geom. Topol. **8** (2004), 735–742 (electronic).

[13] Charles Livingston and Swatee Naik, *Ozsváth-Szabó and Rasmussen invariants of doubled knots*, Algebr. Geom. Topol. **6** (2006), 651–657 (electronic).

[14] Peter Ozsváth and Zoltán Szabó, *Knot Floer homology and the four-ball genus*, Geom. Topol. **7** (2003), 615–639 (electronic).

[15] ———, *Holomorphic disks and knot invariants*, Adv. Math. **186** (2004), no. 1, 58–116.

[16] ———, *Holomorphic disks and topological invariants for closed three-manifolds*, Ann. of Math. (2) **159** (2004), no. 3, 1027–1158.

[17] Ina Petkova, *Cables of thin knots and bordered Heegaard Floer homology*, preprint (2010), arXiv:0911.2679.

[18] Jacob Rasmussen, *Khovanov homology and the slice genus*, preprint (2004), arXiv:math.GT/0402131.

[19] Jacob A. Rasmussen, *Floer homology and knot complements*, Ph.D. thesis, Harvard University, 2003, arXiv:math/0509499.

[20] Lee Rudolph, *Quasipositive annuli. (Constructions of quasipositive knots and links. IV)*, J. Knot Theory Ramifications **1** (1992), no. 4, 451–466.

[21] ———, *Quasipositivity as an obstruction to sliceness*, Bull. Amer. Math. Soc. (N.S.) **29** (1993), no. 1, 51–59.

[22] ———, *Quasipositive plumbing (constructions of quasipositive knots and links. V)*, Proc. Amer. Math. Soc. **126** (1998), no. 1, 257–267.

[23] Sucharit Sarkar and Jiajun Wang, *An algorithm for computing some Heegaard Floer homologies*, to appear, arXiv:math/0607777.

MATHEMATICS DEPARTMENT, BRANDEIS UNIVERSITY, 415 SOUTH STREET, WALTHAM, MA 02453

E-mail address: `levinea@brandeis.edu`

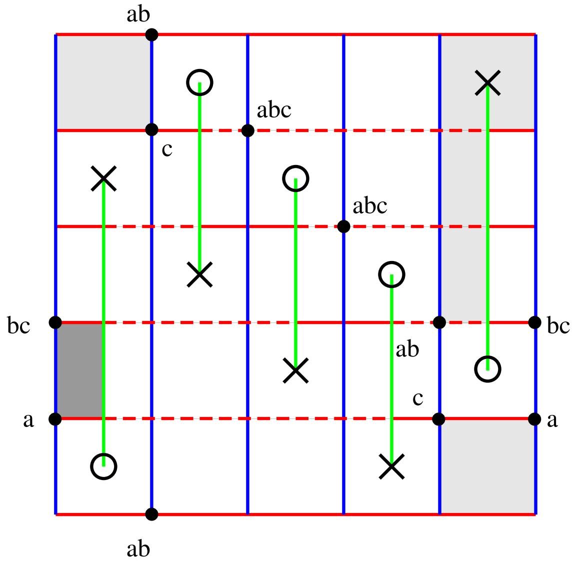
ab
c
abc
abc
bc
bc
ab
a
c
a
ab

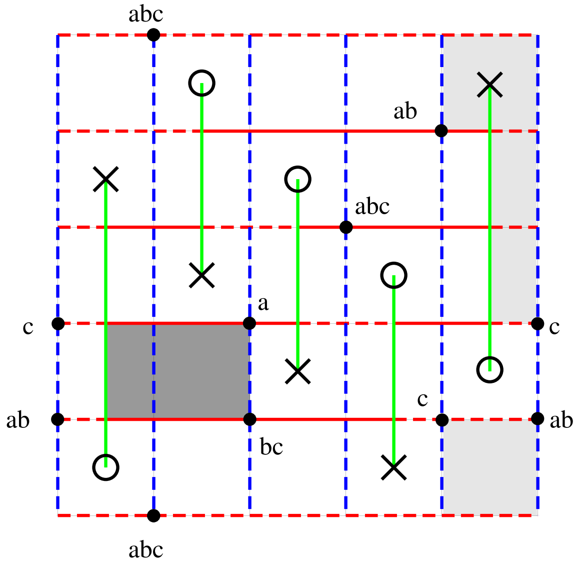
abc
ab
abc
a
c
c
ab
c
ab
bc
abc

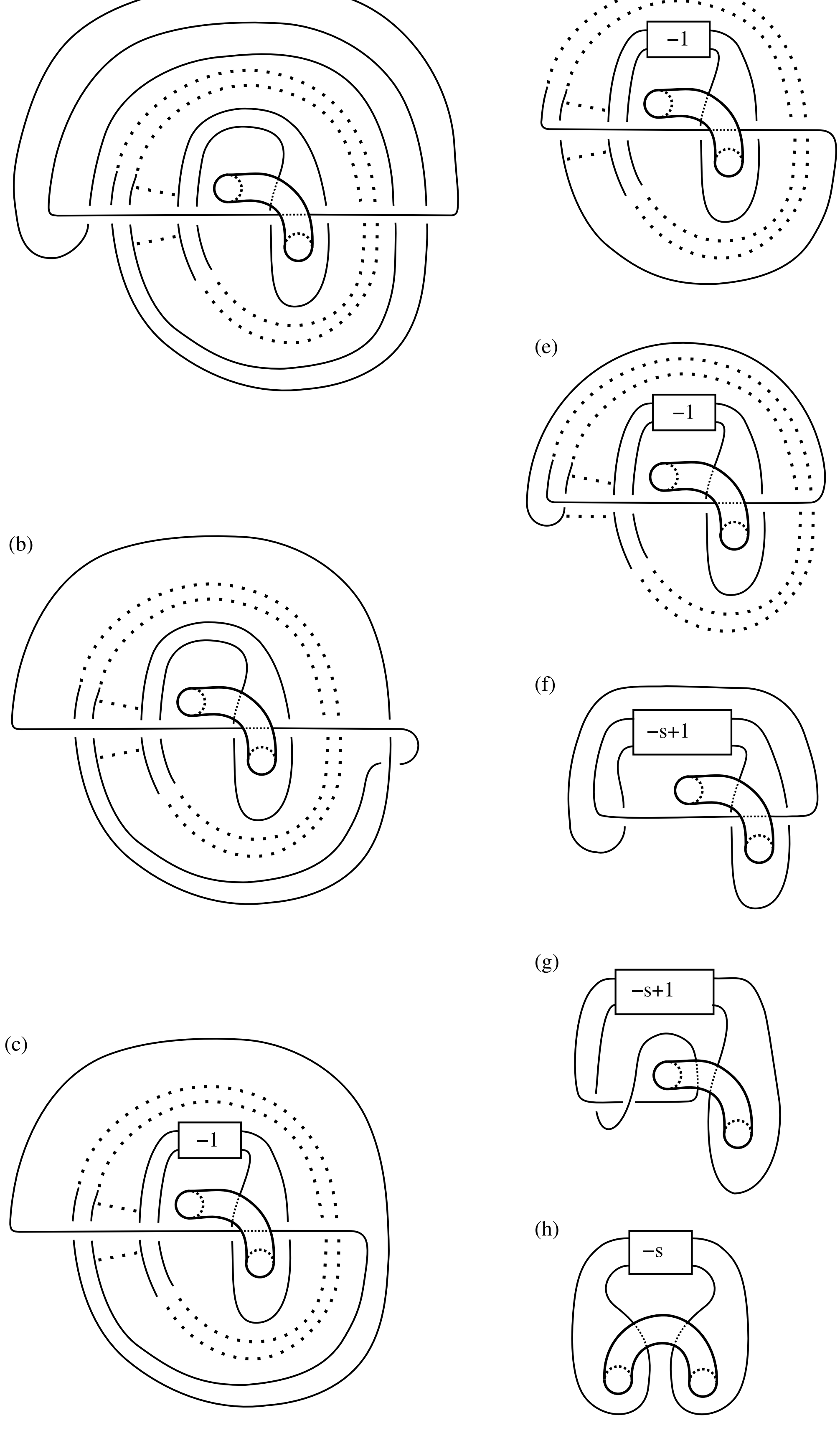
−1
(e)
−1
(b)
(f)
−s+1
(g)
−s+1
(c)
−1
(h)
−s

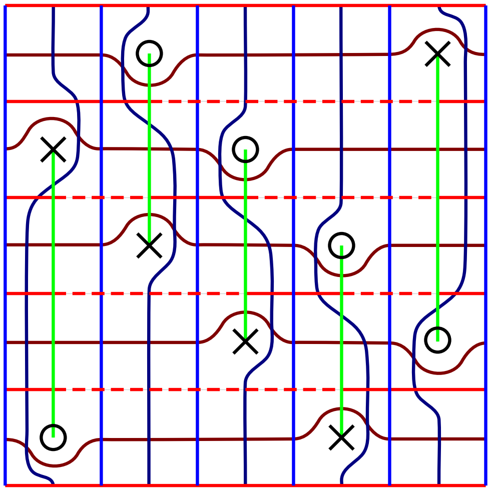

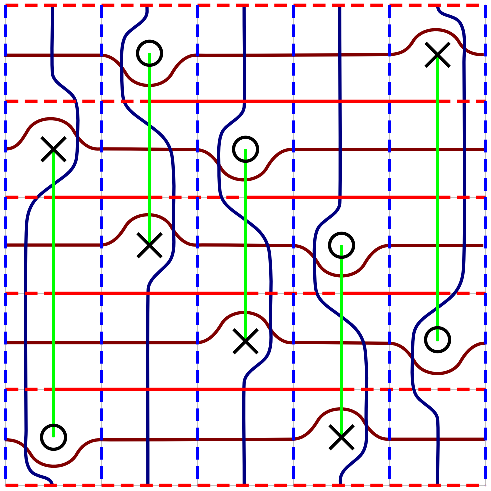

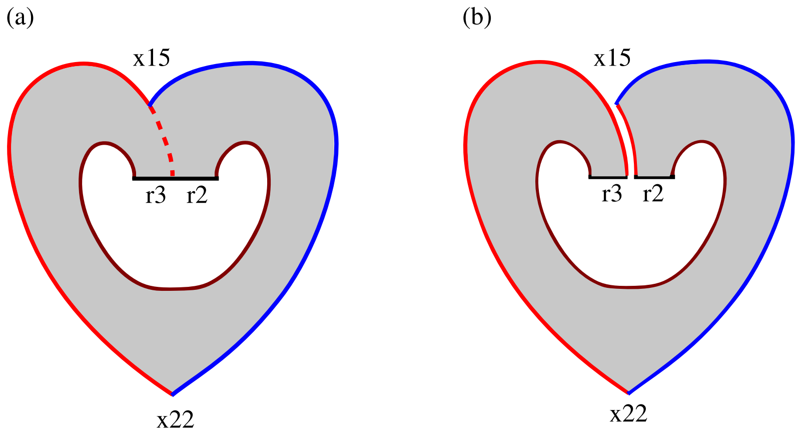
(a)
x15
r3
r2
x22
(b)
x15
r3
r2
x22

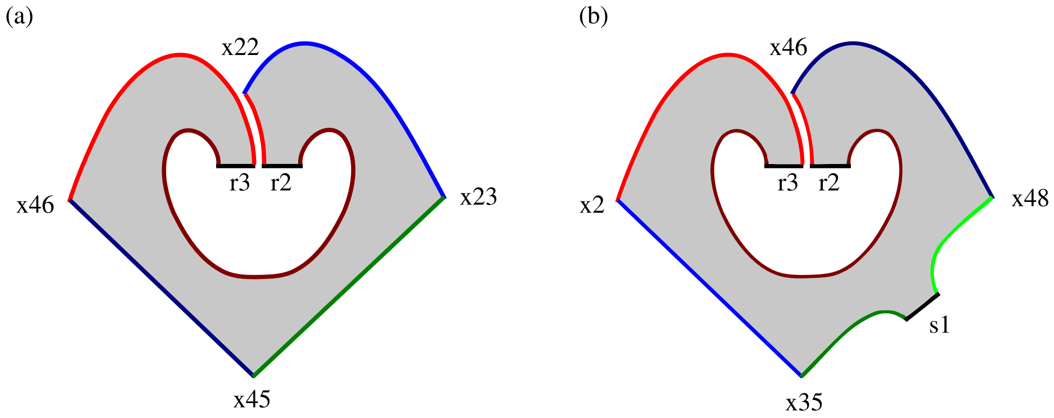
(a)
x22
x46
r3
r2
x23
x45
(b)
x46
x2
r3
r2
x48
s1
x35